"EVALUATION OF THE CHEMOTHERAPEUTIC POTENTIAL OF RESVERATROL ENTRAPPED NANOLIPOSOMES FOR TARGETING HEPATOCELLULAR CARCINOMA"

Thesis submitted to

KLE ACADEMY OF HIGHER EDUCATION AND RESEARCH (BELAGAVI)

(Deemed-to-be-University)

[Declared as Deemed-to-be-University u/s3 of the UGC Act, 1956 vide Govt. of India Notification No.F.9-19/2000-U.3(A)]

Accredited 'A' Grade by NAAC (2nd Cycle)

Placed in Category 'A' by MHRD (GoI)

For the award of the degree of

Doctor of Philosophy
In the Faculty of Pharmacy

By

Satveer Jagwani M.Pharm.

(Registration No: KLEU/Ph.D./14-15/DO1214018)

KLE
EMPOWERING PROFESSIONALS

Under the Guidance of

Prof. (Dr.) Sunil Satyappa Jalalpure Ph.D
Principal, KLE College of Pharmacy, Belagavi,
KLE academy of Higher Education and Research, Belagavi-590010,
Karnataka, India

2020

UNDERTAKING

I, Mr. **Satveer Jagwani** hereby declare that the information and the data mentioned in my thesis entitled **"Evaluation of the chemotherapeutic potential of resveratrol entrapped nanoliposomes for targeting hepatocellular carcinoma"** belongs to me and is original.

I am aware of definition of plagiarism as detailed below:

- An act or instance of using or closely imitating the language and thoughts of another author without authorization and the representation of that author's work as one's own, as by not crediting the original author.
- A piece of writing or other work reflecting such unauthorized use or imitation.
- The deliberate or reckless representation of another's words, thoughts or ideas as one's own without attribution in connection with submission of academic work, whether graded or otherwise.

I hereby declare that the thesis prepared by me is original-one and does not involve plagiarism anywhere. In case at a later stage it is found that I have indulged in plagiarism, then I am solely responsible for the same and the Institution is at liberty to take any disciplinary action against me including cancellation of dissertation or any other penalties imposed by the University.

Date:

Place: Belagavi

Mr. Satveer Jagwani
Full time Ph.D Research Scholar
Reg.No:DO12140018
KAHER, Belagavi-590010.

PLAGIARISM REPORT

KLE ACADEMY OF HIGHER EDUCATION AND RESEARCH
(Formerly known as KLE University)
(Deemed-to-be-University established u/s 3 of the UGC Act, 1956)
Accredited 'A' Grade by NAAC (2nd Cycle) Placed in Category 'A' by MHRD (GoI)
JNMC Campus, Nehru Nagar, Belagavi-590 010, Karnataka State, India
☎: 0831-2444444 FAX: 0831-2493777 Web: http://www.kledeemeduniversity.edu.in E-mail: info@kledeemeduniversity.edu.in

Ref. No. KAHER/AA/20-21/D-001 16th June 2020

Sir,

The soft copy of Ph.D. research thesis of **Mr. Satveer Jagwani, Faculty of Pharmacy** of KAHER, Belagavi has been submitted for anti-plagiarism check at the office of the undersigned through "Turn-it-in" package. The scan has been carried out and the scanned output reveals a match percentage of **8%** which is within the acceptable limit of 10%.

To obtain the comprehensive report of the plagiarism test, research scholar can send a mail to **diracademic@kledeemeduniversity.edu.in** along with the Registration Number, Name of the Scholar, Name of Guide/Co-guide and title of the thesis.

Daksha

(Dr.) Daksha Dixit)
Director, Academic Affairs

DIRECTOR Deemed-to-be University ACADEMIC AFFAIRS

To,

Mr. Satveer Jagwani
Full-Time Ph.D. Scholar,
2014-15 Batch
Faculty of Pharmacy, KAHER,
Belagavi.

Cc to :

1. The Principal, College of Pharmacy, Belagavi.
2. Dr. S. S. Jalalpure. Professor, College of Pharmacy, Belagavi- Guide

KLE ACADEMY OF HIGHER EDUCATION AND RESEARCH

(Deemed-to-be-University)

[Declared as Deemed-to-be-University u/s3 of the UGC Act, 1956 vide Govt. of India Notification No.F.9-19/2000-U.3 (A)]

Accredited 'A' Grade by NAAC (2nd Cycle)

Placed in Category 'A' by MHRD (GoI)

Copyright Declaration

We hereby declare that **KLE ACADEMY OF HIGHER EDUCATIONAND RESEARCH, BELAGAVI, KARNATAKA,** *shall have the rights to preserve, use and disseminate this thesis in print or electronic format for academic/research purpose.*

Signature

Mr. Satveer Jagwani
Full time Ph.D Research Scholar
Reg.No:DO12140018

KAHER, Belagavi-590010.

Place: Belagavi

Date:

Signature Guide

Prof. (Dr.) Sunil Jalalpure

Principal, KLE College of Pharmacy, KAHER, Belagavi-590010.

Place: Belagavi

Date:

KLE ACADEMY OF HIGHER EDUCATION AND RESEARCH

(Deemed-to-be-University)

[Declared as Deemed-to-be-University u/s3 of the UGC Act, 1956 vide Govt. of India Notification No.F.9-19/2000-U.3 (A)]

Accredited 'A' Grade by NAAC (2nd Cycle)

Placed in Category 'A' by MHRD (GoI)

KLE
EMPOWERING PROFESSIONALS

Declaration

I hereby declare that the thesis entitled **"Evaluation of the chemotherapeutic potential of resveratrol entrapped nanoliposomes for targeting hepatocellular carcinoma"** *is a bonafide and original research carried out by me under the guidance of* **Dr. Sunil Satyappa Jalalpure,** *Deputy Director, Dr. Prabhakar Kore Basic Science Research Center, Principal, KLE College of Pharmacy, Belagavi- 590010. The thesis or any part thereof has not formed the basis for the award of any degree/fellowship or similar title to any candidate of any University.*

Place: Belagavi

Date:

Signature

Mr. Satveer Jagwani

Full time Ph.D Research Scholar

Registration No: DO12140018

KLE ACADEMY OF HIGHER EDUCATION AND RESEARCH

(Deemed-to-be-University)

[Declared as Deemed-to-be-University u/s3 of the UGC Act, 1956 vide Govt. of India Notification No.F.9-19/2000-U.3 (A)]

Accredited 'A' Grade by NAAC (2nd Cycle)

Placed in Category 'A' by MHRD (GoI)

Certificate

This is to certify that the thesis entitled **"Evaluation of the chemotherapeutic potential of resveratrol entrapped nanoliposomes for targeting hepatocellular carcinoma"** *is a bonafide record of original research carried out by* **Mr. Satveer Jagwani** *under the guidance of* **Prof. (Dr.) Sunil Satyappa Jalalpure,** *Deputy Director, Dr. Prabhakar Kore Basic Science Research Center, Principal, KLE College of Pharmacy, Belagavi-590010.*

Place: Belagavi

Date:

Signature

Prof. (Dr.) M. S. Ganachari

Dean, Faculty of Pharmacy

KAHER, Belagavi – 590010.

KLE ACADEMY OF HIGHER EDUCATION AND RESEARCH

(Deemed-to-be-University)

[Declared as Deemed-to-be-University u/s3 of the UGC Act, 1956 vide Govt. of India Notification No.F.9-19/2000-U.3 (A)]

Accredited 'A' Grade by NAAC (2nd Cycle)

Placed in Category 'A' by MHRD (GoI)

Certificate

This is to certify that the thesis entitled **"Evaluation of the chemotherapeutic potential of resveratrol entrapped nanoliposomes for targeting hepatocellular carcinoma"** *is a bonafide record of original research carried out by* **Mr. Satveer Jagwani** *under the guidance of* **Prof. (Dr.) Sunil Satyappa Jalalpure,** *Deputy Director, Dr. Prabhakar Kore Basic Science Research Center, Principal, KLE College of Pharmacy, Belagavi-590010.*

Place: Belagavi

Date:

Signature

Prof. (Dr.) Sunil Jalalpure

Principal,

KLE College of Pharmacy

KAHER, Belagavi - 590010

KLE ACADEMY OF HIGHER EDUCATION AND RESEARCH

(Deemed-to-be-University)

[Declared as Deemed-to-be-University u/s3 of the UGC Act, 1956 vide Govt. of India Notification No.F.9-19/2000-U.3 (A)]

Accredited 'A' Grade by NAAC (2nd Cycle)

Placed in Category 'A' by MHRD (GoI)

Certificate

This is to certify that the thesis entitled **"Evaluation of the chemotherapeutic potential of resveratrol entrapped nanoliposomes for targeting hepatocellular carcinoma"** *is a bonafide record of original research carried out by* **Mr. Satveer Jagwani** *for the award of degree of DOCTOR OF PHILOSOPHY IN FACULTY OF* ***Pharmacy*** *under my supervision and guidance.*

Place: Belagavi

Date:

Signature Guide

Prof. (Dr.) Sunil Jalalpure

Principal, KLE College of Pharmacy,

Belagavi, KAHER, Belagavi-590010.

ACKNOWLEDGEMENT

This Ph.D. thesis is the result of a challenging journey, upon which many people have contributed and given their support. At this moment of accomplishment, I wish to express my sincere acknowledgements to many people those who have contributed to this thesis work and supported me in one way or the other during this amazing journey.

Foremost, I would like to express my deep sense of gratitude and heartfelt thanks to my research advisor, Respected Dr. Sunil Satyappa Jalalpure, for his constant guidance and co-operation not only during my study but also during my entire course. He presented me with the opportunity to explore new fields in the area of drug delivery system. His expertise and support helped me throughout my research and writing of this thesis. I could not have imagined having a better advisor and mentor for my Ph.D study.

This project was completed with the continuous support of my senior, Dr. Kiran Jadhav and Dr. Dinesh Dhamecha who helped me throughout the research work. Thanks to them for their extended guidance.

I whole heartedly thank to all my close friends Dr. Shilpa Agrawal, Dr. Rajeshwari HR, Dr. Shabana Shaikh, Dr. Shruti Murthy, Ms. Dhanashree Patil, Mr. Vishal Jakati and Ms. Neha Bulchandani for everlasting support and help during my Ph.D. work.

Humble Pranams to our Honorable former Vice Chancellor, Prof. (Dr.) Chandrakant K. Kokate Sir, respected Vice Chancellor Prof. (Dr.) Vivek A. Saoji and respected Ph.D. expert committee, Dr. P.A. Patil, Dr. B.S. Kodkany, Dr. Alka Kale, and Dr. Subarna Roy for their constructive criticism which helped for the successful completion of my research.

I would extend my acknowledgement to the Dean Dr. M. S. Ganachari and Vive Principal Dr. Mrityunjaya B Patil, KLE College of Pharmacy, Belagavi for their support during my course of Ph.D.

I appreciate the generous support from the KLE Academy of Higher Education and Research, Belagavi for funding my research and my deep sense of gratitude to entire staffs at KLE College of Pharmacy, Belagavi and Dr. Prabhakar Kore Basic Science Research Center for providing all necessary support required during the course of study.

I owe my warmest and humble thanks to Dr. Daksha Dixit - Director of Academic Affairs, KLE Academy of Higher Education and Research for her untiring support and co-operation.

I would like to express my heartfelt appreciation to Prof. (Dr.) Ramesh Chavan, HOD and Mr. Shivanand G. Hiremath, Junior Laboratory technician, Department of Pathology, J. N. Medical College, Belagavi, for helping me in histopathology studies.

I take this opportunity to genuinely acknowledge my seniors and colleagues, who guided and supported me from the early days of my research. Dr. Nitin P Ambhore, Dr. Mukund M Gade, Dr. Bindiya Chauhan, Dr. Vinyas M, Dr. Satish Hedge, Dr. Suneel Dodamani, Mr. Bhaskar, Ms. Vineeta Dhyani, Ms. Damita Cota, Dr. Nagaraj Nannapaneni, Dr. Sudhirgouda Patil, Dr. Sameer Haveri, Dr. Tejas Shah, Dr. Sushant Shengule and Dr. Ritiha Patil for being a constant support during my research.

Special thanks to Sami Labs, Bangalore, India and Lipoid GmbH, Ludwigshafen, Germany for providing the gift sample of Resveratrol and Lipids for my research work.

I am indebted to all my family members and friends for providing me the strength and enthusiasm to reach my goals.

Above all, I thank the Lord Almighty, the author of knowledge and wisdom, for his countless grace and love.

Date: **Mr. Satveer Jagwani**

Place: Belagavi

Table of contents

List of abbreviations

AASLD: American association for the study of liver diseases

ACN: Acetonitrile

AFP: Alpha fetoprotein

ALP: Alkaline phosphatase

ALT: Alanine transaminase

ANOVA: Analysis of variance

AST: Aspartate transaminase

AUC: Area under curve

BCLC: Barcelona clinic liver cancer

bcl: B-cell lymphoma

BL: Blank liposomes

BUN: Blood urea nitrogen

Chol: Cholesterol

CL: Coumarin6 loaded liposomes

CLSM: Confocal laser scanning microscope

cm: Centimeter

CO_2: Carbon dioxide

C6: Coumarin 6

DAPI: 4', 6-diamidino-2-phenylindole

DDS: Drug delivery system

DMEM: Dulbecco's Modified Eagle's medium

DMSO: Dimethyl sulphoxide

DSC: Differential scanning calorimetry

EE: Entrapment efficiency

EPR: enhanced permeation and retention

FBS: Fetal bovine serum

FT-IR: Fourier Transform infrared spectroscopy

g: Gram

GGT: Gamma glutamyl transpeptidase

HCC: Hepatocellular carcinoma

HepG2: Hepatoma G2

IC_{50}: Half maximal inhibitory concentration

ICH: International Council for Harmonization

KBr: Potassium bromide

LOD: Limit of detection

LOQ: Limit of quantification

L929: Normal mouse fibroblast

M: Metastatis stage

mg: Milligram

Minimum inhibitory concentration **(**MIC)

Minimum bactericidal concentration **(**MBC)

ml: Milliliter

MTT: 3-(4,5-dimethylthiazol-2-yl)-2,5-diphenyltetrazolium bromide

N: Number of theoretical plates

N: Nodal stage

NCDs: Non-communicable diseases

NDEA: N-Nitrosodiethylamine

ng: Nanogram

nm: Nanometer

ns: No significant

P: Probability

PBS: Phosphate buffer saline

PC: Phosphatidylcholine

PDI: polydispersity index

PEG: Polyethylene glycol

PEI: Percutaneous ethanol injection

pH: power of hydrogen/ povouir hydrogen

PS: Phosphatidylserine

PTA: Phosphotungustic

r^2: Correlation coefficient

RCL: Resveratrol loaded cationic liposomes

RES: Reticuloendothelial system

RFA: Radio frequency ablation

ROS: Reactive oxygen species

RP-HPLC: Reversed-phase high performance liquid chromatography

RSD: Relative standard deviation

RSV: Resveratrol

S: Slope

SA: Stearyl amine

SD: Standard deviation

SL: Soya lecithin

T: Tumor stage

T: Tailing factor

$t_{1/2}$: Half life

TACE: Transarterial chemoembolization

TDDS: Targeted drug delivery system

TEM: Transmission electron microscopy

Tf: Transferrin

TfR: Transferrin receptor

USA: United States of America

USFDA: United States Food and Drug Administration

UV spectroscopy: Ultra violet spectroscopy

VS: Vesicle size

WHO: World Health Organization

ZP: Zeta potential

µg: Microgram

µl: Microliter

µm: Micrometer

v/v: Volume by volume

w/w: Weight by weight

1L: First-line

2L: second-line

°C: Degree centigrade

%: Percentage

<: Less than

>: Greater than

List of tables

List of figures

Abstract

Background

Hepatocellular carcinoma (HCC) is one of the leading causes of cancer-related death worldwide. The destructive nature of the disease makes it difficult for clinicians to manage the condition. Hence, there is an urgent need to find new alternatives for HCC, as the role of conventional cytotoxic drugs has reached a plateau to control HCC associated mortality. Antioxidant compounds of plant origin with potential anti-tumor effect have been recognized as alternate modes in cancer treatment and chemoprevention. Resveratrol (RSV) is a model natural nonflavonoid drug known for its anti-cancer activity. However, its clinical application is limited due to its poor bioavailability.

Objectives

The current research work aims to formulate, optimize, and characterize RSV loaded cationic liposomes (RCL) for specific delivery in HCC. Hence the objectives of the study are:

1. Formulation and optimization of RCL using 3^2 factorial design.
2. Characterization of prepared RCL drug delivery system.
3. In-vitro cytotoxicity studies, cytocompatibility and cellular uptake studies of RSV and RCL.
4. In-vivo pharmacokinetic profiling and anticancer pharmacodynamic study of RSV and RCL in NDEA induced HCC bearing rats.

Methodology

The resveratrol loaded cationic liposomes (RCL) were prepared by thin film hydration method. A 3^2 factorial design was used for the optimization of the RCL using Design-Expert® software. The prepared formulations were characterized for entrapment efficiency,

vesicle size, shape and zeta potential. The optimized RCL5 formulation was subjected to in-vitro release study, in-vitro cell culture studies (cytocompatibility, cytotoxicity and cell uptake studies). In-vivo Pharmacokinetic and pharmacodynamic (prophylactic and therapeutic treatment modalities) studies of RSV and optimized RCL were performed in N-nitrosodiethylamine (NDEA carcinogen) induced HCC in rats.

Results

The optimized liposomes formulation (RCL5) was spherical with a vesicle size (VS) of 145.78 ± 9.9 nm, zeta potential (ZP) of 38.03 ± 9.12 mV, and encapsulation efficiency (EE) of 78.14 ± 8.04%. In-vitro drug release of RSV from RCL5 at pH 5.5 and 7.4 showed a faster release trend at pH 5.5 when compared to pH 7.4. Cell compatibility studies of RSV and RCL5 was evaluated against mouse fibroblast culture (L929) which showed no significant difference in cell viability, which confirms its cytocompatibility. In-vitro cytotoxicity studies in HepG2 cells demonstrated an improved anticancer activity of RCL5 in comparison with free RS. These outcomes were supported by a cell uptake study in HepG2 cells, in which RCL5 exhibited a higher uptake than free RS. Furthermore, confocal images of HepG2 cells after 3 and 5 h of incubation showed higher internalization of coumarin 6 (C6) loaded liposomes (CL) as compared to those of the free C6. Pharmacokinetic evaluation of RCL5 demonstrated increased localization of RSV in cancerous liver tissues by 3.2- and 2.2-fold increase in AUC and Cmax, respectively, when compared to those of the free RSV group. A pharmacodynamic investigation revealed a significant reduction in hepatocyte nodules in RCL5 treated animals when compared to those of free RSV. Further, on treatment with RCL5, HCC-bearing rats showed a significant decrease in the liver marker enzymes (alanine transaminase, alkaline phosphatase, aspartate transaminase, total bilirubin levels, γ-glutamyl transpeptidase, and αfetoprotein), in comparison with that of the disease control group. These findings were supported by

histopathological analysis, which demonstrated that NDEA induced detrimental effect on rat livers was successfully reversed with the treatment of RL5 formulation.

Conclusion

These results implied that delivery of RSV loaded cationic liposomes substantially controlled the severity of HCC and that they can be considered as a promising nanocarrier in the management of HCC.

Keywords: Resveratrol; cationic liposomes; hepatocellular carcinoma; cell uptake; pharmacokinetic; pharmacodynamic

1. INTRODUCTION

1.1. BACKGROUND

Non-communicable diseases (NCDs) are now responsible for the majority of worldwide deaths and cancer is anticipated to become the foremost reason of mortality and the only significant obstacle to increased life expectancy in each country of the world, in the 21st century. As per the GLOBOCAN 2018 report, cancer accounts for 20.3, 14.4, 57.3 and 7.3 percent mortality rate in Europe, USA, Asia and Africa respectively (1). Among all the cancers, hepatocellular carcinoma (HCC) is the fourth leading cause of cancer related deaths with 8.2% in the year 2018, which is approaching closer to lung cancer every year, accounting for 18.6% of total death. Given its asymptomatic nature in the early stages of the disease, most HCC cases are diagnosed at advanced stages especially in developing countries where screening processes are insufficient, which have led to total of 841,080 new cases and 781,631 deaths in the year 2018 worldwide (2).

Barcelona Clinic Liver Cancer Staging and Treatment Strategies

The Barcelona Clinic Liver Cancer (BCLC) staging system was developed by Llovet and colleagues in the late 1990s, to help stratify patients with HCC based on survival outcomes and to direct patients to the best available therapy. The classification system combines multiple variables (eg, tumor stage, liver function, performance status, cancer-related symptoms) in an algorithm and recognizes 5 stages for the disease (Figure 1). The BCLC staging system has been adopted as a standard by the American Association for the Study of Liver Diseases (AASLD) and the European Association for the Study of the Liver. Patients with very early HCC (stage 0) are candidates for tumor resection or radiofrequency ablation (Figure 1). Early-stage HCC (stage A) can

be treated with curative-intent radical therapies such as resection, liver transplantation, percutaneous ethanol injection, or radio frequency ablation. Intermediate-stage HCC (stage B) is generally treated with transarterial chemoembolization. Advanced HCC (stage C) is treated with systemic agents. End-stage HCC (stage D) patients have a survival of less than 3 months either due to poor liver functions or very advanced HCC and may benefit from palliative care. Patients who fail or are not eligible for a certain treatment modality should be offered an alternative option within the same stage or the next BCLC stage (3).

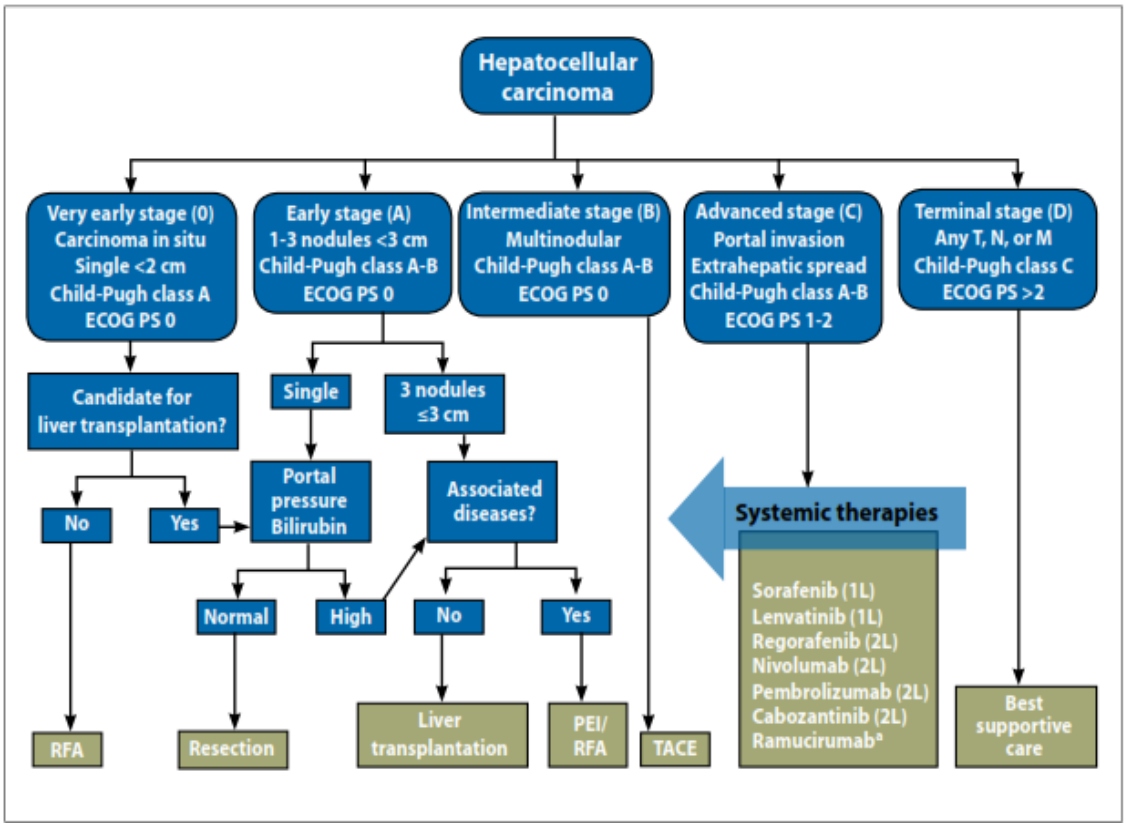

Figure 1: Barcelona Clinic Liver Cancer staging system and corresponding treatment options [adapted from ref]. first-line (1L); second-line (2L);Eastern Cooperative Oncology Group (ECOG); metastasis stage (M); nodal stage (N); percutaneous ethanol injection (PEI); performance status (PS); radiofrequency ablation (RFA); tumor stage (T); transarterial chemoembolization (TACE) [adapted from (3,4)**].**

Hepatitis B and Hepatitis C viral infections dominate as the attributable cause in a lion's share of HCC cases, but additional causes which are involved are iron overload, alcohol consumption, obesity as well as environmental and chemical carcinogens (5). Currently surgical resection and liver transplantation are considered the single curative treatment modalities, however less than twenty percent of liver cancer patients are prime invasive candidates because of hepatic decompression, multifocality, tumor size, and vascular invasion. The reappearance rates are possibly as high as fifty percent in between several years of surgery for those undertaking resection (6). Radiotherapy and conventional chemotherapy both have been found to be ineffective or less effective in severe malignancy (7). Considering the limited treatment options and negative diagnosis of liver cancer, protective control approaches and notably chemoprevention, has been measured to be the best strategy in dropping the present prevalence of the disease (8). The discovery of monoclonal antibodies has contributed greatly to open a new avenue in the management of cancers. Currently, sorafenib (Nexavar) is the only USFDA approved drug for systemic administration in the management of advanced HCC. Active efforts have been made in the past to develop similar therapies with some of the ongoing phase III trials focused on shedding light on the cancer therapy with better outcomes and minimal/no side-effects (9). Hence, HCC critically demands crucial attention to improve therapeutic strategies.

In the human body, liver is the principal detoxifying organ that helps in eliminating the metabolic byproducts/toxins to achieve homeostasis. However, the vital organ is susceptible to accumulation of reactive oxidative species (ROS) due to imbalance between pro-oxidant and antioxidant compounds. Scientific literature suggests that there is a significant co-relation between the increased levels of oxidative stress

generated by these reactive oxygen species (ROS) and the severity of chronic liver diseases. It should be noted that HCC occurs in the background of chronic liver disease, due to which it is often difficult to diagnose at an initial stage (10).

Antioxidant compounds of plant origin with potential anti-tumor effect have been recognized as an alternative mode in cancer chemoprevention. Different phytochemicals, including nutrients and dietary agents have been found to be effective against numerous types of cancers (11). Additionally, natural bioactive compounds in comparison with synthetic compounds normally have better safety profiles, are well accepted by the public (opinion) and are relatively inexpensive. However, its establishment as an active therapeutics, is hindered due to its low water solubility, weak absorption *in-vivo*, and rapid hepatic first pass metabolism (12). Among the various available groups of natural products and plant metabolites, polyphenols particularly have added wide attention as preventive agents and strong therapeutic in the management of various diseases (13).

Active Natural compound Resveratrol

Plant polyphenol resveratrol (RSV) a phytoalexin (plant antibiotic and antioxidant) found in more than seventy plant species including peanuts, grapes, pines, berries, and various herbs such as *Polygonum cuspidatum* and *Vitis vinifera L.*, plays an important role as an antioxidant (14), antitumor (15), antiaging (15), antidiabetic (16), anti-inflammatory (17), cardiotonic (17) and antiobesity (17). RSV (chemical name: 3,5,4'-trihydroxystilbene), molecular formula $C_{14}H_{12}O_3$, having low molecular weight (228.25g/mol) lipophilic compound mainly occurs in a delicate trans (*Z*)-resveratrol form, which transformed to cis (*E*) form because of isomerization under UV light exposure (Figure 2) (18). As per the definition of European Pharmacopeia, the water

solubility of RSV is 3mg/100mL having log P value of 3.1, makes it "almost insoluble" in an aqueous medium (19,20). On the topic of in-vivo evidence, direct application of RSV in the treatment of human cancer possess certain limitations owing to the rapid metabolism and swift elimination from systemic circulation resulting in low bioavailability (<1% oral viability) and low biological half-life (30-45 min) (18,21).

Since RSV is a naturally occurring compound, it has been highly studied for various inflammation-associated illnesses, containing neurodegenerative diseases, ischemic injury, cancer, and viral infections, as well as control uninvited effects of oxidative stress and significantly extend the lifespan of mammals (5). RSV appears to have multiple anti-tumor effects on different cancer by affecting cellular growth and proliferation, apoptosis, invasion, inflammation, metastasis and angiogenesis (22). Additionally, RSV has been widely envisioned as therapeutic molecule, and proven as an effective chemopreventive and chemotherapeutic agent against human cancer (23).

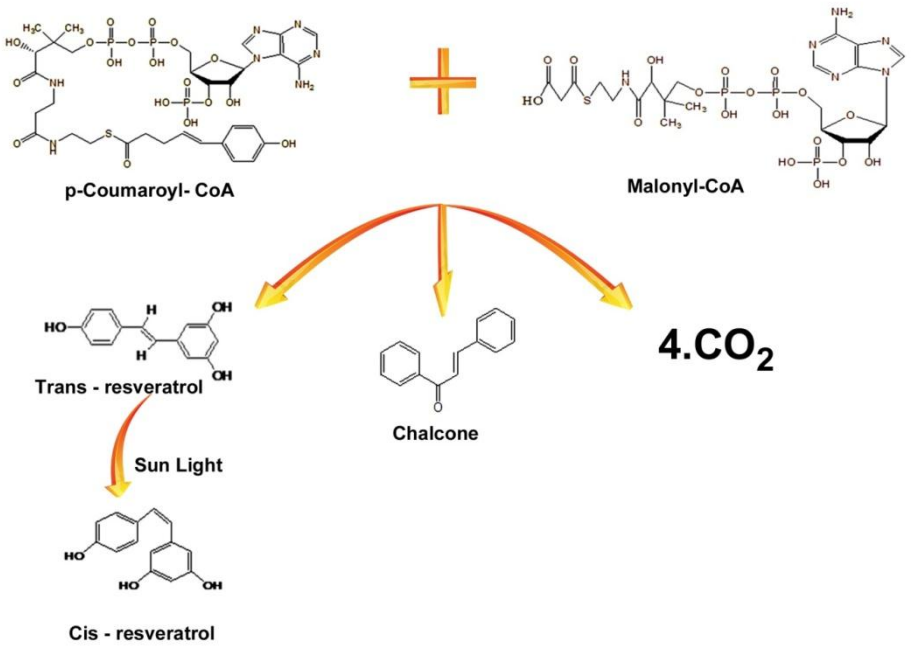

Figure 2: Synthesis of trans-resveratrol, Carbon dioxide (CO_2)

Drug delivery systems (DDS)

DDS is an interesting field of pharmaceutical research which mainly encompasses the process of releasing the drug/pay loads at the specified cite and at a specific rate. Current advances have proved multimodal capabilities of targeted drug delivery systems (TDDS), which offers improved therapeutic efficacy and reduce drug toxicity. The breakthrough potential of nanoparticle delivery systems attracts the attention of pharmaceutical industry to expand commercial drug markets. By encapsulating the therapeutic entity inside a TDDS serves various advantages (24,25) like:

1. Improved patience compliance
2. Improved product shelf life
3. Reduced costing
4. Reduced drug toxicity and
5. Better therapeutic efficacy

Therefore, developments of techniques which are focused on TDDS are on rise in the present pharmaceutical drug delivery research. Emergence of nanotechnology in the field of drug delivery is well known for its potential to effectively deliver multiple therapeutic agents at targeted diseased tissue and proved for its improved therapeutic and diagnostic potential.

Nanocarrier in drug delivery systems:

Nanocarriers are solid, colloidal particles with a size in the range of 10-1000 nm. These are well appreciated for their application in various sectors and specifically healthcare system where it increasing and replacing conventional systems (25).

Various nanocarrier involved in drug delivery systems represented in figure 3 are mentioned below.

1. Polymeric nanoparticles
2. Dendrimers
3. Liposomes
4. Inorganic/metallic nanoparticles
5. Hybrid nanoparticles
6. Micelles
7. Magnetic and bacterial nanoparticles
8. Solid lipid nanoparticles
9. Self nanoemulsifying drug delivery system

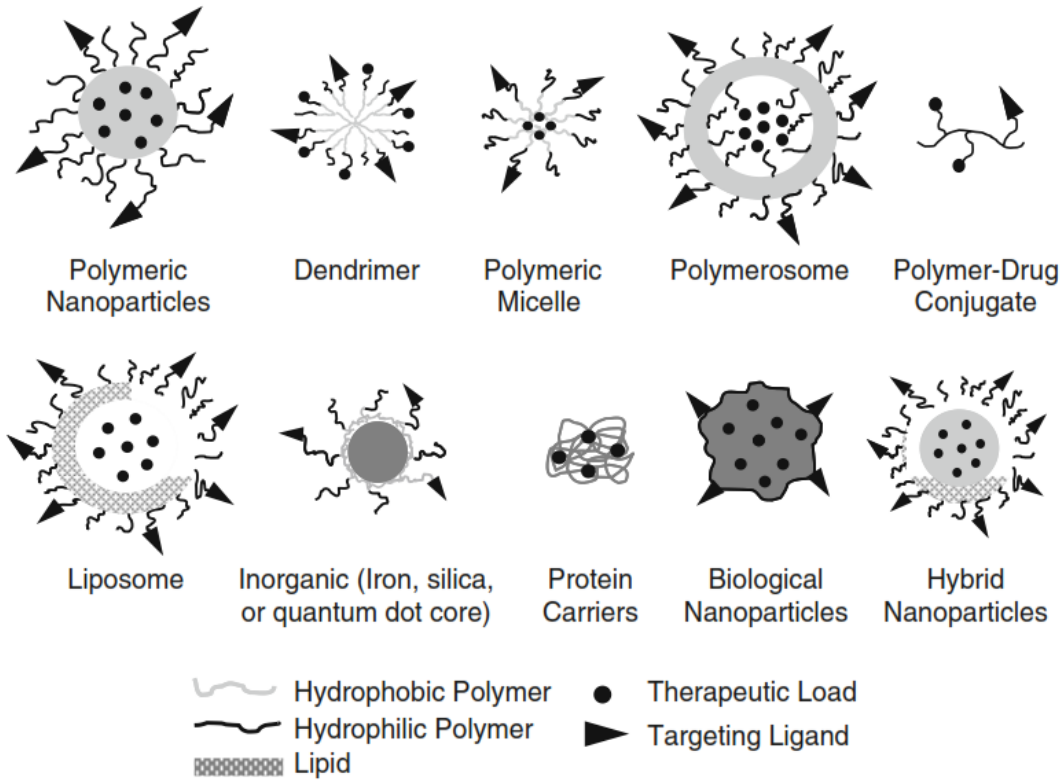

Figure 3: Typical representation of various types of nanocarrier for drug delivery [adapted from (25)].

Benefits of nanocarrier drug delivery system (DDS):

1. Improves the aqueous solubility of drug
2. Imparts protection to drug from photo degradation, acidic environment, etc.
3. Provides sustained release of the drug
4. Improves the bioavailability of drug
5. Improved targeting ability of the drug (active or passive targeting)
6. Reduction in side effects of the drug
7. Offer appropriate choices for various routes of drug administration
8. Allows rapid formulation and development of drugs.

Liposomes

Lipid vesicles were the first Nanoscale DDS, defined in the 1960s and later turned out to be famous as liposomes (Bangham et al. 1965). Ability to incorporate different substances and having fundamental feature to mimic the biological cellular membranes make liposomes to be a model DDS (26).

Liposomes formation of bilayer in continuous parallel packing is grounded on hydrophobic interactions in which hydrophilic head groups located in the direction of the aqueous atmosphere (Figure 4). The architecture of liposomes strengthen due to the Vander Waals forces and hydrogen bonds. Wherein, Vander Waals force organized the hydrocarbon chain and hydrogen bond creates the interaction between the polar heads of lipids in the aqueous environment which makes the stable organization of liposomes.

In addition, liposome vesicles have the capability to entrap the hydrophilic drug molecules in the internal aqueous phase whereas hydrophobic molecules can be entrapped between the lipid bilayer which is called as hydrophobic domains (27). Physical-chemical properties of liposome vesicles can be altered by controlling

functionality, size and surface charge by simply adding of different lipid molecules which are commercially available. Liposomes proposed a notable benefit among other nanocarriers carriers that involve much more chemical modifications and controlled synthesis (27).

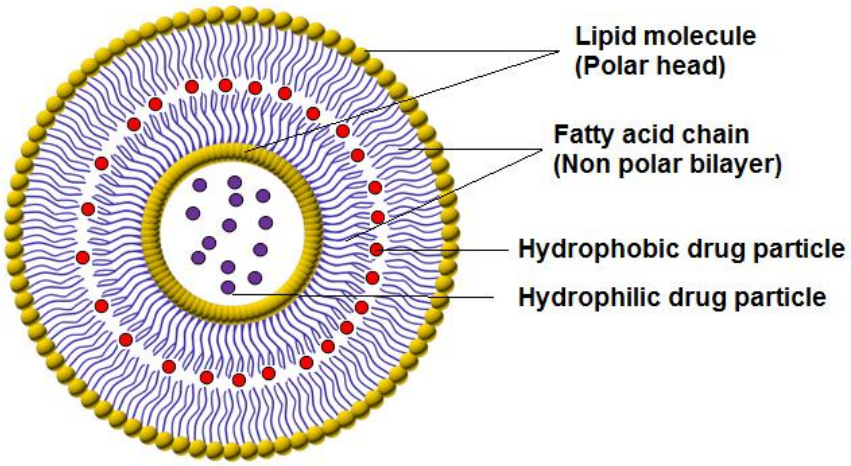

Figure 4: A representative scheme of Liposomes

As a DDS, liposomes offer various advantages comprising ability to encapsulate large drug payloads, capacity of self-assembly, biocompatibility, protecting the encapsulated agents from metabolic processes, increased efficacy and therapeutic index by improving its pharmacokinetics effect (28).

Injectable DDS application in cancer therapy has witnessed significant advances in the last decade. These approaches comprise the use of different nanoparticles and liposomes as biological carriers and drug conjugates. In the field of nanomedicine, the design of site specific nano-scaled devices and their cellular targets interactions are rapidly evolving. Typical classes of nanomedicine like liposomes are currently prepared using different approaches at the nanosize range. Doxil was the first

doxorubicin liposomes formulated by using polyethylene glycol (PEG) approved by USFDA, whereas Ambisome was produced for the fungal infection treatment (29).

Types of liposomal drug delivery

In general, liposomal DDS are having four key types—conventional liposomes, sterically-stabilized liposomes, ligand-targeted liposomes, and a combination of the above (Figure 5). Conventional liposomes were the 1st generation of liposomes to be developed. Liposomes comprise of a lipid bilayer that can be composed of neutral (phospho) lipids, cationic or anionic lipid, and cholesterol, which surrounds an aqueous volume (Figure 5A).

Conventional liposomes have the ability to decrease the in-vivo toxicity of loaded compounds, by the way of altering pharmacokinetics and improve the targetability to diseased tissue relative to free drug. However, the delivery have many problems including fast drug release, insufficient drug loading and prone to swift elimination from the bloodstream, thereby limiting its therapeutic efficacy (28).

This shorter circulation in the blood was owing to opsonization of liposomes by plasma protein and enhanced uptake by RES system macrophages, mainly in the liver and spleen (26). To enhance the circulation time in the blood and stability of liposomes, sterically-stabilized liposomes has been explored. PEGylation with hydrophilic polymer, polyethylene glycol (PEG), helps to obtained sterically-stabilized liposomes (Figure 5B). Steric barrier formation enhances the potency of loaded drugs and helps liposomes escape the RES. This not only reduces the side effects of the drug but also providing accumulation at pathological sites (28). Ligand-targeted smart liposomes propose a huge potential for *in-vivo* delivery of therapeutic molecule to the actively target sites (cell type or organs), which are specific ligands over-express on cells (e.g., receptors or cell adhesion molecules) at disease site (24).

Glycoproteins, monoclonal antibodies, carbohydrates, antibody fragments, peptides/proteins, and vitamins, are usually grafted on the liposome to actively target the cancer site (Figure 5C) (28). The inadequate *in-vivo* results of immune liposomes, owing to its low pharmacokinetics and immunogenicity, liposomes of newer generation have developed a blend of the above formulated design to expand liposomal targeting which involves ligand mediated active targeting, triggered release in response to various stimulations. Overall as a DDS, liposomes propose a dynamic and versatile technology for improving the therapeutics efficacy of drugs in various diseases.

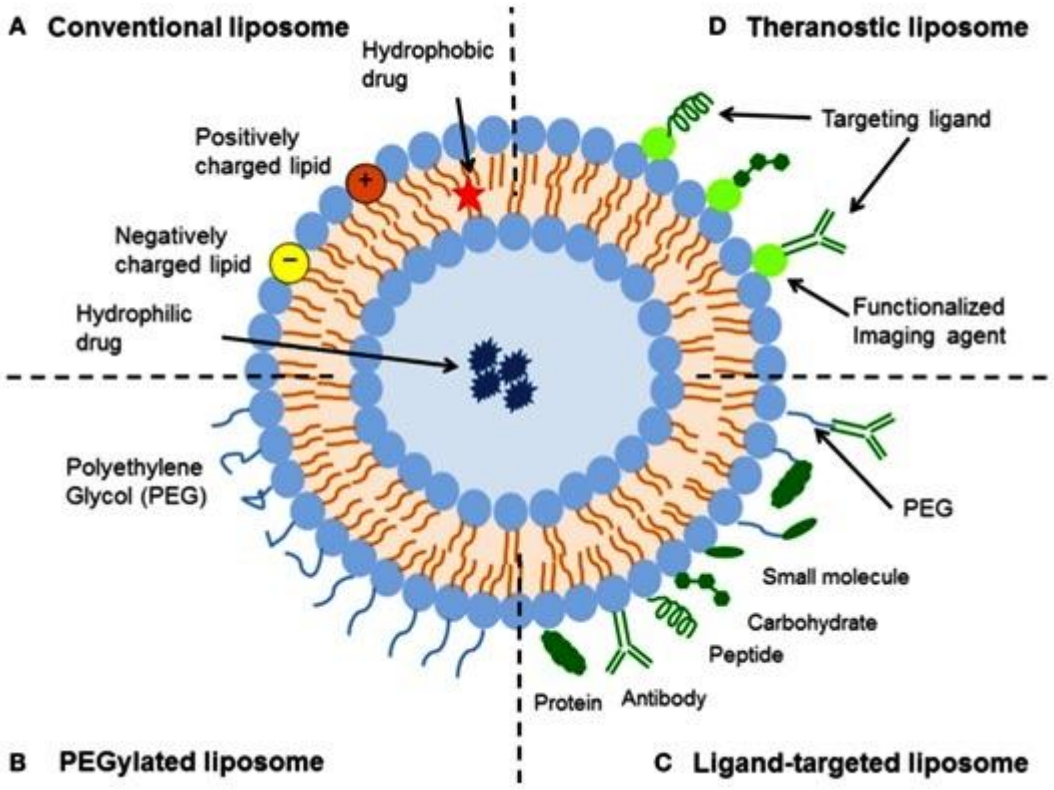

Figure 5: Diagrammatic representation of the different types of liposomal drug delivery systems, adapted with permission (28)**, under CC By 4.0 license .**

The density and nature of the charge on the liposomes surface significantly altered the mechanism and interaction of liposomes with cells. Through altering the composition of lipid, both of these parameters can be amended. Charge components can be included in the liposomes that confer the gross neutral, positive or negative charge. Dearth of surface charge on liposomes (neutral liposomes) shows lack of physical stability and increases the aggregation of liposomes. Additionally, liposomes having neutral charge resulted in less cell interaction which could be the reason for fast drug release in the extracellular space from the liposomes (26). Conversely, compared with neutral liposomes, charged liposomes present several advantages. For example, charge containing liposomes generates the zeta potential either positive or negative resulted in repulsion and avoids aggregation. Felgner et al. in 1987, first described the cationic liposomes for gene delivery, based on the electrostatics between positively charged lipids and negatively charged nucleic acids (30). Carrier system like cationic liposomes are used for the anticancer agents delivery to tumor endothelial cell by interacting with anionic molecules, like proteoglycans anionic phospholipids, and glycoproteins, in the tumor microvasculature (26). Physiological difference between cancer and normal tissue can however be manipulated to improve selective drug delivery in cancer cells based on vascular endothelial pores, heterogeneous blood supply and heterogeneous architecture for successful cancer treatment. It leads to prolonged retention of the drug in tumor mass and thereby limits the severe side effects on normal tissues (31). Anionic phospholipid; mainly phosphatidylserine (PS) is presented on the external surface of viable vascular endothelial cells in tumors, probably due to oxidative stress in the tumor microenvironment (32). These exposed anionic moieties become an easy target and attract cationic liposomes for targeting of liposomes (Figure 6B).

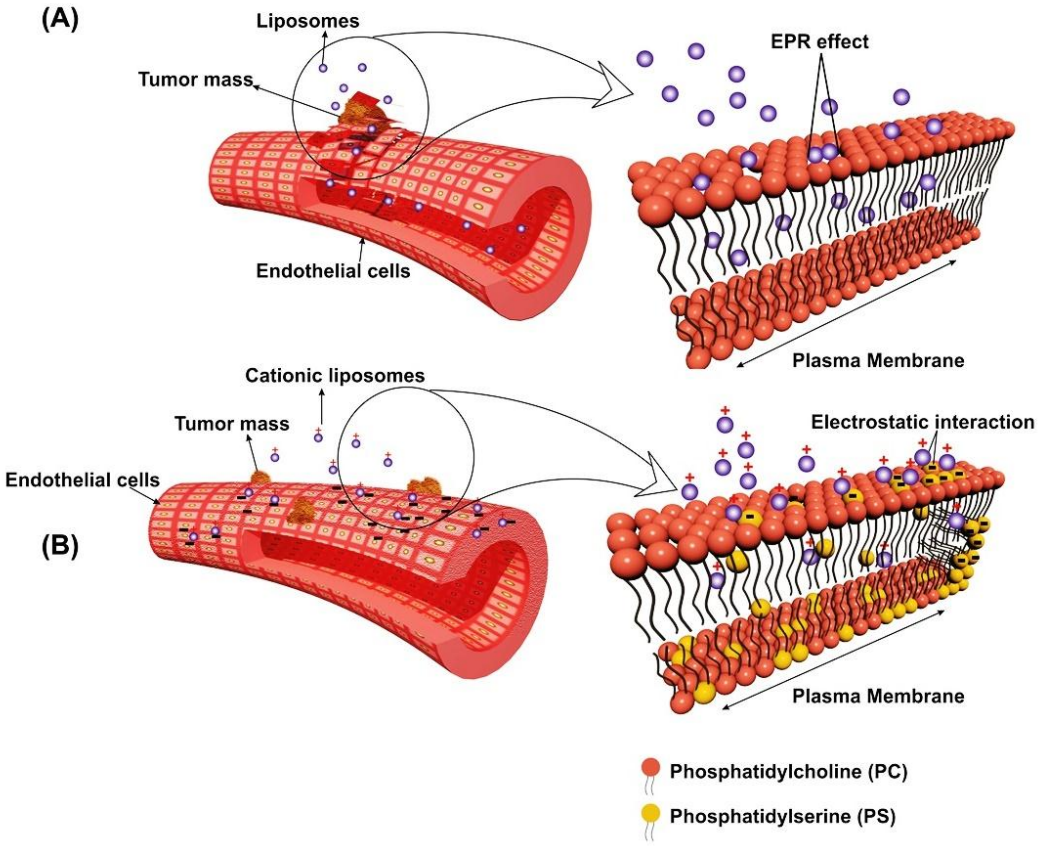

Figure 6: Schematic figure depicting the accumulation of cationic liposomes in tumor microenvironment.

Liposomal targeting to tumors

Two main strategies of liposomes for targeting tumor sites are spontaneous/passive and active targeting via functionalized liposomes to identify several overexpressed biomarkers on cells, and triggered release of a therapeutic payload on local stimuli (33).

Passive targeting

The normal endothelium having a gap size of 5-10 nm between the cells, whereas depending on the cancer type it ranges from 100 - 780 nm in tumor capillaries. Owing to this leaky nature, nanosized and biomacromolecules DDS easily get passed through the tumor-associated blood vessels, and ingress into the interstitial space

(Figure 6A). Lack of sufficient lymphatic drainage in the solid tumors, macromolecules and nanoparticles will get accumulated in the tumor microenvironment. Systemic circulation of the liposome for a longer period allows its prolonging interaction with the target (33). Coating of the liposomes with polymers such as PEG enhances its circulation in blood and protects them from recognition by the RES. To produce the `steric stabilization' effect, liposomes surface was coated with PEG. This hydrophilic layer coating of liposomes avoids its aggregation and interaction with the blood components (34). Thus, attaching of polymers like PEG onto the surface of liposomes resulted in prolongs blood circulation and decreases it uptake by mononuclear phagocytic system cells (macrophages) (33).

Active targeting

In order to reduce the off-target effects actively targeted liposomes are designed. These are prepared by conjugating with monoclonal antibodies, small molecule ligands, aptamers, and peptides on the surface of liposomes. After accumulation of the liposomes in the tumor microenvironment it gets endocytosed due to its attraction with cell specific receptor (Figure 7) (33).

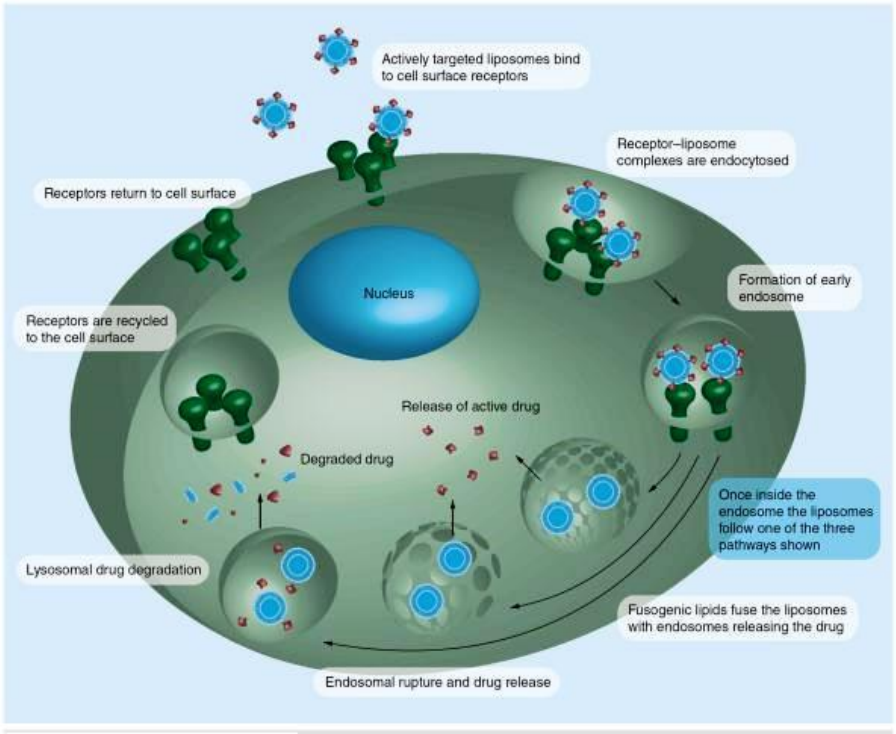

Figure 7: Surface receptor mediated endocytosis [adapted from (33)**].**

1.2 REVIEW OF LITERATURE

According to the WHO, cancer is the 2nd foremost cause of mortality globally, with practically 9.5 million cancer-related deaths stated in 2018. Among cancers, HCC accounting 781,631 deaths in the year 2018 globally (3). Conventional cytotoxic drugs have reached a plateau to control this mortality rate in this life-threatening disease. The ongoing efforts with immunotherapy are promising but still needs further evidence to prove their effectiveness in HCC. Further, the asymptomatic nature of the disease makes it very difficult for the clinicians to manage the disease (35).

Dietary polyphenols have been reported to hold anti-cancer and anti proliferative effect on malignancies including HCC (36). In this context, RSV has emerged as the lead promising molecule. Multiple in-vitro anticancer studies of RSV on Hep G2, Hep 3B and Huh-7 cells demonstrated the inhibition of cell proliferation, cell cycle arrest

and apoptosis via up-regulated p21/WAF1 expression and down-regulated the expression of cyclin E, cyclin A, and cyclin-dependent kinase 2 (37).

Bishayee et al., (2009) first time evaluated the inhibitory effect of RSV using a two-stage model of rat hepatocarcinogenisis in Sprague-Dawley rats. They observed a dose dependent suppressive effect of RSV on hepatocarcinogenesis by decreasing the incidence, total number and multiplicity of visible hepatocyte nodules. Immunohistochemical results indicated the increase in apoptotic cells and decrease in cell proliferation in the RSV-supplemented rats livers. Up regulation in the pro-apoptotic protein Bax expression, and down regulation in the expression of anti-apoptotic Bcl-2 was suggested as the possible mechanism through which RSV exerts its action. The authors suggested that additional studies on the effect of RSV on other signaling pathways xenobiotic metabolism systems are needed to confirm the anti-HCC activity (38). **Pangeni et al., (2014)** extensively reviewed the therapeutic properties of RSV reported in the literature. They also discussed about the limitations such as poor water solubility, low stability, high photosensitivity and low bioavailability which restricted its application in-vivo. Authors suggested to prevail to these limitations of RSV by using different novel drug delivery system approaches have been formulated to bring this potential candidate to the first line of disease treatment. Further new strategies to improve the bioavailability should be researched and subjected to clinical trail to approve the usefulness (22). **Le Bu et al., (2013)** formulated RSV loaded chitosan nanoparticles with the surface modified by biotin and avidin to improve the physicochemical properties and investigated the targetability in HCC. Pharmacokinetic study revealed the improved RSV bioavailability and liver targeting index as compare to free drug solution. Moreover, cytotoxicity experiments indicated enhanced inhibitory rate towards HepG2 cell lines

as compared to free drug. These finding proposed that biotin and avidin modified nanoparticles are promising drug delivery system for HCC treatment (39). **Bilensoy (2010)** extensively reviewed the, cationic nanosize carrier systems as a therapeutic choice for targeting tumor due to its better cell internalization and strong cellular interaction. Author suggested, cationic polymer vectors due to its electrostatic interaction with the negative charge of tumor membrane could be an option for cancer therapy. Additional studies are required to clarify the use of cationic liposomes in cancer therapy (40). **Manjarika et al., (2017)** developed novel stearylamine bearing cationic liposomes for targeting cancer. Cationic liposomes composed of phosphatidylcholine and stearyl amine were used to target the externalized phosphatidylserine, an anionic phospholipid on tumors vasculature. Authors reported the induction of the apoptosis and showed anticancer effects against majority cancer cell lines owing to its strong affinity of cationic liposomes with phosphatidylserine. These findings suggested that stearyl amine bearing cationic liposomes has potential anticancer activity (31).

Though there are various reports for the use of resveratrol encapsulated liposomes in cancers such as cervical cancer (41), skin cancer (42–44), Glioblastoma (45), breast cancer (46) and prostate cancer (47). However, the efficacy of resveratrol (RSV) loaded cationic liposomes (RCL) was never assessed for its use in the treatment of HCC. Hence, the aim of the research is to develop and optimized the cationic liposomes on the ground of ZP, VS and EE(%) . The potential of optimized formulation was assessed with in-vitro cellular uptake, cytotoxicity assay, cytocompatibility, in-vivo pharmacokinetic profile and pharmacodynamic study in NDEA induced HCC bearing rats.

1.3 JUSTIFICATION

Hepatocellular carcinoma (HCC) is the fourth leading cause of cancer-related death accounting for mortality of 8.2% in the year 2018, which is approaching closer to lung cancer every year, accounting for 18.6% of total death. Given its asymptomatic nature in the early stages of the disease, most HCC cases are diagnosed at advanced stages, which has led to total of 841,080 new cases and 781,631 deaths in the year 2018 worldwide. Hence, HCC critically demands crucial attention to improve therapeutic strategies. Currently, HCC is treated with invasive surgical and chemotherapeutical approaches, which often leads to serious side effects such as hand–foot syndrome, gastrointestinal, skin and endocrine disorders. Furthermore, these conventional approaches have not been successful in reducing the overall mortality rate. The discovery of monoclonal antibodies has contributed greatly to open a new avenue in the management of cancers. Currently, sorafenib (Nexavar) is the only USFDA approved drug for systemic administration in the management of advanced HCC. Active efforts have been made in the past to develop similar therapies with some of the ongoing phase III trials focused on shedding light on the cancer therapy with better outcomes and minimal/no side-effects.

Antioxidant compounds of plant origin with potential anti-tumor effect have been recognized as alternate modes in cancer chemoprevention. Different phytochemicals, including nutrients and dietary agents have been found to be effective against numerous types of cancers. Among the various available groups of natural products and plant metabolites, RSV a phytoalexin (plant antibiotic and antioxidant) found in peanuts, grapes, pines, berries, and various herbs such as *Polygonum cuspidatum* and *Vitis vinifera L.*, plays an important role as an

antioxidant, antitumor, antiaging, antidiabetic, anti-inflammatory, cardioprotective and antiobesity.

Looking towards the potential benefits of RSV, its use in prophylaxis and therapeutics would be of great importance in the treatment of HCC. However, direct application of RSV in the treatment of human cancer possess certain limitations owing to the rapid metabolism and swift elimination from systemic circulation resulting in low bioavailability and low biological half-life. Amid various possible approaches, liposomes nanometer scale systems are the most clinically acceptable system and provide various advantages including biocompatibility, higher stability, sustained release of drug, biodegradability and safety. Due to their unique properties and simple manufacturing process along with the use of relatively cost effective excipients offer high level of industrial scalability and applicability for drug delivery.

Several reports confirmed the use of RSV loaded liposomes in cancer therapy. However, the applicability of the RCL in the treatment of HCC has not been described so far. In HCC, the physiological changes in the surface properties of liver tissue causes to generate large fenestration in endothelium and anionic charge due to exposed phosphatidylserine (PS). These anionic moieties are exposed to outer surface which makes it an easy target to attract cationic liposomes for active targeting of liposomes. With this background, the present study was stemmed to encapsulate RSV in a unique blend of lipid and charge generator for the formulation of cationic liposomes for selective delivery in HCC.

1.4 AIM AND OBJECTIVES

Aim

The aim of the present research was to develop, statistically optimize and evaluate the targeting potential of resveratrol loaded cationic liposomes (RCL) in the treatment of NDEA induced hepatocellular carcinoma (HCC) in rats.

Objectives

1. Analytical RP-HPLC method development and validation.
2. Formulation and optimization of RCL using 3^2 factorial design.
3. Characterization of prepared RCL drug delivery system.
4. In-vitro cytotoxicity studies, cytocompatibility and cellular uptake studies of RSV and optimized RCL.
5. In-vivo pharmacokinetic profiling and anticancer pharmacodynamic study of RSV and optimized RCL in NDEA induced HCC bearing rats.

2. Materials and Method

Table 1: List of Instruments

S.No	Instrument name	Model	Make
1	Electronic balance	AUW 220D	Shimadzu
2	Magnetic stirrer	RCT Basic	IKA
3	FTIR	IRAffinity-1S	Shimadzu
4	Differential-scanning calorimetry	DSC-60	Shimadzu
5	High-Performance Liquid Chromatography	LC-20AD Prominence	Shimadzu
6	pH meter	Cyber Scan pH 510	Eutech Instruments
7	Rotavapor	R-210	Buchi
8	Probe sonicator	Rivotek™ Ultrasonic sonicator	Riviera Glass Private Limited
9	Bath sonicator	CPX 1800 H-E	Branson
10	Inverted microscope	TCM 400	Labomed
11	Transmission electron microscope	H-7500	Hitachi
12	Zetasizer	Nano ZS	Malvern instruments
13	Homogeniser	RQT-127A	Remi Laboratory Instruments
14	confocal laser scanning microscope	Olympus FV1000	Olympus
15	Ultra-low temperature freezer	U410-86	New Brunswick
16	Freeze dryer	Alpha 1-2 LD plus	Christ
17	CO_2 incubator	Galaxy 170R	New Brunswick
18	Microtiter plate reader	Lisa Plus	Rapid Diagnostic Pvt. Ltd.
19	Micro centrifuge	Spinwin MC-02	Tarson Products Pvt. Ltd.

Table 2: List of chemicals

S.No	Chemical	Supplier
1	Resveratrol	Sami Labs Limited, Bangalore, India
2	LIPOID S 100	Lipoid GmBH, Germany
3	Ethanol absolute	SD Fine-Chem Ltd, India
4	Sodium cholate	Sigma Aldrich, USA
5	Cholesterol	Loba Chemie Pvt. Ltd. Mumbai, India.
6	Stearylamine (SA- 74750)	Sigma Aldrich, USA
7	Sodium hydroxide	Merck, India
8	Coumarin 6(442631)	Sigma Aldrich, USA
9	Mannitol	Himedia Laboratories, India
10	3-(4,5-dimethylthiazol-2-yl)-2,5-diphenyltetrazolium bromide (MTT)	Sigma Aldrich, USA
11	4',6-Diamidino-2-phenylindole (DAPI)	Sigma Aldrich, USA
12	Acetonitrile	Fisher Scientific, India
13	Methanol	Fisher Scientific, India
14	Chloroform	Fisher Scientific, India
15	Formic acid	Fisher Scientific, India
16	Paraformaldehyde	Qualigens, India
	Fetal bovine serum	HiMedia Laboratories Pvt. Ltd, India.
17	Pen strep (mixture of streptomycin and penicillin)	HiMedia Laboratories Pvt. Ltd, India.
18	Dulbecco's modified Eagle's medium (DMEM)	HiMedia Laboratories Pvt. Ltd, India.
19	Serum aspartate amino transferase (AST), serum alanine transaminase (ALT), alkaline phosphatase (ALP), total bilirubin (TB), gamma glutamyl transpeptidase (GGT)	ERBA Diagnostics Mannheim GmbH (Manufactured by Transasia Bio-Medicals Ltd., Baddi, Himachal Pradesh, India).
20	Rat alpha- fetoprotein (AFP) ELISA kit	Qayee-Biotechnology Co., Ltd (Shanghai, China)
21	HepG2 and normal mouse fibroblasts cell lines	National Centre of Cell Sciences, Pune, India.

2.1 Identification of the pure drug

2.1.1 Fourier transform infrared spectroscopy (FTIR)

The FTIR spectrum of the pure resveratrol was recorded using FTIR spectrometer (IR Affinity-1S, Shimadzu, Japan) by mixing the resveratrol thoroughly with potassium bromide (KBr) and the spectra were noted in the range of 4000 – 400 cm^{1}.

2.1.2 Melting point determination

The melting point of resveratrol was determined by using differential scanning colorimetry (DSC 823, Mettler Toledo). The sample (4−5 mg) was weighed, compressed into an aluminum pan, and scanned in the temperature range from 50 to 300 °C at a heating rate of 10 °C/min under the influence of nitrogen.

2.2 Analytical HPLC method for the estimation of RSV

The Shimadzu HPLC system (LC-20AD prominence system, Kyoto, Japan) comprising of a pump, degasser, auto sampler, diode array detector and communication bus module coupled with a Shimadzu LC solution software (version 1.25) was used to process the chromatogram. The analysis was carried out by using a reverse-phase C18 column (4.6 × 150 mm, particle size 5 µm, Phenomenex, USA) with isocratic mobile phase which was mixture of ACN: water (30:70 v/v). The flow rate was kept at 1.0 ml/min under a controlled temperature (30°C) and detection wavelength of 306 nm was used for the assay of RSV throughout the experiment. The injection volume was 10 µl and chromatographic run time was set at 12 min.

2.2.1 Preparation of standard solutions

Stock solution of 1mg/ml of RSV and carbamazepine as the internal standard (IS) were prepared by dissolving in methanol. From which six working solutions of RSV (2-12 µg/ml) and working solution of IS (20 µg/mL) were made by suitable dilution of RSV and IS solution in the mobile phase respectively. The experiments were performed in dim light to prevent the possibility of photochemical isomerization.

2.2.2 Validation studies

As per the International Council for Harmonisation (ICH) guidelines, the RP-HPLC method was developed and validated (48) for several parameters such as system suitability, linearity, precision, recovery, robustness, limit of detection (LOD) and limit of quantification (LOQ). The linearity for analytical samples were evaluated by analyzing six different concentrations (2-12 µg/ml) of RSV in triplicates. A calibration curve was attained by plotting the concentration of the RSV versus peak area. The slope, y-intercept and correlation coefficient (r^2) were calculated for defining the linearity. The intraday precision/repeatability was assessed by analyzing three different concentrations in triplicates within the same day. Intermediate/interday precision was performed by following the same method for three different days under the same experimental conditions. The % RSD of the peak area less than 2.0 % was set as acceptance criteria. Accuracy (recovery studies) was conducted by mixing known quantities of pure RSV to the pre-analysed sample and its percentage recovery was estimated by comparing the actual and measured concentrations. Percentage recovery within 80-120% and percent relative standard deviation (% RSD) less than 2% were set as acceptance criteria. Limit of detection (LOD) and quantification (LOQ) was calculated based on the SD of the y- intercept and slope (S) values (LOD = 3.3 (SD/S) and LOQ = 10(SD/S).

2.3 Preparation of resveratrol loaded liposomes

On the basis of preliminary studies, RCL was optimized by using 3^2 factorial design approach in which the molar ratio of soya lecithin: cholesterol (SL:Chol) and stearyl amine (SA) were selected as independent variables. The mean vesicle size (VS), zeta potential (ZP) and encapsulation efficiency (EE) were selected as dependent variables

(Table 3).The generated polynomial equation was used for the evaluation of the response.,

$Y = b_0 + b_1X_1 + b_2X_2 + b_{12}X_1X_2 + b_{11}X_1^2 + b_{22}X_2^2$.

Thin film hydration method was used for the preparation of RCL (49). Briefly, 20mg of RSV was dissolved with given molar ratio of SL and Chol in the mixture of organic solvent chloroform and methanol (2:1v/v). The organic solvent was evaporated on rotavapor R-210 under a reduced pressure (vacuum pump, V-700 Buchi, Switzerland) for 1 h at 40ºC to obtain a thin film. For removal of solvent traces, the film was purged with the nitrogen gas and kept in vacuum oven for overnight. For the formation of liposome vesicles, the lipid film was hydrated by using phosphate buffer (pH 6.4) as aqueous medium at 40ºC for 1 h. Formulated RCL were sonicated for 2 min (15 s on/off pulse) using a high intensity probe ultrasonic generator (Rivotek, India) having probe diameter of 15mm. Following sonication, the resulting liposome dispersion was subject for centrifugation at 4ºC for 10 min on 2000 rpm to separate the undissolved RSV. RSV loaded liposomes were then filtered five times using syringe filters (0.44 µm and 0.22µm) successively to yield monodispersed RCL. Finally, 5% w/v mannitol (cryoprotectant) was mixed to RCL dispersion and lyophilized (CHRIST Alpha 1-2 LD plus, Germany) for further studies. For lyophilization, RCL dispersion was frozen at -80 ºC for 24 hours followed by freeze drying for 48 hours. The lyophilizer was set with -55ºC as condenser temperature and 0.023 mbar as vacuum pressure. The lyophilized formulation was evaluated for the appearance of cake, reconstitution time, ZP, VS and EE (50). Liposomes containing coumarin6 (C6) (1µg/ml) were also formulated by using the similar procedure for carrying out the in-vitro qualitative cellular uptake studies.

Table 3. Factorial design (3^2) applied by using different Independent and dependent variables

Independent variables	Levels			Dependent variables
	-1	0	+1	
Molar ratio of SL and Chol	6:2	7:2	8:2	Y1= Encapsulation efficiency (EE)
Concentration of SA (mg)	2.5	5.0	7.5	Y2= Vesicle size (VS) and Y3= Zeta potential (ZP)

2.4 Characterization of RCL

2.4.1 Vesicle size (VS), size distribution (PDI), zeta potential (ZP) and vesicle morphology

Dynamic light scattering was used to measure VS, PDI and ZP of all RCL formulations and the surface morphology was examined by using a transmission electron microscopy. For TEM analysis, aqueous dispersion of RCL was stained with 1% phosphotungustic acid (PTA) and was visualized under TEM. The liposome suspension was diluted with appropriate volume of distilled water for all the measurements.

2.4.2 Entrapment efficiency (EE)

The amount of RSV inside the liposomes was determined using an indirect method, which involves measuring the amount of free drug available in nano dispersion. RCL dispersion was centrifuged (Kubota 6500, Japan) at 2000 rpm (using rotor model AG-1212) at 4°C for 10 min, and the supernatant was then separated. Pellet of unentrapped drug (free drug) was determined by using the developed HPLC method (Shimadzu, LC-20AD prominence system, Japan). Percent EE was determined as:

Percent EE= D– d / D ×100; where D: concentration of drug used for liposome formation; and d: concentration of free drug (51).

2.4.3 In-vitro drug release studies of RCL

In-vitro release of RSV from liposomes was performed by ready-to-use dialysis tubes (Spectrum Laboratories, Rancho Dominguez, CA, U.S.A.) having MWCO: 12,400 Da, pore size of <10 nm, 10 cm length with membrane diameter of 10 mm with seal at one end and attached to a floatable cap. Release studies were performed in phosphate buffer saline (PBS) (pH 7.4- to simulate pH of blood) and PBS (pH 5.5- to simulate pH of tumor micro environment) both containing 0.1 % v/v polyethylene glycol (PEG-400) to solubilize the released drug. Briefly, RCL (5 ml equivalent to 4 mg RSV) was transferred to dialysis bag, which was immersed into a 200 ml bottle containing 100 ml of PBS (pH 5.5 and 7.4). Bottles were placed on a magnetic stirrer pre-equilibrated at 37 ± 0.5 ºC with stirring speed of 100 rpm. At specific time intervals, the aliquots (0.5ml) were withdrawn and replaced with equal amount of fresh PBS. All aliquots were filtered by using a 0.45 µm syringe filter and the amount of drug released was analysed by HPLC. In order to understand the kinetics and the drug release mechanism of optimized formulation (RCL5) different kinetics models such as zero order, first order, Highuchi model, Korsemeyer-peppas model, and Hixon Crowell model were evaluated (52,53).

2.5 Freeze-drying

In order to perform the DSC and FTIR studies of optimized RCL, liposomes were lyophilized using mannitol 5% w/v as cryoprotectant. Samples were frozen using -20°C followed by -80°C freezer for 24h and then subjected to lyophilization using freeze dryer (Christ, Germany). Primary drying was performed by using standard

conditions as -55ºC as condenser temperature and 0.023 mbar as vacuum pressure and for main drying was set with -60 °C as condenser temperature and 0.0054 mbar as vacuum pressure. The dried powder was stored in a desiccator for further studies.

2.5.1 DSC

For differential scanning colorimetry (DSC) studies, dried samples of raw materials and optimized RCL were analysed by using a DSC (DSC-60, Shimadzu, Japan). Briefly, each sample (4 – 5 mg) was weighed, compressed into an aluminum pan and scanned under nitrogen atmosphere (40 ml/min) in the temperature range from 50 to 300 ºC at a heating rate of 10 ºC/min. DSC thermograms of pure RSV, lyophilized RCL, soya lecithin, stearyl amine, cholesterol and mannitol were recorded.

2.5.2 Fourier transform infrared spectroscopy (FTIR)

FTIR analysis of each chemical components of formulation and lyophilized liposomes were analyzed by using FTIR spectrophotometer. The grounded samples were mixed thoroughly with KBr and the spectrum was noted in the range of 4000 – 400 cm^{-1}.

2.5.3 Stability studies of liposomes

The stability stabilities of liposome dispersion and lyophilized formulation, different characteristics like EE, VS, and ZP were observed according to ICH guidelines at storage condition (2-8°C), for a period of 3 months (50,54).

2.6 In-vitro cell culture studies

The human liver cancer epithelial cell line ($HepG_2$) and mouse fibroblast cell lines (L929) were procured from the National Centre for Cell Sciences (NCCS), Pune, India. The cells were cultured in growth medium comprised of Dulbecco's modified Eagle's medium (DMEM) supplemented with 10% Fetal Bovine Serum (FBS) and

1% Pen step antibiotic solution and maintained under 5% CO_2 atmosphere at 37°C. The growth medium was changed on alternate day (55).

2.6.1 In-vitro Cytocompatibility assay

The cytocompatible behavior of RSV and RCL5 on normal mouse fibroblasts (L929) cell lines was assessed by using standard MTT assay. Briefly, cells were seeded at the density of 10000 cells/well in the 96 well plate and incubated for 24 h in a CO_2 incubator to allow cell adhesion. The media was discarded and swapped with fresh media with varying concentrations of RSV and RCL5 (250, 125, 62.5,31.25, 15.63 and 7.81µg/ml) equivalent to free RSV and the same amount of media without any test compound was used for control wells followed by incubation for a period of 24 h. After the completion of incubation period, the media in each well was discarded and wells were gently washed with PBS. Cells were then treated with 100 µl of MTT solution (0.5 mg/ml in phosphate buffer saline) and the plate was incubated at 37°C for 4 h. After 4 h, the supernatant was discarded and DMSO (100 µl) was added to each well to dissolve formed formazan crystals and analyzed by plate reader (Lisa plus, India) to calculate percent cell viability (56).

2.6.2 In-vitro cytotoxicity assay

RSV and RCL5 cytotoxicity against $HepG_2$ cell lines was performed as per the procedure mentioned in section 2.6.1. $HepG_2$ cell lines were incubated with RSV and RCL5 of varying concentrations (250, 125, 62.5, 31.25, 15.63 and 7.81µg/ml) equivalent to free RSV for 24 and 48h. After the completion of incubation period, percent cell viability was estimated by MTT assay method.

2.6.3 Qualitative and Quantitative cell uptake assay

For qualitative cell uptake analysis, coumarin 6 (C6) was used as a model fluorescent dye to evaluate the extent of cellular uptake of liposomes. HepG2 cells were seeded in 6-well culture plates (50 000/well) and were incubated overnight for the attachment of the cells. The efficacy of cellular uptake as a function of RCL5 was evaluated by in-vitro incubation of HepG2 cells with free C6 and C6 loaded liposomes (CLs) (equivalent to 1 μg/mL C6) for 3 and 5 h. The free C6 solution was prepared by solubilizing in 0.1% DMSO to yield a final concentration of 1 μg/mL. CLs were prepared by following the method mentioned in section 2.3 and replacing RSV with C6. After the given time of incubation of C6 and CL, the medium was aspirated and cells were washed with PBS five times, fixed with 4% paraformaldehyde (Merck), and were observed under a confocal laser scanning microscope (CLSM) (Olympus FV1000). For quantitative cell uptake analysis, HepG2 cells were treated with RSV and RCL5 (equivalent to 10 μg/mL RSV) and further incubated for 3 and 5 h to determine cell uptake over time. Media was removed, and cells were washed thrice with PBS and then lysed with 0.1% Triton X-100. Lysed cells were then extracted with ACN for the complete dissolution of internalized RSV. Finally, the cell lysate was centrifuged at 10000 rpm for 10 min and supernatant was analyzed by HPLC (57).

2.7 Animal experiments

Male Wistar rats of 220 ± 250g were supplied by the animal facility, KLE College of Pharmacy (KAHER), Belagavi, India. Protocols for all the animal studies were duly approved by the Institutional Animal Ethics Committee (KLECOP/IAEC/Res.22-10/10/2015), KAHER, India. Rats were housed in groups of 6 at 25–30 °C with a 12 h

light-dark cycle and were allowed access to pellet diet (VRK Nutritional solutions, Pune, Maharashtra, India), and water ad libitum for one week before experiments.

2.7.1 In-vivo organ toxicity studies

Biochemical parameters of hepatic and renal functions such as alanine transaminase (ALT), aspartate transaminase (AST), Blood urea nitrogen (BUN) and creatinine was assessed by commercially available diagnostic kits (Erba Diagnostics, Inc., U.S.A.). Furthermore, histopathological evaluation of liver, kidney and spleen tissues were performed after staining with hematoxylin and eosin (H&E).

2.7.2 Pharmacokinetic study

For in-vivo pharmacokinetic study, hepatocellular carcinoma (HCC) in rats was induced by using NDEA solution administered intragastrically at a dose of 10mg/kg bodyweight with the frequency of 5 times a week for 12 week (58). HCC induced animals were randomly divided in 2 groups (n=3 for each time point); and were administered with 20 mg/kg body weight of RSV and equivalent RCL5. Free RSV was solubilized in a mixture of 1% DMSO and 1% Tween-80 solution in phosphate buffer saline (PBS). Experimental rats were anesthetized and blood samples (1 mL) were collected in heparinized tubes via cardiac puncture at 15, 30, 60, and 120 min and sacrificed by cervical dislocation. Major organs such as heart, spleen, liver, lung and kidney were excised, washed twice with ringer's solution and immediately frozen until analysis. For estimation of RSV in rat plasma, blood samples were centrifuged at 4,000 rpm for 10 min at 4 ºC for plasma separation and were preserved at –20 ºC for further sample analysis. On similar lines, RSV from frozen isolated organs was estimated by using optimized RP-HPLC method. Isolated organs were weighed, minced thoroughly and homogenized (RQT – 127AD, Remi Elektrotechnik Ltd., Vasai, India) in 50% aqueous acetonitrile. Homogenized samples were centrifuged

(12,000 rpm for 12 min) and the supernatant was preserved at -20ºC for further analysis. Separated biological sample (150 µl) was vortex-mixed with 150 µl of ACN (containing IS 20 µg/mL) for deproteinization followed by centrifugation at 12,000 rpm for 12 min. Supernatants were separated, filtered through 0.22 µm membrane filter (Millipore) and finally analyzed by the HPLC system. The pharmacokinetic investigation was performed by using Kinetica software (Thermo-Scientific, USA) to estimate the parameters such as area under curve (AUC), peak plasma concentration (Cmax), half-life ($t_{1/2}$), and mean residence time (MRT).

2.7.3 Pharmacodynamics activity: prophylactic and therapeutic anti-cancer activity

Hepatocellular carcinoma was induced in male Wistar rats weighing 200-250 g by intragastric administration of NDEA at a dose of 10 mg/kg body weight 5 times a week for 12 weeks. The experimental animals were divided into six groups (Table 4) comprised of six animals in each group. Group 2 (positive control group) consisted of two more rats for the confirmation of the induction of HCC at the end of 9th week of the experiment. At 13th week, rats in each group were sacrificed and liver specimens were removed and weighed. Plasma was collected from the blood by centrifugation at 3000 rpm for 5 min at 4 °C for biochemical estimation of alanine transaminase (ALT), alkaline phosphatase (ALP), aspartate transaminase (AST), total bilirubin levels, gamma glutamyl transpeptidase (GGT) and alpha fetoprotein (AFP). After dissection, liver was isolated and the tumor nodules were counted and stored in buffered formalin for histopathological examination.

Table 4 Experimental groups used in the study to evaluate the effect of prophylactic and therapeutic treatment in HCC induced rats.

Group I (normal group)	Rats fed with standard diet and were administered with vehicle (a mixture of 1% DMSO and 1% Tween 80 in PBS) twice a week.
Group II (disease control)	NDEA (carcinogen) intragastric administration until 12th week
Prophylactic treatment	
Group III received RSV	NDEA administration until 12th week + simultaneous intraperitoneal dosing of RSV (20 mg/kg body weight/twice a week)
Group IV received RCL5	NDEA administration until 12th week + simultaneous intraperitoneal dosing of RCL5 (equivalent to RSV 20 mg/kg body weight/twice a week)
Therapeutic treatment	
Group V received RSV	NDEA administration until 12th week + intraperitoneal dosing of RSV (20 mg/kg body weight/twice a week) starting from 9th week
Group VI received RCL5	NDEA administration until 12th week + intraperitoneal dosing of RCL5 (equivalent to RSV 20 mg/kg body weight/twice a week) starting from 9th week

3. STATISTICAL ANALYSIS

The optimization the RCL formulations was accomplished using Design-Expert® software version 7.0.0. Statistical analysis of in-vitro tests was carried out by Student's t-test using Prism software version 5.1 and data was expressed as the mean standard deviation (S.D.) of the mean. (*p< 0.05, **p<0.01 and ***p< 0.001). A value of P < 0.05 was considered statistically significant and ns represent not significant. The Statistical analysis of in-vivo results were performed by using GraphPad Prism software utilizing one-way ANOVA.

4. RESULTS

4.1 Identification of RSV

4.1.1 FTIR

The infrared spectrogram of the pure RSV (figure 8) which revealed the intense absorption band of phenolic hydroxyl group at 3288 cm^{-1} and benzene ring absorption peaks of C=C at 1606 and medium absorption peak at 1514 cm^{-1}.

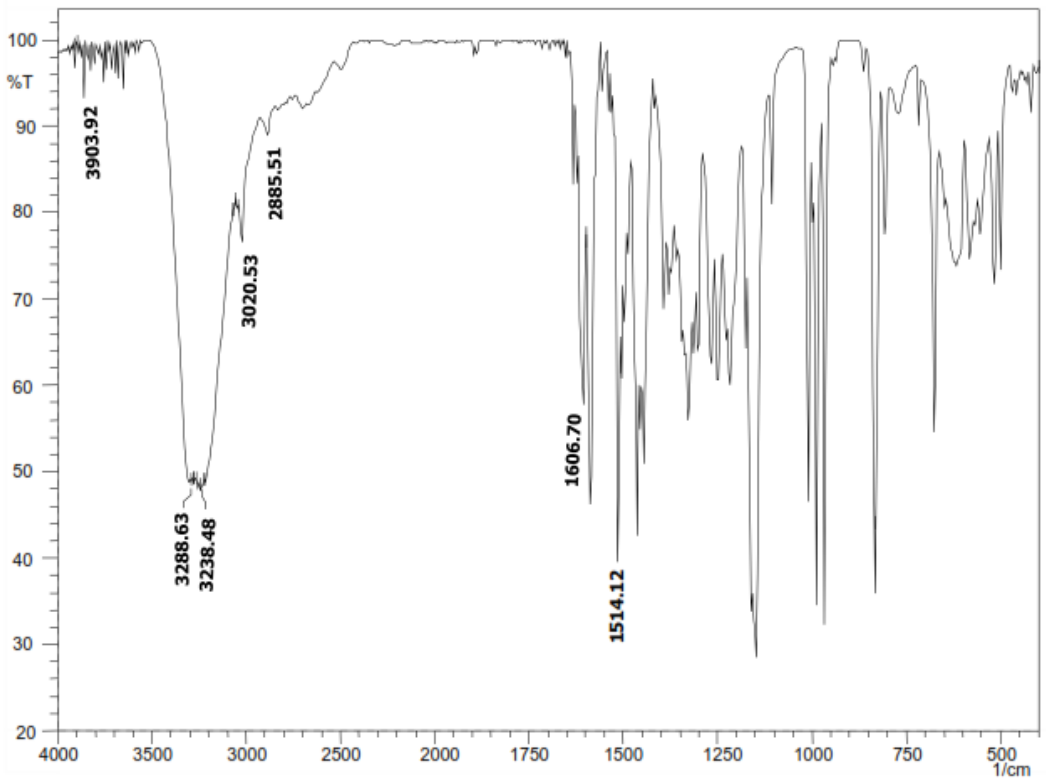

Figure 8: FTIR spectra of pure resveratrol

4.1.2 Melting point

DSC was used to determine the melting point of RSV. The DSC thermogram of RSV, shows a sharp endotherm at 256.45 °C, indicating the melting point of RSV (figure 9).

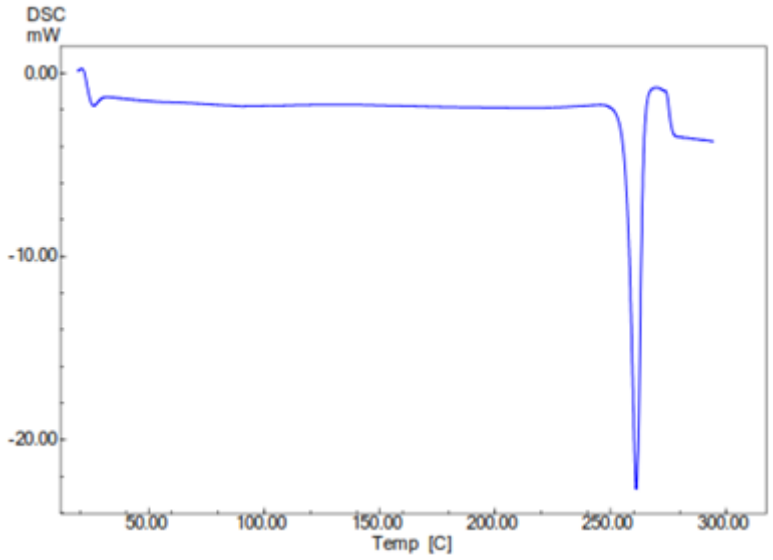

Figure 9: DSC thermogram of pure resveratrol

4.2 Analytical HPLC method for the estimation of RSV

The developed RP-HPLC method displayed the retention time of 6.1 and 11.2 min for RSV and IS respectively (Figure 10) and it was validated according to the ICH guidelines Q2 (R1) for various parameters. The system suitability parameters were found to be within the acceptance limits; tailing factor (T < 2.0), number of theoretical plates (N > 2000) and relative standard deviation of the peak area (%RSD < 2.0%). The calibration curve for RSV was linear (r^2 = 0.9999) in the concentration range of 2.0-12.0 µg/ml (Figure 10). The regression equation for calibration curve was y = 80745x – 35857. The %RSD values for both intra- and interday precision were ranged from 0.670 to 1.676. The mean percentage recovery of RSV was in the range of 97.97 and 102.80%. The LOD and LOQ values for RSV were found to be 0.008 µg/ mL and 0.024 µg/mL respectively. During the method validation the slight modifications in the flow rate, column oven temperature and mobile phase ratio has insignificant effect on the chromatographic parameters such as tailing factor (T < 2.0), %RSD of the peak area (<2.0%), and theoretical plates (N >2000).

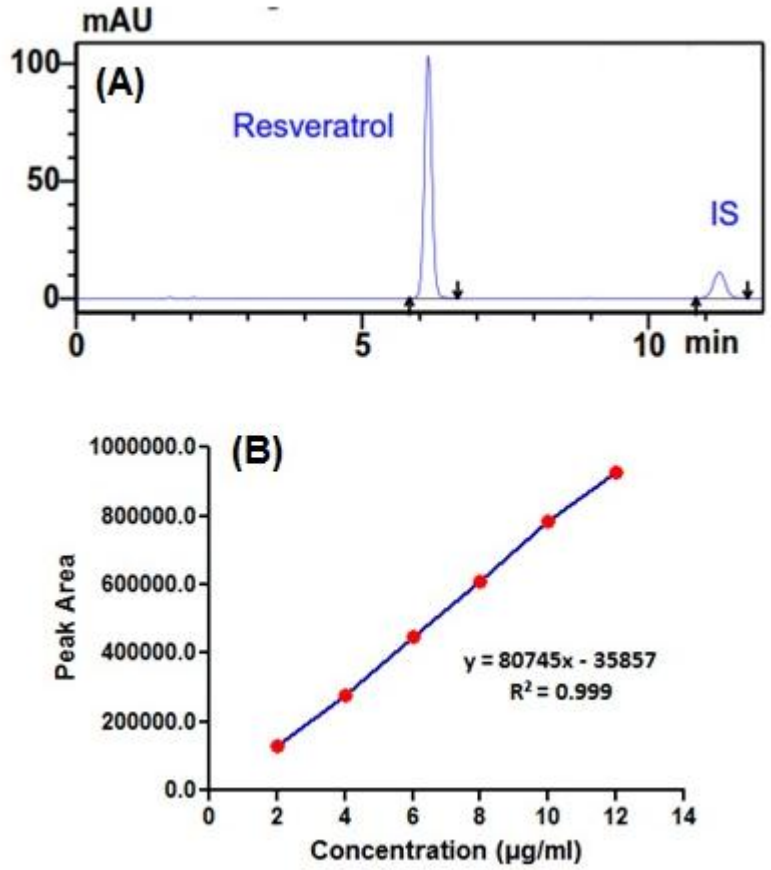

Figure 10: (A) HPLC chromatogram of resveratrol with internal standard (IS) and (B) Calibration curve of pure resveratrol.

4.3 Preparation and optimization of RCL

The resveratrol loaded liposomes was prepared by a thin film hydration method as described by Bangham et.,al (1965). The method was selected because it provides high entrapment efficiency for lipophilic drugs like RSV into liposomes. Using Design-Expert® software two-factor, 3-level (3^2) factorial design was applied to optimize the

RCL formulation. For optimization of liposomes Independent variables like (A) Molar ratio of SL: Chol (where Chol concentration is fixed on the basis of preliminary studies) and (B) concentration of stearyl amine (SA) were selected. Percent

entrapment efficiency (Y1), vesicle size (Y2), and zeta potential (Y3) were selected as the dependent variable. As per 3^2 factorial design total nine formulations were formulated and evaluated for vesicle size, % EE and zeta potential is shown in Table 5.

Table 5. The independent variables, observed responses, %EE, VS, ZP of resveratrol loaded cationic liposomes according to factorial design

Formulation code	Independent variable		Dependent variable		
	A+	B	Y1	Y2	Y3
RCL1	-1	-1	49.26 ±9.72	153.33 ±7.50	07.57 ±3.66
RCL2	-1	0	62.57±7.45	140.30 ±10.16	25.98 ±5.82
RCL3	-1	1	58.91±7.06	134.73 ±5.09	29.26 ± 7.40
RCL4	0	-1	62.76±6.17	176.43 ± 7.16	15.88 ± 4.27
RCL5	**0**	**0**	**78.14 ± 8.04**	**145.78 ± 9.9**	**38.03 ±9.12**
RCL6	0	1	65.31±5.59	138.18 ± 12.35	62.58 ± 4.13
RCL7	1	-1	63.65±4.63	187.54 ± 7.29	11.73 ±2.58
RCL8	1	0	70.74 ±5.99	152.46 ± 7.52	35.00 ± 7.04
RCL9	1	1	65.85 ±7.54	148.91 ± 7.27	56.43 ± 9.14

A: molar ratio of SL: Chol B: SA (mg) Y1: entrapment efficiency (%), Y2: vesicle size (nm) and Y3: zeta potential (ZP)

Quadratic equation represents the effect of selected independent variables on EE.

$Y1 = 75.09 + 4.92A + 2.40B – 1.86AB – 6.91A^2 –9.53B^2$,

The equation indicates that EE is directly proportional to both the independent variables A and B. The ANOVA results for the measured response are illustrated in Table 6 confirm the significance of the model from F value and P values. The Model

F-value of 10.52 suggests the model is significant ($p< 0.04$). There is only a 4.0% possibility that a "Model F-Value" this large could arise due to noise. The p-value (Prob>F) less than 0.0500 specify model terms are significant. Values greater than 0.1000 indicate the model terms are not significant.

$$Y2= 145.46 + 10.25A - 15.32B - 6.40AB -0.38A^2 + 9.92B^2,$$

The equation indicates that VS is directly proportional to A (molar ratio of SL: Chol) and the negative sign indicates inversely proportionality to B (concentration of SA).The Model F-value of 20.39 suggests the model is significant ($p< 0.016$). There is only a 1.0% possibility that a "Model F-Value" this large could arise due to noise.

$$Y3= 38.53 + 5.36\ A + 20.41B + 3.40AB -9.84A^2 + 1.05B^2$$

Based on the result, the positive sign indicates that the ZP is directly proportional to A and B. The Model F-value of 52.44 suggests the model is significant ($p< 0.004$). There is only a 0.04% possibility that a "Model F-Value" this large could arise due to noise. Surface contour plots and response curve figure 11, demonstrated the effect of the A and B on the EE, VS and ZP.

Table 6: Results of ANOVA for measured response for EE, VS and ZP

Parameters	Degree of freedom	Sum square value	Mean square value	F value	p value	R^2 value
For Y_{EE}						
Regression	5	470.40	94.08.07	10.52	0.0405	0.9460
Residual	3	26.83	8.94			
Total	8	497.23	-			
For Y_{VS}						
Regression	5	2398.79	479.76	20.39	0.016	0.9714
Residual	3	70.6	23.53			
Total	8	2469.39	-			
For Y_{ZP}						
Regression	5	2914.69	582.94	52.44	0.0040	0.9887
Residual	3	33.35	11.21			
Total	8	2948.04	-			

p-value: significant probability value, R^2: multiple correlation coefficient

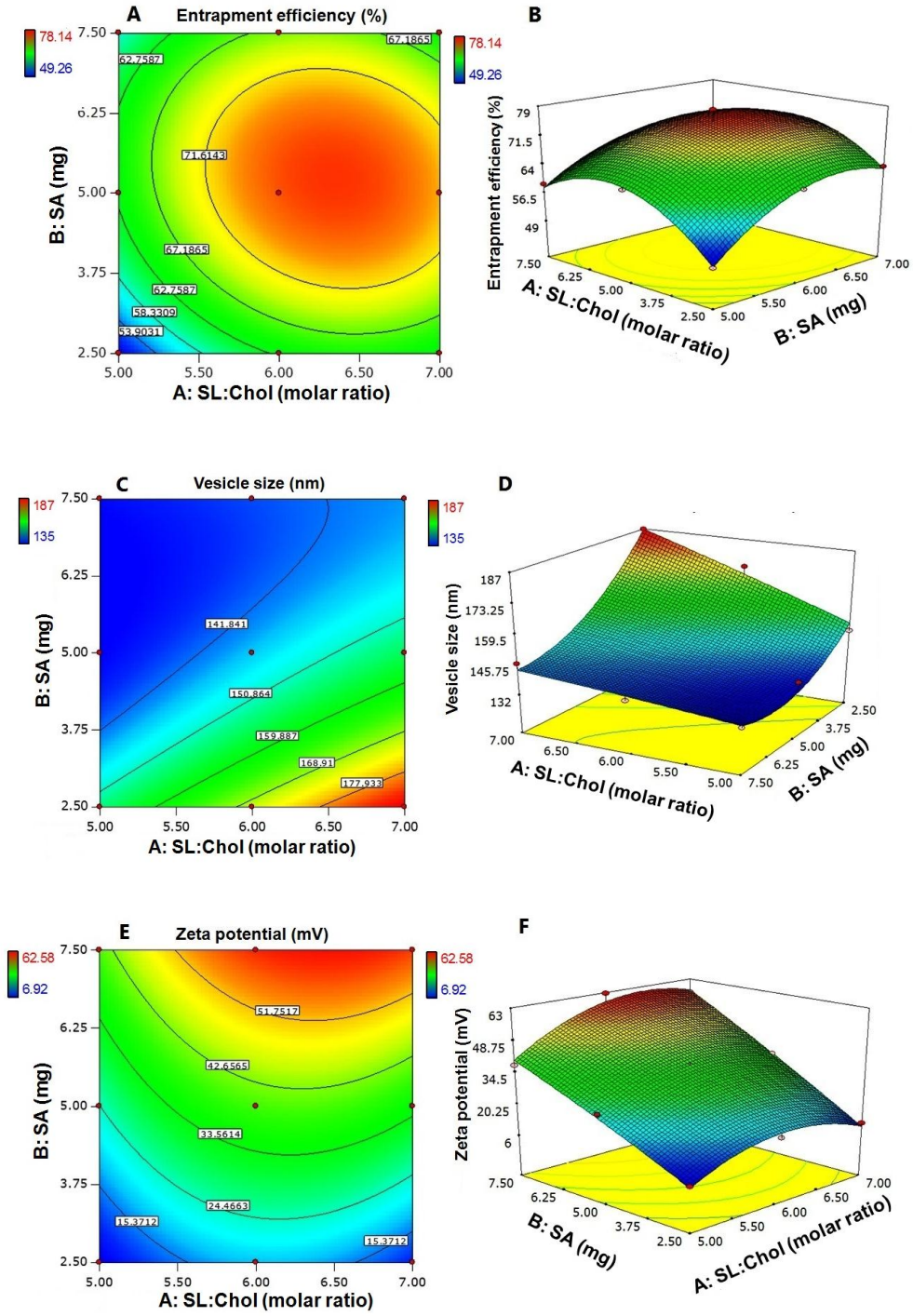

Figure 11: 2D-contour (A, C and E) and 3D-Response (B, D and F) surface presenting the effect of SL: Chol molar ratio and SA concentration on EE, VS and ZP of RCL formulations.

4.4 Evaluation of RCL

As per the applied factorial design, nine formulations were prepared from which optimized RCL was selected on the basis of maximum entrapment efficiency, lowest vesicle size, and high zeta potential (Figure 12). Finally, the optimized liposomes was lyophilized by using cryoprotectant mannitol and used for DSC and FTIR analysis. After a thorough evaluation, it was found that RCL5 (SL:Chol ratio 7:2 and SA 5mg) fulfilled the requisites of an optimum formulation. EE, VS, ZP and PDI of the optimized resveratrol loaded liposomes (RCL5) was found to be 78.14 ± 8.04%, 145.78 ± 9.9 nm, 38.03 ± 9.12mV and 0.359 ± 0.03 respectively. The vesicle size distribution and ZP of optimized liposomes (RCL5) were shown in figure 13.

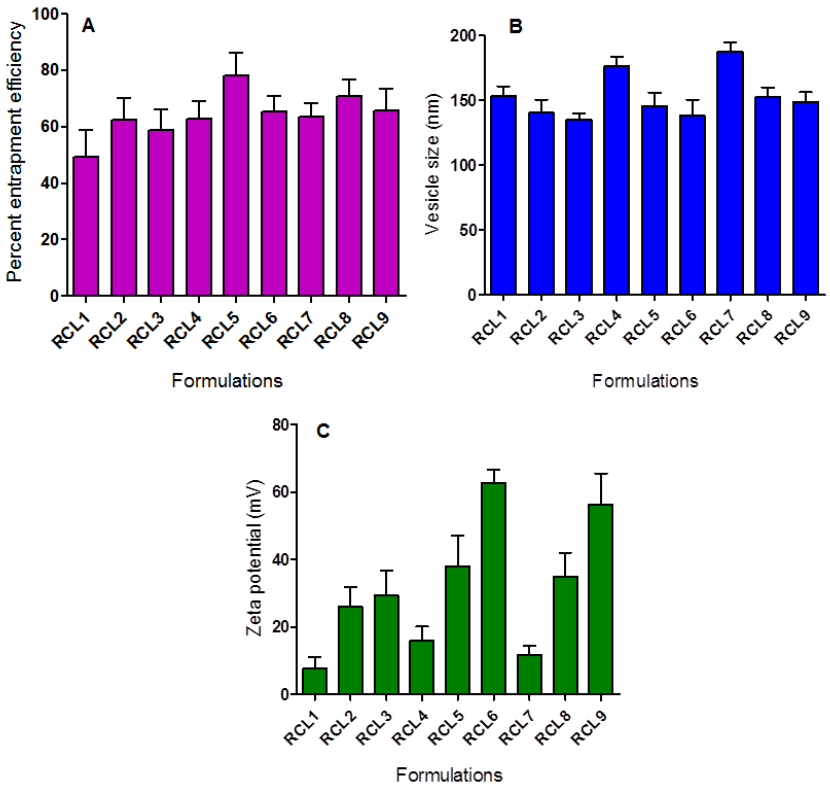

Figure 12: (A) Percent entrapment efficiency, (B) vesicle size (nm) and (C) zeta potential (mV) of RCL1 – RCL9 by varying the ratio of SL:Chol and SA concentration. All results are expressed in mean ± SD (n=3).

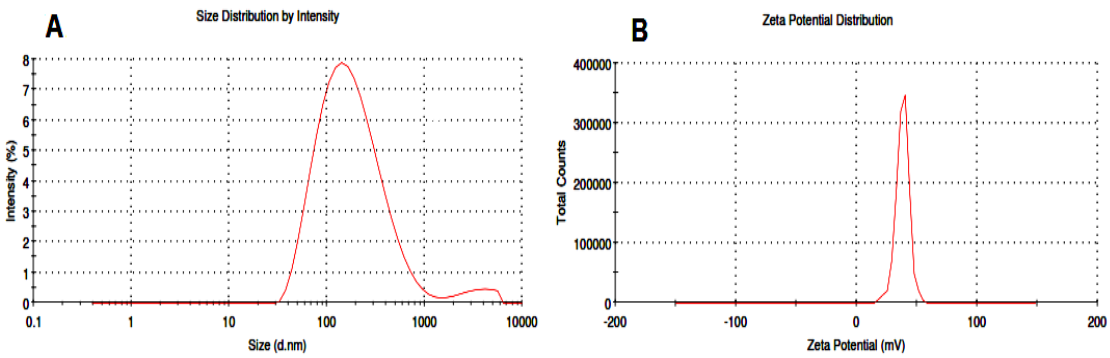

Figure 13: The vesicle size distribution (A) and zeta potential (B) of optimized resveratrol loaded cationic liposomes (RCL5).

Morphological examination of liposomes was evaluated by TEM after negative staining using phosphotungstic acid and images clearly showed spherical morphology with uniform size distribution (Figure 14). In addition, TEM images of RCL5 also confirm the nanosize. The results are consistent with the results achieved with the particle size measurements by zeta sizer.

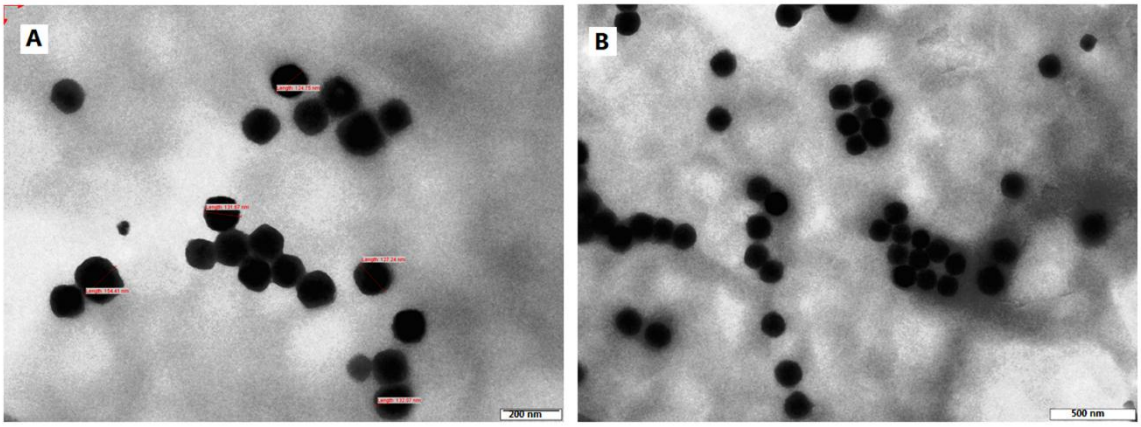

Figure 14: TEM photomicrographs of optimized RCL5

4.5 Freeze drying

The lyophilized RCL5 cake was found to be intact and fluffy in nature with a reconstitution time less than 35 s.

4.5.1 DSC

Figure 15 represent the DSC thermograms of RSV, SL, SA, Cholesterol, mannitol and freeze-dried RCL5. RSV thermogram exhibited a sharp endotherm at 256.45ºC which indicates the crystalline state of RSV and confirms its melting point. DSC of pure SL exhibited endothermic peaks at 20.5°C indicates the transition temperature (Tm), which serves as the basis for optimize the temperature required for the film formulation of lipids. Further, SA and Chol thermograms showed a strong endotherm at 52 °C and 149°C corresponding to their melting points respectively confirming their purity. RCL5 however shows clear peak of mannitol at 166.0 ºC which was used as a cryoprotectant for lyophilization and resveratrol peak was absent.

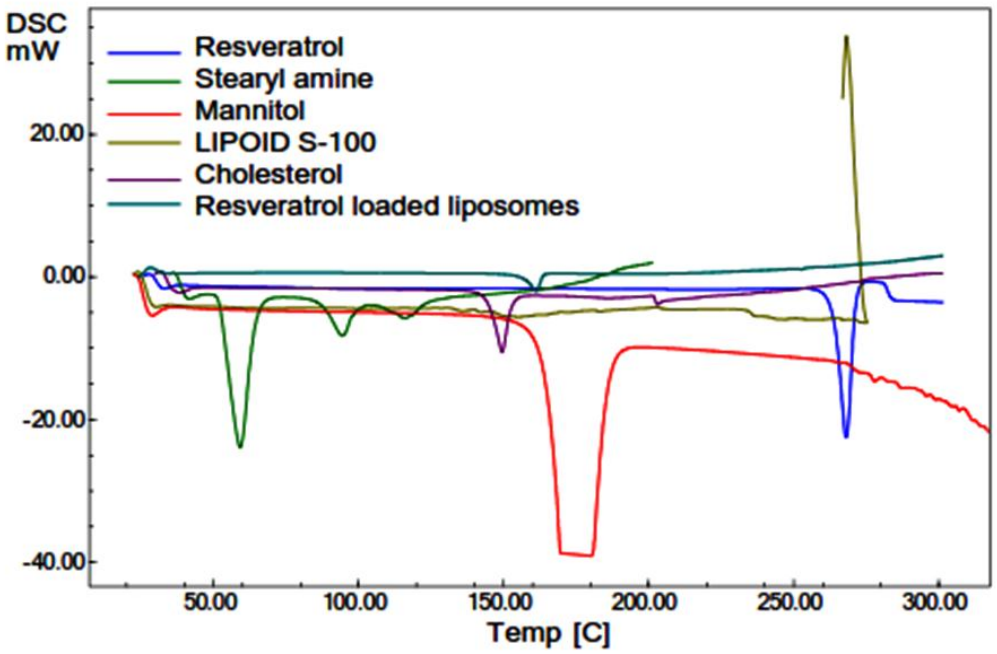

Figure 15: Differential scanning calorimetry thermograms of resveratrol, stearyl amine, Mannitol, soyalecithin, cholesterol and lyophilized resveratrol loaded liposomes (RCL5).

4.5.2 FTIR

FTIR spectroscopic studies were performed to analyze the drug and polymer/excipients interaction. Figure 16A shows the infrared spectrogram of the pure RSV which revealed the intense absorption band of phenolic hydroxyl group at 3288 cm^{-1} and benzene ring absorption peaks of C=C at 1606 and medium absorption peak at 1514 cm^{-1}. Figure 16B shows the FTIR spectrum of SL (LIPOID S100), in which characteristic peaks at 2954 cm^{-1} (Hydroxyl stretching); 2900 and 2856 cm^{-1} (C-H stretching of long fatty acid chain); 1739 cm^{-1} (carbonyl stretching of the fatty acid ester); 1246 cm^{-1} (P = O stretching band); 1097 cm^{-1} (P-O-C stretching) and 972 cm^{-1} ($N^{+}(CH_3)_3$ stretching were observed. FT-IR spectrum of Cholesterol (Figure 16C) displayed a characteristic band between 2866–2931 cm^{-1} representing asymmetric and symmetric stretching vibrations of CH_2 and CH_3 groups and broad and intense band nearly at 3377.36 cm^{-1} due to -OH stretching. Additional band at 1463 and 1375 cm^{-1} is due to asymmetric stretching vibrations and bending vibration of -CH_2 and -CH_3 groups. FT-IR spectrum of SA (Figure 16D) showed peaks at 2916 and 2,850 cm^{-1} owing to -C – H stretching and 1463 cm^{-1} owing to -N-H bending. Further, a sharp peak at 1,315 cm^{-1} could be attributed to C – N stretching and 721 cm^{-1} representing -N-H wagging vibration. FT-IR spectrum of mannitol (Figure 16E) showed a broad characteristic peak at 3280 cm^{-1} assigned to the hydroxyl group. FT-IR spectra of lyophilized RCL5 (Figure 16F) showed characteristics peaks of mannitol, Chol, and SA but did not show any characteristics peaks of RSV, which indicates the entrapment of RSV inside the liposomes.

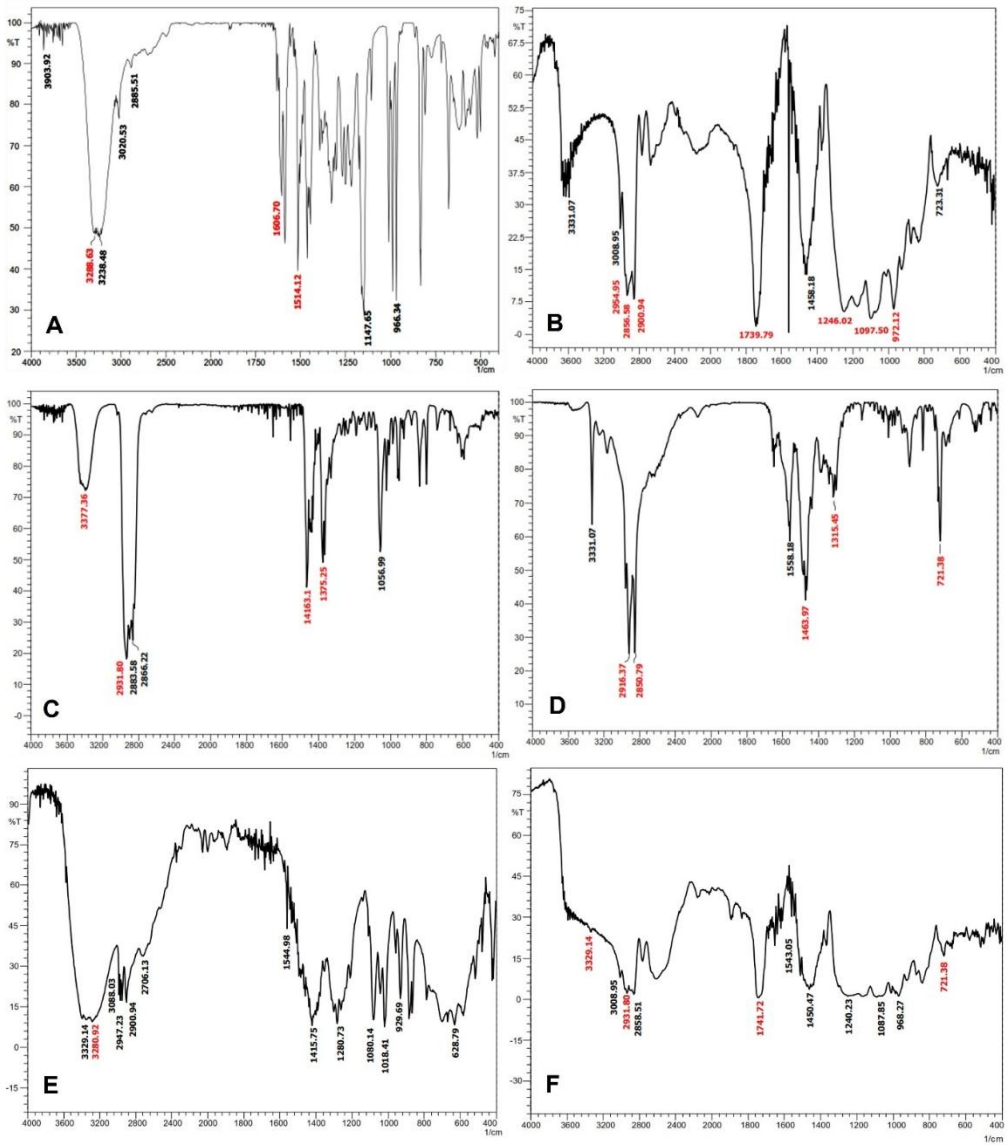

Figure 16: FTIR spectra of (A) pure resveratrol; (B) soya lecithin (LIPOID S100); (C) cholesterol; (D) stearyl amine; (E) mannitol; (F) lyophilized RCL5.

4.6 Stability studies

The storage stability studies of optimized RCL5 in both dispersion and lyophilized form (reconstitute with water) were tested on storing them at 4 °C for 3 months. Table 7 summarizes there was no significant difference in the VS, ZP and EE after 3 months which indicates a good long term stability of formulation.

Table 7: Stability studies of optimized liposomes RCL5 at 4 °C for 3 months

Parameter→	Vesicle size (nm)		Zeta potential (mV)		EE (%)	
Storage condition ↓	Initial	After 3 months	Initial	After 3 months	Initial	After 3 months
RCL5, liquid dispersion at 4ºC	142.17 ± 6.20	149.14 ± 12.62	37.3 ± 4.53	34.43 ± 4.80	76.57 ± 2.51	72.77 ± 3.05
RCL5, Lyophilized at 4ºC	143.76 ± 4.77	147.80 ± 10.30	36.66 ± 2.65	35.03 ± 3.27	76.44 ± 2.27	75.36 ± 0.929

Values are expressed as Mean ± SD (n=3).

4.7 In-vitro release study of RCL

In-vitro drug release profile of RSV from liposomes at pH 5.5 and 7.4 were obtained by plotting the graph of cumulative percentage of the drug released with respect to time (Figure 17). Initially, a burst release phase, releasing approximately 30% of RSV in both pH medium was observed in first 2h followed by sustained and complete drug release in 48h. Faster release of RSV at pH 5.5 (tumor microenvironment) was observed as compared to pH 7.4. The release data was subjected for model fitting

using the zero order, first order, Higuchi, Korsemeyer-Peppas and Hixon-crowell models (Figure 17). The Hixon-crowell model showed the highest R^2 value for RCL5 at pH 5.5 (R^2 value: 0.937) and pH 7.4 (R^2 value: 0.971) indicating it as the best fit model for RSV release from liposomes at both pH.

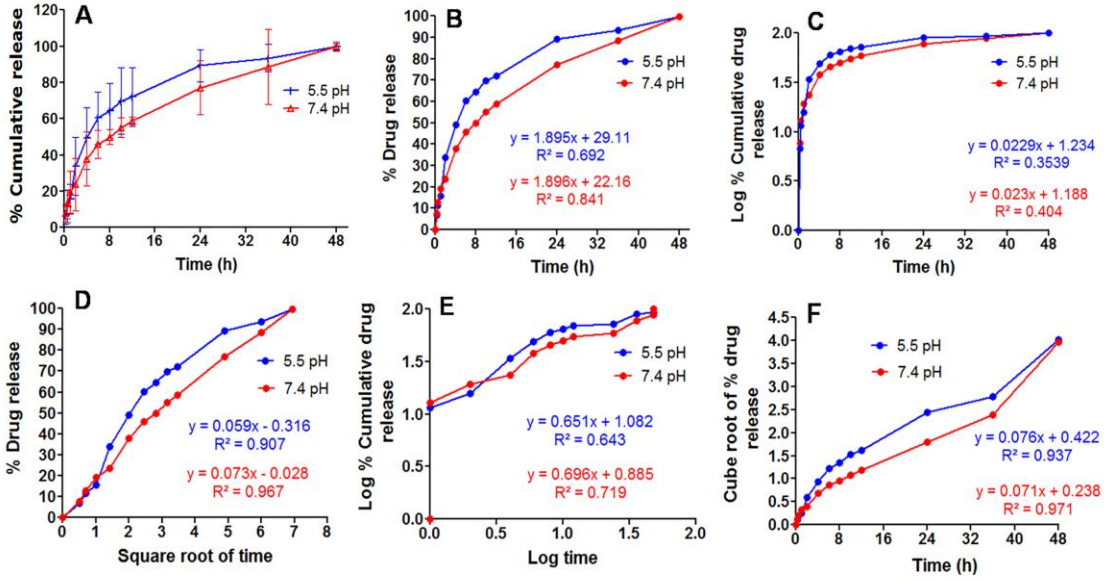

Figure 17: (A) In-vitro drug release of RSV from liposomes at pH 5.5 and 7.4 showed faster release trend at pH 5.5 when compared to pH 7.4.; The release data subject to different release model (B) Zero order release, (C) First order release, (D) Higuchi model, (E) Kosmeyer-pepas model, and (F) Hixon-crowell model.

4.8 In-vitro cytocompatibility assay

Figure 18 revealed the in-vitro cytocompatibility of RSV, blank liposomes and RCL5 against L929 cell line after 24 h incubation. The L-929 cells viability after treatment with RSV and RCL in the concentration range of 7.812 - 250 µg/ml showed approximately 90% of viable cells, which is insignificant difference as compared to untreated cells, confirms its cytocompatibility.

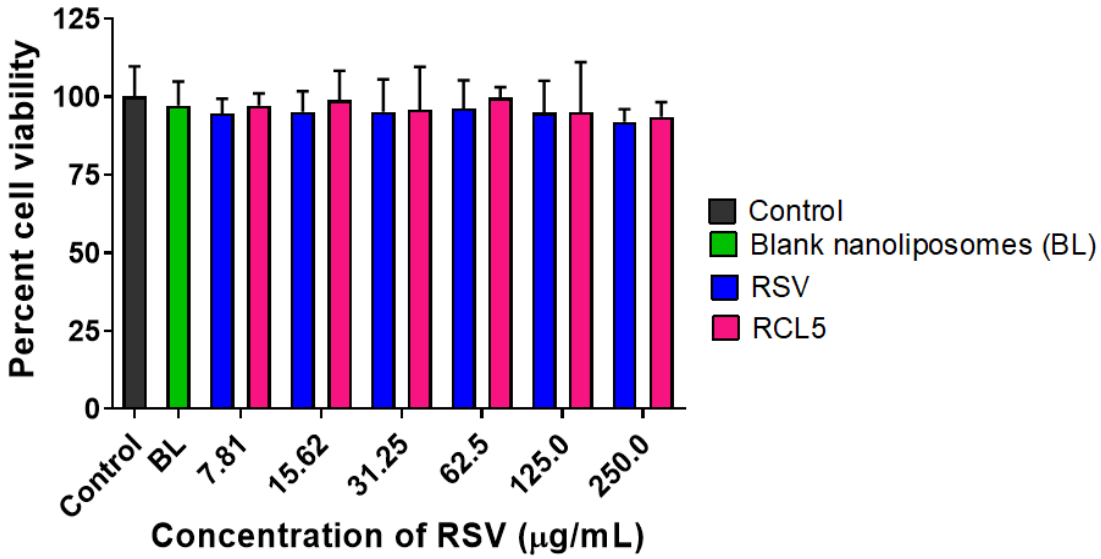

Figure 18: In-vitro cytocompatibility of RSV, BL and RCL5 on L-929 normal mouse fibroblast cells for 24 h.

4.7 In-vitro cytotoxicity assay

Cytotoxicity studies of RSV, BL and RCL5 were tested on HepG2 cell line over a period of 24 and 48h using MTT viability assay at different drug concentration (Figure 19). The HepG2 cells viability was considerably decreased after treatment with free drug and optimized liposomes. BL was found to be biocompatible and showed no significant cytotoxicity against HepG2 when compared to control. RSV and RCL5 showed dose and time dependent changes in which RCL5 demonstrated significantly higher cytotoxicity against HepG2 when compared to RSV. The IC50 values of RSV at 24h and 48h time point were 84.49 µg/mL, 68.23 µg/mL and, 63.65µg/mL, 42.26 µg/mL for RCL5 respectively.

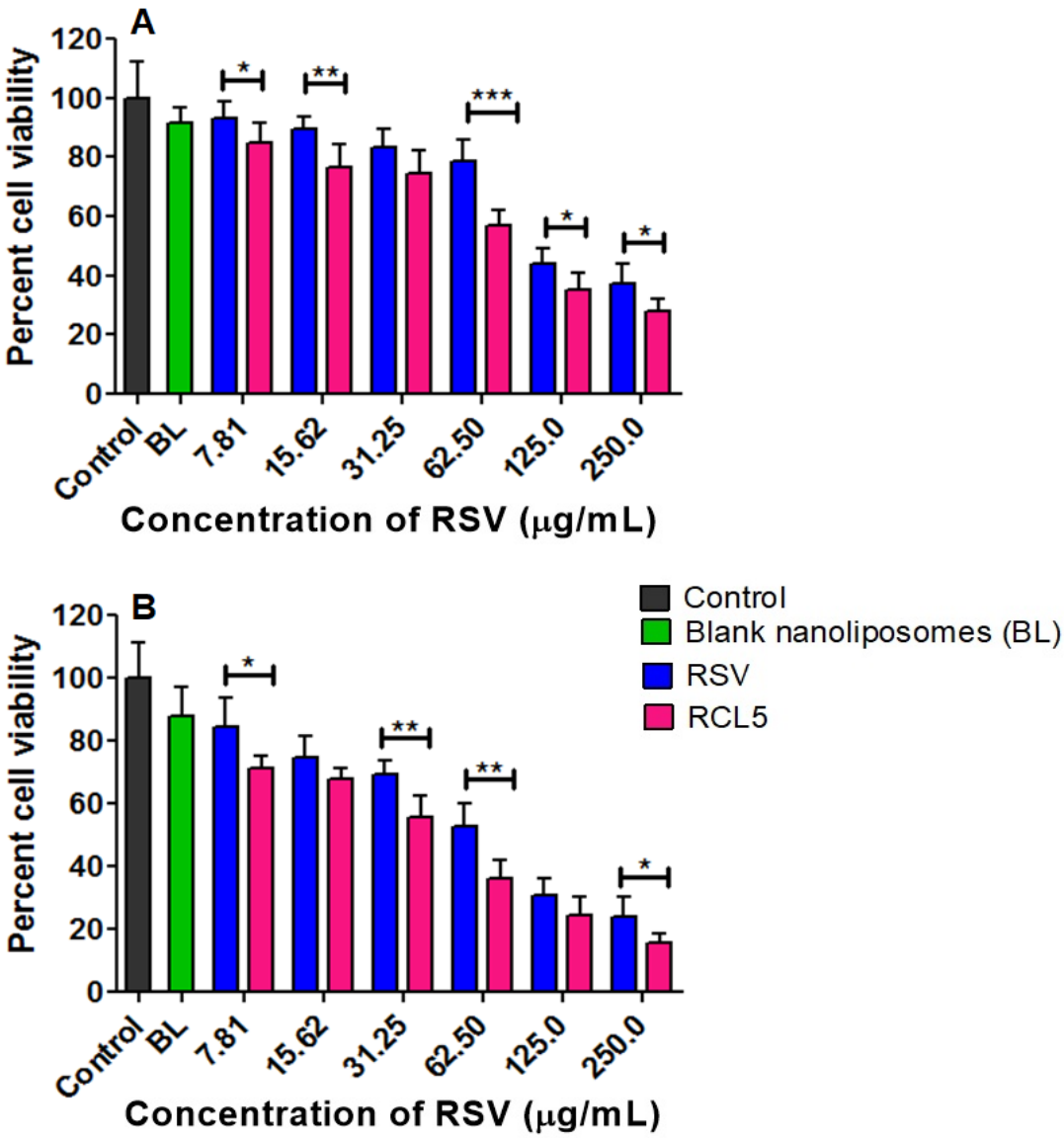

Figure 19: In-vitro cytotoxicity effects of BL, RSV, and RCL5 on HepG2 cells (A) for 24 h and (B) for 48 h. Data are mean ± SD (n=3). Significant difference specified as *** p < 0.001, ** p <0.01,* p<0.05 between RSV vs RCL5.

4.8 In-vitro quantitative and qualitative cellular uptake studies

The results indicated that cells treated with RCL5 showed significant ($p<0.01$) accumulation of RSV as compared to cells treated with free RSV after 3 and 5 h incubation. HPLC analysis of cell extract after 5 h showed 54.16 ± 9.61% and 74.98 ± 6.33 % cellular internalization of free RSV and RSV from RCL5, respectively (Figure

20). The in-vitro qualitative cellular uptake of C6 and CL in HepG2 cell lines was visualized by CLSM scanning microscope. CL was prepared by the similar method as reported in the methodology section, except that C6 was used in place of RSV. Images of HepG2 cells treated with C6 and CL for 3 and 5 h were shown in Figure 21. Almost negligible fluorescence was observed in the cells treated with C6 after 3 h. In contrast, CL incubated with HepG2 cells for both time points observed rapid internalization as confirmed by the persistent fluorescence signals recorded.

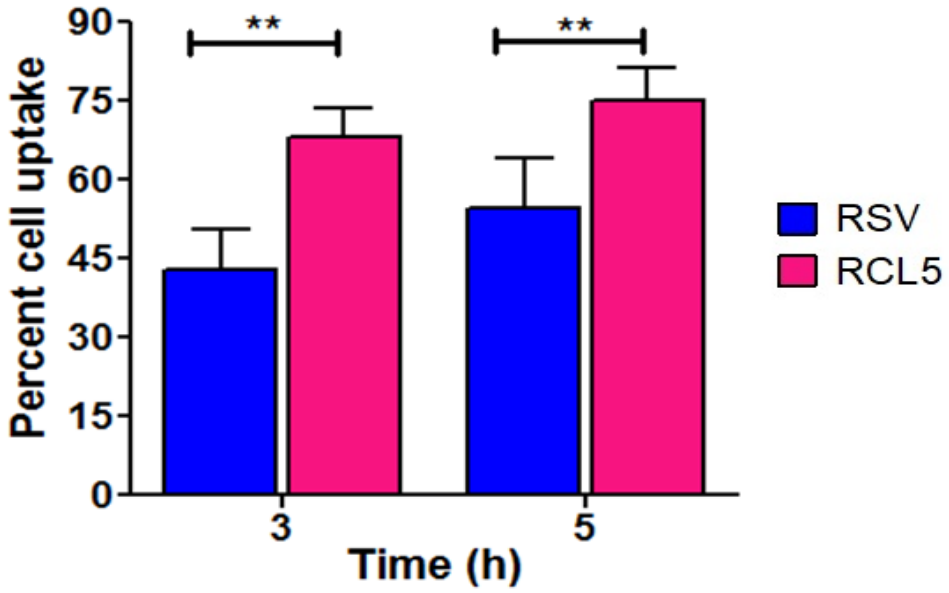

Figure 20: Quantitative uptake of RSV and RCL5 byHepG2 cells after 3 and 5h. Significance difference was specified as ** $p \leq 0.01$ between RSV vs RCL5

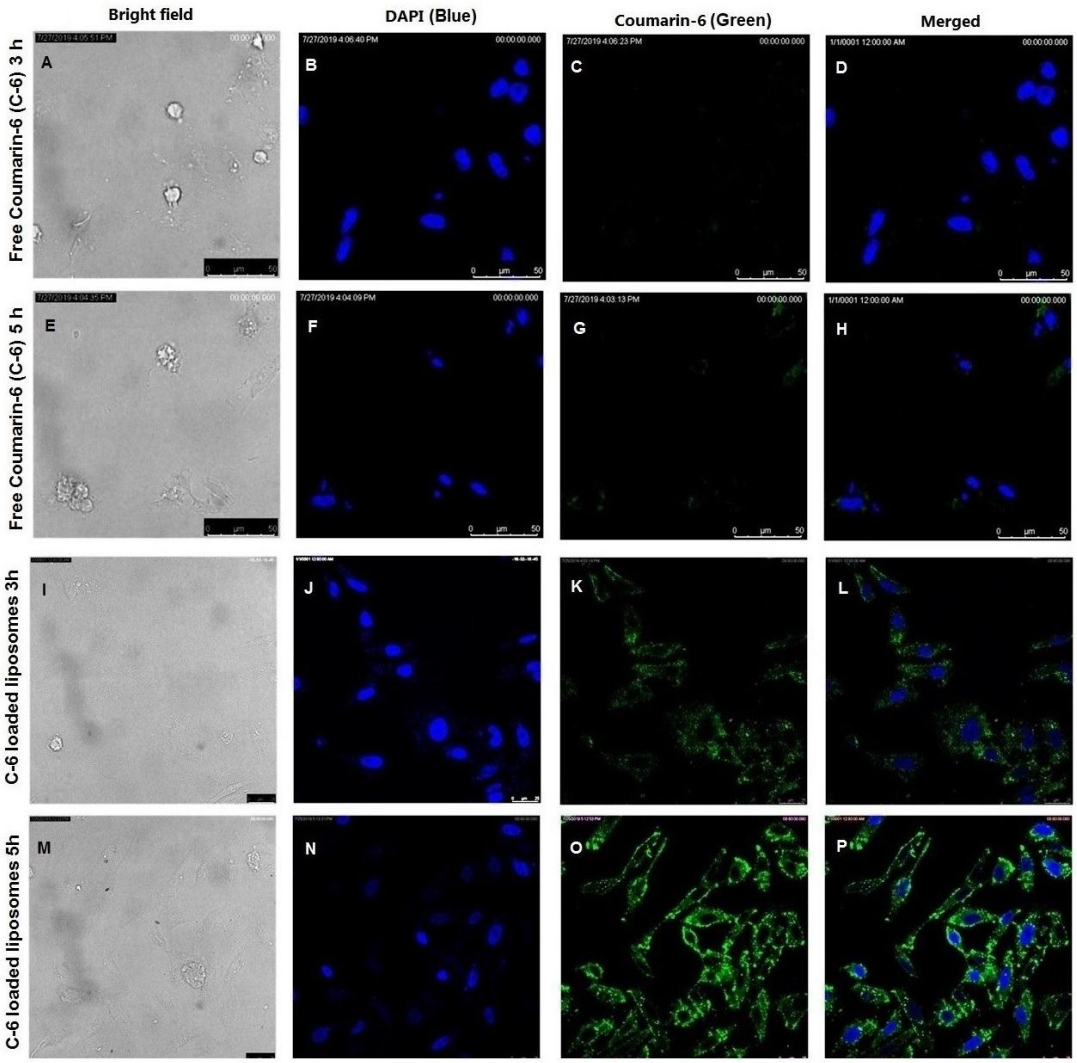

Figure 21: Confocal microscope fluorescence images presenting the in-vitro cellular uptake of free C6 and C6 loaded liposomes in HepG2 cell lines after 3 and 5 h. Aming to observe the intracellular distribution, green fluorescence dye coumarin-6 was incorporated into the liposomes and blue fluorescence dye DAPI was used after the incubation of coumarin-6. Scale bar is 50 µm.

4.9 In-vivo toxicity studies

RSV and RCL5 were subjected to toxicity profiling by using different markers. For nephrotoxicity, creatinine and BUN levels in plasma were evaluated whereas for hepatotoxicity, ALT and AST levels were determined. Untreated animals served as control for the comparison. As shown in figure 22, animals treated with RSV and RCL did not induce toxicity in the liver, spleen and kidney. The biochemical evaluation was further corroborated with histopathological examinations suggesting nontoxic behavior of free RSV and RCL5. Histological sections of liver, kidney and spleen (Figure 23), demonstrated normal parenchymal cell physiology indicating no signs of inflammation and necrosis.

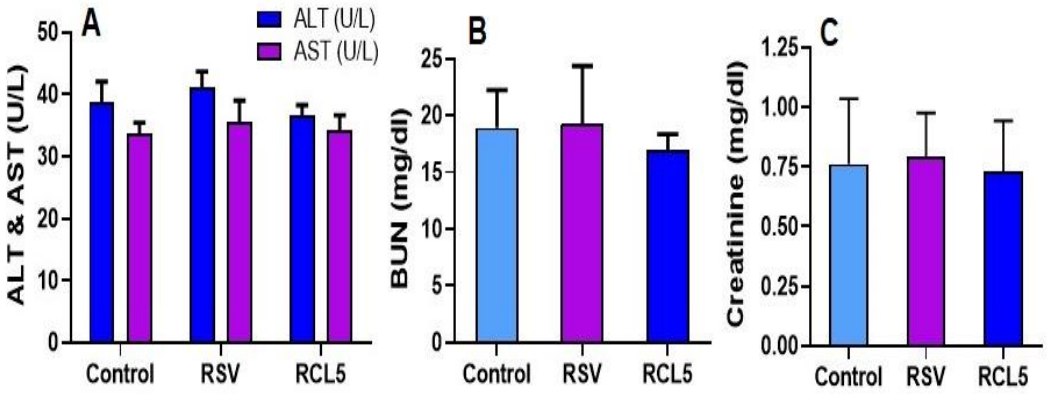

Figure 22: Biochemical markers (A) AST and ALT (B) BUN and (C) creatinine levels in plasma after 7 days administration of RSV and RCL. Values are expressed as Mean ± SD (n = 3)

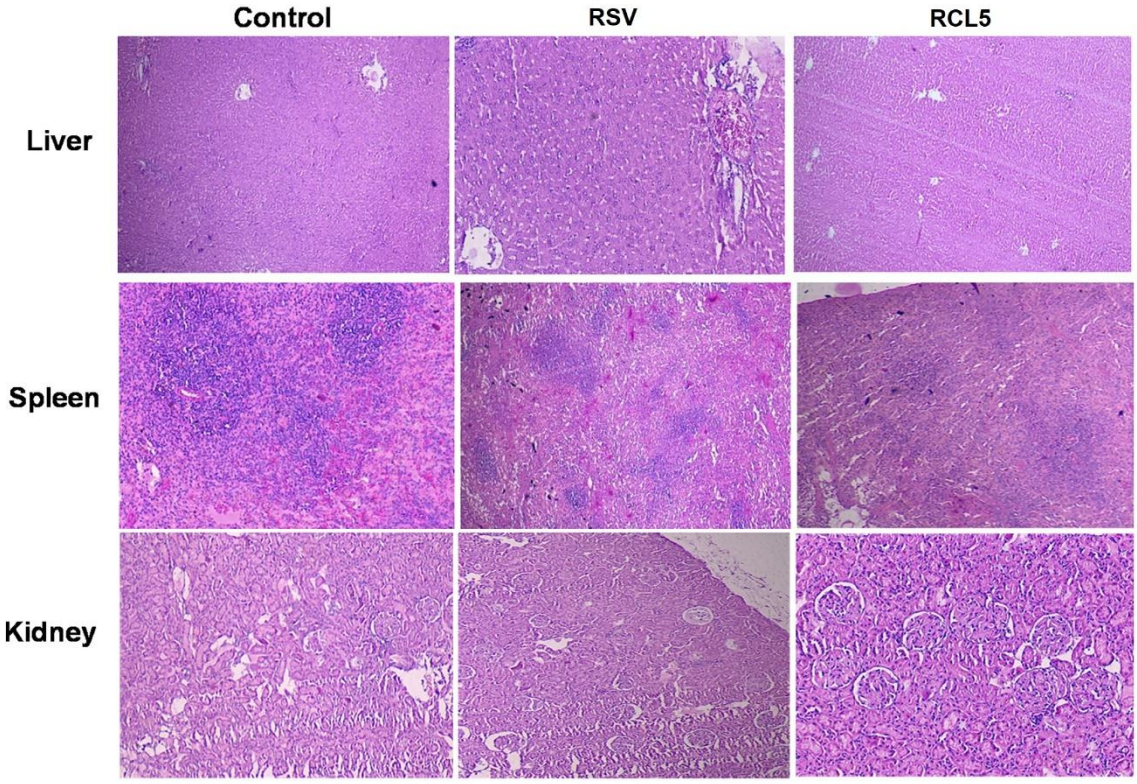

Figure 23: Histopathological examinations of liver, spleen and kidney sections suggesting nontoxic behavior of free RSV and RCL5.

4.10 In-vivo pharmacokinetic studies

Results of pharmacokinetic evaluation of RCL5 after intraperitoneal injection in Wistar rats are shown in Table 8. Higher concentration of RSV from RCL5 in the plasma and liver was achieved when compared to the animal group, which received free RSV. In terms of distribution, cationic liposome was concentrated maximum in the liver followed by spleen (C_{max} 2.82 µg/ml, half-life of 30 min) as compared to other organs.

Table 8. Pharmacokinetic parameters of RSV and RCL in rat plasma and organs following i.p. administration

Parameters		C_{max}	AUC_{total} (μg/ml*min)	$T_{1/2}$ (min)	MRT (min)
Blood	RCL5	2.15	225.98	56.24	95.70
	RSV	1.74	125.06	48.86	83.58
Liver	RCL5	3.51	223.54	35.75	72.16
	RSV	1.50	69.85	37.36	58.29
Spleen	RCL5	2.83	74.32	18.92	40.99
	RSV	2.50	113.15	18.65	38.66
Lung	RCL5	0.49	10.56	-	-
	RSV	1.10	19.66	-	-
Heart	RCL5	0.39	19.01	33.09	56.00
	RSV	0.22	23.40	65.40	102.00
Kidney	RCL5	2.34	63.53	29.30	39.70
	RSV	2.82	132.25	26.25	45.07

4.11 Anticancer efficiency of RSV and RCL5 in experimentally HCC induced animal model.

Prophylactic and therapeutic, anticancer properties of RCL5 was assessed in NDEA induced HCC rats. Morphology of liver (Figure 24), histopathology, relative body/liver weight ratio, tumor nodules, liver enzyme levels (alanine transaminase (ALT), alkaline phosphatase (ALP), aspartate transaminase (AST), total bilirubin levels, gamma glutamyl transpeptidase (GGT) and alpha fetoprotein (AFP) were assessed in all groups to compare the efficiency of RCL5 with free RSV. The liver specimens of all the groups were investigated for its morphology on 13^{th} week (Figure 24A-F). Normal group liver tissue appears normal with no macroscopically detectable pathological

changes (Figure 23A). Disease control group liver tissues (Figure 24B) demonstrated significant changes in terms of color, consistency, and the surface texture. Tissue appeared pale pink in color with increased size and corrugated surface with multiple macroscopic nodules (yellow arrows). Prophylactic and therapeutic RSV treated groups (Figure 24C & E) demonstrated very few nodules (yellow arrows) and lesions. Prophylactic and therapeutic RCL5 treated group (Figure 24D & F) in rats showed marked reduction in the number of nodules and damaged caused by NDEA.

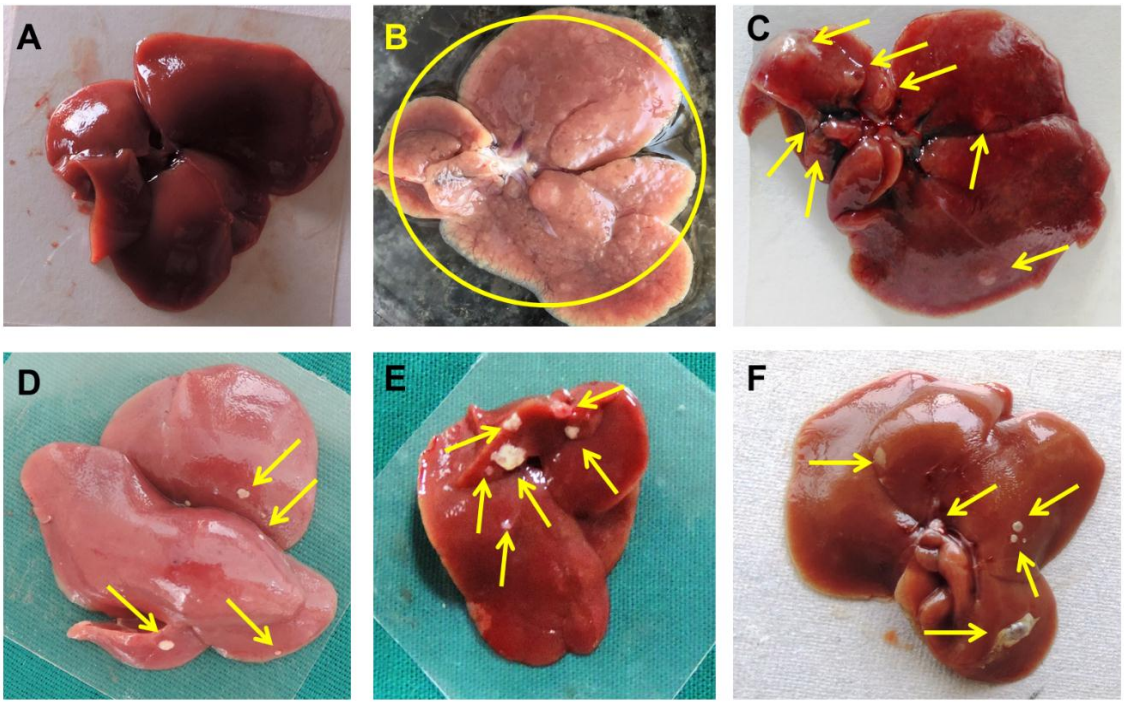

Figure 24: Representative images of rat's livers: (A) Control group; (B) NDEA treated group; (C) Prophylactic RSV treated group; (D) Prophylactic RCL5 treated group; (E) Therapeutic RSV treated group; (F) Therapeutic RCL5 treated group.

Administration of RSV and RCL5 to HCC-initiated rats (group III–VI) exhibited very few hepatic nodules (Figure 25A) in comparison with NDEA alone treated rats (group II). The marked suppression in the development of tumor was noticed with significant ($P<0.05$) changes in liver morphology, when rats treated with RCL5 in both

preventive and therapeutic condition (group IV and VI) as compare to NDEA administered rat. NDEA treated rats showed marked raise in AST, ALT, ALP total bilirubin and GGT levels in serum as shown in figure 25C-G, which is an indicative of damage in liver. RCL5 treatment to HCC-induced rats displayed a significant reduction in the AST, ALT, ALP and GGT levels in serum as compared to the NDEA induced HCC (group II). The effect of RSV and RCL5 on alfa-fetoprotein levels in NDEA induced liver damage is shown in figure 25H. Preventive and curative treatment with RCL5 showed significant decrease (P<0.001) in AFP levels compared to group II HCC bearing rats.

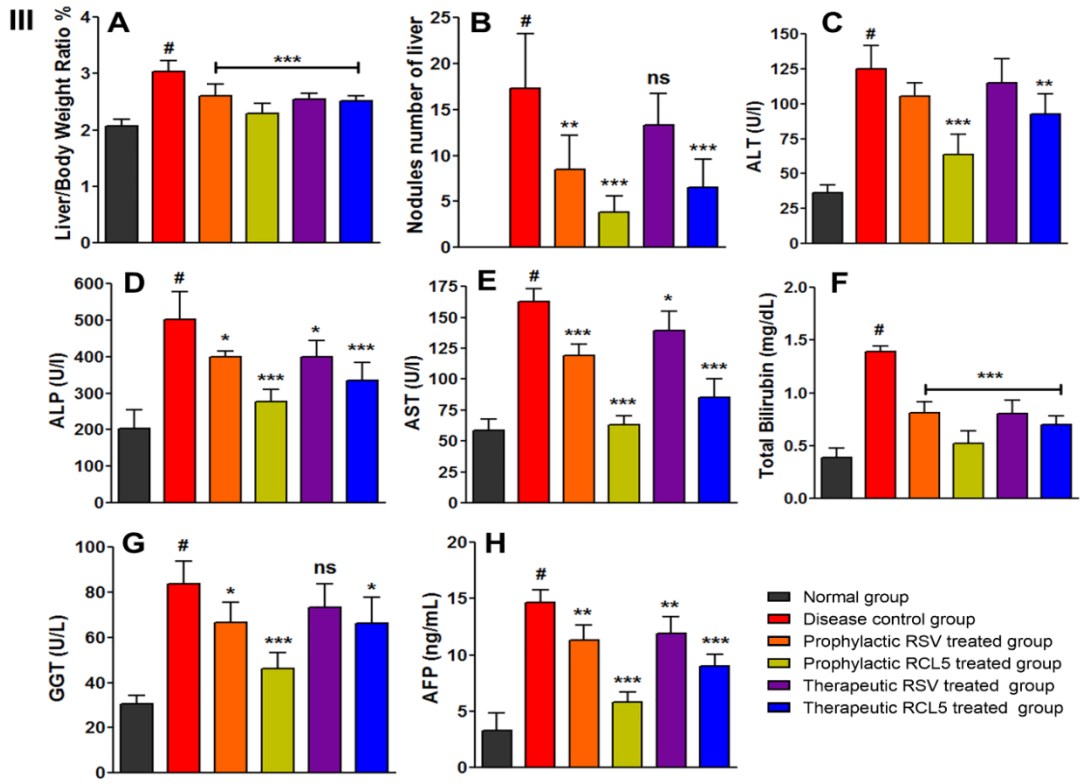

Figure 25: (A) number of nodules; (B) liver/body weight ratio; Results of biochemical estimation of serum levels:(C)serum alanine transaminase (ALT); (D) alkaline phosphatase (ALP); (E) aspartate transaminase (AST); (F) total bilirubin levels; (G) gamma glutamyl transpeptidase (GGT) and (H) alfa-fetoprotein (AFP). Data are shown as mean ± SD of six animals, # P<0.001 vs normal group; (* P<0.001, ** P<0.01, * P<0.05 and ns: no significant) vs disease control group.**

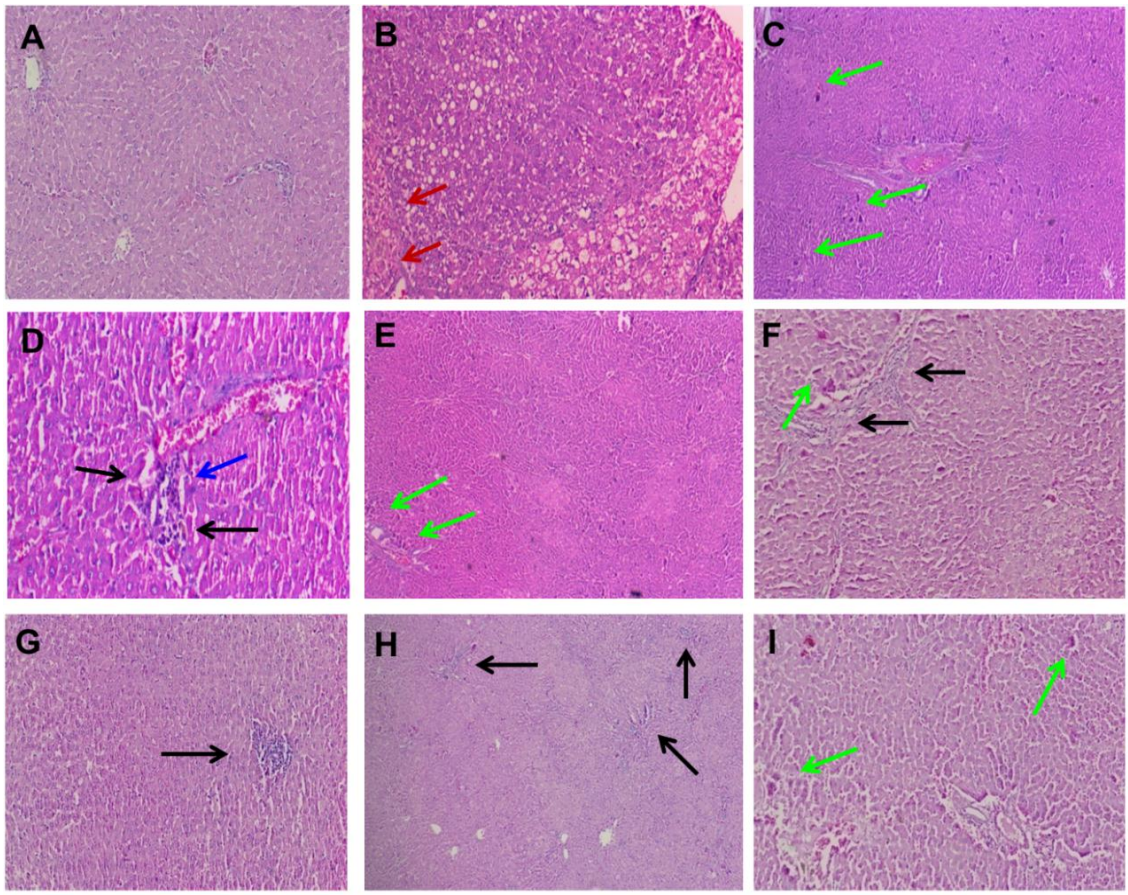

Figure 26: Histopathological images of rat's livers: (A) Control group; (B-E) Toxicant group;(F)Prophylactic RSV treated group; (G) Prophylactic RCL treated group; (H)Therapeutic RSV treated group; and (I) Therapeutic RCL treated group

5. DISCUSSION

Identification of the pure drug was done by FTIR and DSC to check the identity of RSV obtained from Sami Labs Limited, Bangalore, India. The FTIR spectra of RSV show all the characteristic peaks at different wave numbers corresponding to the various functional groups exist in the RSV. A sharp endotherm peak of RSV displays at 256.45 °C conforming its glass transition temperature/melting point. FTIR spectrum and melting point of RSVwere in conformity with the literature reports. Thus the results confirmed that the obtained drug was RSV.

A simple and precise RP-HPLC method validated as per ICH guidelines was used for the estimation of RSV. All the parameters were found to be within the acceptable limits.

Physicochemical properties and stability are the key factors to be considered while developing a new drug delivery system in all the formulation stage, especially those proposed for parenteral administration. This ensures acceptable bioavailability of administered drugs and biocompatibility. In the present investigation, the RCL obtained from the factorial design (3^2 level) confirmed that the independent variables such as (A) Molar ratio of SL: Chol (where Chol concentration is fixed on the basis of preliminary studies) and (B) concentration of SA had a significant effects on dependent variables such as EE, VS and ZP.

Percent entrapment efficiency (%EE) states the total quantity of drug that is successfully entrapped inside the liposomes. To analyze the %EE is one of the essential parameter which determines the drug holding capacity and decisive delivery potential of a system. Although both hydrophilic and hydrophobic drugs can be entrapped into the liposome vesicles, however it was mentioned in the literature that

%EE is considerable higher for hydrophobic drugs as compared to lyophobic drugs (59). The EE of the liposomal formulation was dependent on the molar ratio of soya lecithin and cholesterol as well as the amount of stearyl amine used in their preparation. Increasing in the SL:Chol molar ratio from 6:2 to 8:2 increased in the drug EE. The positive effect of phospholipid concentration on %EE attributed to the lipophilic interaction of the hydrophobic drug with the vesicle membrane and thus increases the % EE (60).

Furthermore, the accessibility of lipid phase could be increased with the increase in the concentration of phospholipid for drug molecule, resulted in accommodation in the lipid bilayers (61). At the same time stearyl amine plays an important role which may affect the EE of RSV in liposomes could be due to alters in the membrane permeability or the electric charge density (62). A nonlinear increase in the encapsulation efficiency of RSV was observed in the liposomes. At low levels of SA tended to enhance the EE till its intermediate levels, followed by curvilinear decline at its higher levels could be due to the changes in the lateral packing of the liposomes bilayer at higher concentration of stearyl amine (62).

The average size and size distribution of liposomes are important parameters especially when the liposomes are intended for therapeutic use by inhalation or parenteral route (63). Moreover, the Liposomes particle size is one such property that affects the half-life of liposomes in the vascular system and may range from few minutes to many hours. The particle size has an influence on the vesicles removal from circulation by the reticuloendothelial system (RES), phagocytosis by kupffer cells, distribution and accumulation in specific organs (28). Smaller liposomes (0.1-1 μm) are located principally in the liver and spleen whereas liposomes larger than 3 μm are deposited in the lungs (64). In the present research, the vesicle size of

optimized liposomes was below 300 nm, signifying that these vesicles have lesser uptake into the RES and decreased rate of the clearance from plasma. In addition, nanoparticle of appropriate size (upto 4,000 kDa/500nm) can permit through the vessel walls of the tumor and move into the neoplastic lesion due to EPR effect (28). The concentration of soya lecithin has direct positive effect on vesicle size of RCL formulations. Increasing the phospholipid concentration resulted in the formation of larger liposomes which could be due to the propensity of SL molecules coalescence leading to rise in VS (65).

All the formulations were analyzed for ZP during formulation development process. ZP is a useful tool to indicate vesicle surface charge, which is used to predict the stability of colloidal dispersion. In general, ZP is the balance between the surface positive and negatives charges and is directly proportional to the magnitude of the potential (66). Based on the result, ZP is directly proportional to the stearyl amine concentration and our experiments are supported by literature which states that the increase in the concentration of SA consequently increases the ZP. In the present investigation, the observed ZP of optimized liposomal formulation was 38.03 ± 9.12 mV and in all the formulation ZP was maintained towards positive side due to the charge imparted by SA. Cationic lipid SA is an amphiphilic molecule which have a lipophilic region (hydrocarbon chain) and a hydrophilic region comprising of positive charged polar amine group. Previous reported literature by Casals et al., clearly shows that SA is asymmetrically distributed in the lipid bilayer which was predominantly on the outer surface as compared to the inner core. High positive zeta potential value of the formulated liposomes confirms that significant SA is available on the outer surface imparting the cationic charge on the liposomes (67,68). Parameter like PDI used to assess vesicle size distribution or the homogeneity of the nanoparticles. It is

also used to evaluate the stability and efficiency of the preparation technique. Small values of PDI (less than 0.10) state a homogenous population, while high values of PDI (greater than 0.3) specify a vesicles of heterogeneous population (69). In the present study, the PDI of all liposomal formulations were near about 0.3 indicating the narrow size distribution with high degree of homogeneity.

Morphological examination of liposomes was evaluated by TEM after negative staining using phosphotungstic acid and images clearly showed spherical morphology with uniform size distribution. The reason for the formation of sphere-shaped morphology may be attributed to the hydrophobic nature of the lipids. When lipids exposed to an aqueous environment led to the spontaneous formation of closed bilayers exposing the polar hydrophilic later to the outer surface of liposomes (24). The shape and surface morphology of the liposome was found to be smooth with no vesicular aggregation which indicates the stability of the prepared liposomes. These results can be attributed to the inclusion of a charge inducer (SA) in liposomes which projects the amine group towards aqueous phase.

To check the physical state of the drug loaded into the nanoparticles was confirmed by using DSC analysis. DSC is the most preferred thermal analytical technique extensively used in many pharmaceutical industries, analytical, quality assurance and R & D laboratories to investigate the numerous physicochemical phenomena such as melting, purity, polymorphism, crystallization, glass transition, drug–excipients compatibility, degradation and stability determinations. The thermograms of RCL5 showed the disappearance of RSV endothermic melting peak, which specifies that conversion of the crystalline drug to an amorphous state when encapsulated into the liposomal system. This also suggests that the RSV is entirely loaded inside the lipid

matrix of liposomes. The results are corroborated with Abdellatif et.al, wherein the endothermic peak of sertaconazole nitrate was disappeared after entrapped inside the vesicular system due to its alteration from crystalline state to amorphous state (70). However, RCL5 shows clear peak of mannitol at 166.0 ºC which was used as a cryoprotectant for lyophilization.

FTIR studies were done to confirm further the entrapment of RSV into the liposomal systems. The FTIR spectra of RCL5 showing all the peaks related to soya lecithin, stearyl amine and mannitol which suggest no alteration of these used excipients. Furthermore, the absence of characteristic peaks of RSV from the FTIR spectra of RCL5 can indicate effective entrapment of RSV into nanocarrier systems. These results corroborate with the study, where the disappearance of RSV peaks was associated with nano-encapsulation (71). Results concluded that as the RSV molecules were protected in the inner core of the spherical amphiphilic nanovesicles and the IR radiation could not be passed through the entrapped molecules.

Physical unstability of liposomal nanodispersions might become apparent after an aggregation or fusion of unstable liposomes during the process of formulation and or upon long-term storage resulted in an increase in particle size. The increase in the diameter of liposomes, resulting in a short half-life due to rapid uptake by the RES system with subsequent clearance (26,28). Therefore, preparing stable liposomes with small and uniform size distribution is the most significant aspect in drug product development. After 3 months of storage at 4 ºC of optimized liposome formulation in both dispersion and lyophilized form (reconstitute with water), there was no significant difference in the VS, ZP and EE which indicates a good long term stability of formulation.

The in-vitro drug release studies were carried out to provide valuable information on the in-vivo performance of the nanovesicular formulations (liposomes). In-vitro drug release profiles of RSV from RCL5 at pH 5.5 (simulate pH of tumor micro environment) and 7.4 (simulate pH of blood) showed sustained and complete drug release in 48h. No significant difference was found for the release of RSV from RCL5 over the entire study period. A comparative faster release of RSV at pH 5.5 (tumor microenvironment) could be due to use of heterogeneous lipids (SL and SA) used in the formulation of liposomes. SL (Lipoid S 100: lipid mixture) (72) and SA has 18 carbon chain as their backbone. Liposomes prepared with heterogenous lipids when exposed to decreased pH leads to an increase in the membrane permeability and ultimately release the payloads. Our results are in corroboration with the studies performed by Karve et al., wherein they assessed the release behaviour of vesicles formulated by different sets of lipids (DPPC (16 carbon containing lipid; 1,2-dipalmitoyl-sn-glycero-3-phosphocholine,) and DSPA (18 carbon containing; 1,2-Distearoyl-sn-glycero-3-phosphate, sodium salt) lipids, DPPC and DPPA lipids, and DSPC and DSPA lipids) in different pH. Vesicles prepared with different chain lengths (DPPC and DSPA) showed increased membrane permeability and higher release of encapsulated calcein at lower pH when compared to the vesicles prepared by lipids with same chain length (DPPC - DPPA and DSPC - DSPA) (73).

The drug release mechanism can be defined as the way of the release of payload from the nanocarrier. It is dependent on the nature of the polymer/lipid used in the formulation and the release conditions which can follow several mechanisms such as dissolution, diffusion, swelling, erosion and degradation (74). To examine the release mechanism of RSV from the RCL5, five kinetic models were applied to fit the release data. Based on the analysis, the Hixson-Crowell model showed the highest R^2 value

for RCL5 at pH 5.5 (R^2 value - 0.937) and 7.4 (R^2 value - 0.971). Hence the release of RSV from RCL5 follows Hixson-Crowell model which occurs through surface dissolution and is dependent on the surface area and the diameter of vesicle (75,76).

Cytocompatibility is the key parameter to be assessed for any bio-nanomaterial proposed for in-vivo drug delivery system. In the present investigation, cytocompatibility of RSV and RCL5 was evaluated against primary mouse fibroblast culture (L929) using colorimetric MTT assay. The results confirmed the cytocompatible nature of RSV, BL and optimized RCL5 against L929 cell lines (~ 90% cell viability) indicating their suitability as a drug carrier system. Literature suggest that drugs are often recognized as biocompatible with cell viability more than 80 percent (77).

Before the beginning of the in-vivo experiment it is important to evaluate the in-vitro cytotoxicity of the developed formulation for their possible anticancer use. Cytotoxic activity of RSV, blank liposomes and RCL5 against HepG2 were assessed by using MTT assay. The results showed no toxic effect of blank liposomes in HepG2 cell lines when compared to control. RSV and RCL5 showed dose and time dependent changes in which RCL5 demonstrated significantly higher cytotoxicity against HepG2 when compared to RSV. The reason for improved activity of RCL5 in comparison to RSV could be because of enhanced uptake of liposomes and improved solubility of RSV in nanoliposomes formulation. Further, negative charge on cancer cell is more likely to attract positively charged liposomes which increase the cell uptake of nanovesicles (78). Similar outcomes were reported by Manjarika et al., wherein they developed SA based camptothecin loaded cationic liposomes. They reported that camptothecin loaded cationic liposomes demonstrated a manifold enhancement in the

anticancer therapeutic efficacy both in-vivo and in-vitro in comparison with free camptothecin. This enhanced anticancer effect of liposomes was due to the attraction between the SA containing cationic liposomes towards the exposed PS group present on liver cancer cells (31). These results are also supported by the existing literature which suggests that cationic liposomes have been demonstrated for selective delivery of anti-cancer drugs to the tumor vasculature based on electrostatic charges on the diseased cancer tissues (40).

In order to find out the mechanism of improved cytotoxicity of RSV nanovesicular formulations, cellular uptake studies were performed on HepG2 cell lines using HPLC and confocal laser scanning microscopy (CLSM). The time dependent cellular uptake showed enhanced cellular internalization of optimized liposomes as compared to native RSV solution throughout the incubation time. Particle size, shape, and surface charge are the physico-chemical properties of the nanocarriers which strongly influencing the cellular uptake efficacy of nanocarriers (79). Small size nanoparticle (10-500 nm) is one of the key parameter and has the ability to enter without restraint into the cell and is advantageous for passive targeting to tumor tissue by enhanced permeation and retention effect (27,80). In the present research, we found enhanced uptake of RSV in HepG2 cell for the optimized RCL5 formulation compared to the native RSV solution. We found same results in qualitative study, wherein liposomes loaded with C6 co-localized into the subcellular region of HepG2 cells leading to the enhanced therapeutic efficacy which was demonstrated by MTT assay. The improved intracellular internalization of RCL5 in our study could be due to their nano size and cationic charge on the liposomes (mechanism explained for figure 6). Cationic nanoparticles with net positive surface charge emerge as a promising option owing to their very strong cellular interaction and desirable cellular uptake (40). Apart from PS

on the surface of cancerous cells, it also contains strong negatively charged elements such as chorionic gonadotropin, sialic acid and anionic residues of RNA as compared to normal cell surfaces (81,82). Based on this fundamental electrostatic interaction, cationic liposomes have a high tendency to accumulate in cancer cells through endocytosis (81).

Toxicity testing of new compounds is essential for drug development process. The preclinical toxicity testing on various biological systems reveals the species, organ and dose specific toxic effects of an investigational product. Toxicity profiling was carried out for RSV and RCL5 formulation using different toxicity markers. Nephrotoxicity was determined by evaluating the BUN, and plasma creatinine levels whereas, plasma ALT and AST levels were evaluated for hepatotoxicity. After one week treatment of RSV and its liposomal formulation (RCL5) did not induce toxicity in the liver, spleen and kidney. The biochemical evaluation was further corroborated with histopathological examinations suggesting nontoxic behavior of free RSV and its liposomal formulation. Histological results of liver, kidney and spleen demonstrated normal parenchymal cell physiology indicating no sign of inflammation and necrosis.

Liposomes drug delivery system (DDS) are excellent candidates to circumvent the non-ideal properties of drugs. Assessment of pharmacokinetic profile of RCL5 in comparison with free RSV was performed by using standard protocols. Higher concentration of RSV from RCL5 in the plasma and liver was achieved when compared to the animal group which received free RSV. Increase in the plasma concentration of RSV in animals treated with RCL5 could be due to opsonization and phagocytosis of the liposomes. Moreover, the positive charge on the liposomes slow down the absorption rate due to the electrostatic interaction with the negative surface

of the peritoneal mesothelium, consequently with a low uptake of positive liposomes by peritoneal macrophages (83). Tissue distribution and clearance of the RSV followed by intraperitoneal injection of RCL5 is mainly dependent on the vesicle size distribution for the optimized liposomes. Results shows that administration of cationic liposomes showed maximum RSV concentration in liver followed by spleen (Cmax 2.82 μg/ml) with the half life of 30 min as compared to other organs. Maximum concentration of RSV in liver for animals which received RCL5 could be due to EPR effect and/or electrostatic interaction. Electrostatic interaction between the negatively charged hepatocellular cancer cells and positively charged liposomes makes this drug delivery system as a potential way of targeting anticancer drugs to liver cancer. Generally, liver is comprised of phosphatidylserine (PS) which is positioned internally (unexposed) in normal liver tissue and is mediated by a membrane protein or ATP-dependent transporter, amino phospholipid translocase (32,84). This symmetry of PS phospholipid is lost in cancer tissues because of decreased functional activity of enzyme - translocase or oxidative stress in the tumor micro environment or activation of the scramblase enzyme. The loss of symmetry exposes the PS on the surface of cancer tissue which is the salient and universal feature of cancerous cells specifically endothelial cells (ECs) (85,86). Exposure of PS on the surface of cells, known as the death knell, generates a negative charge on liver cancer tissue (31,87). Pharmacokinetic evaluation therefore serve as a clear indicative of this mechanism explaining the use of cationic liposomes as a potential targeting approach to the hepatocellular carcinoma.

Prophylactic and therapeutic, anticancer properties of RSV and RCL5 were assessed in NDEA induced HCC rats. *N*-nitrosodiethylamine (NDEA) a hepatocarcinogen, is known to cause perturbations in the nuclear enzymes involved in deoxyribonucleic

acid (DNA) repair/replication and is normally used as a carcinogen to induce liver cancer in animal models. Experimental, clinical, and epidemiological studies have provided evidence supporting the role of reactive oxygen species in the etiology of cancer. NDEA has been suggested to cause oxidative stress and cellular injury due to the enhanced formation of free radicals (88,89). Aiming to previse the ability of the liposomes, it was found that RCL5 administered either prophylactically or therapeutically significantly ($P<0.001$) reduced the number of neoplastic lesion without causing any changes in the body weight as compare to NDEA administered rat. Though free RSV treated group animals showed decrease in the number of nodules but the results are not significant as the group treated with liposomes. This result corroborates with earlier findings wherein, RSV significantly decrease the incidence and number of nodules in chemically induced HCC animal model (6). RSV has shown to inhibit the hepatic carcinogen-activating enzymes such as cytochrome P450 1A1(CYP1A1) and CYP3A/2 in-vitro and in-vivo. The resultant effects of these enzyme modulation by RSV could be due to the reduced exposure of cells to carcinogensdue to inhibition of carcinogen activation and/or elevated carcinogen detoxification and elimination (5). Administration of NDEA in rats leads to a noticeable rise in levels of serum AST, ALT, ALP total bilirubin and GGT levels, which is an indication of hepatocellular damage. Metabolism of NDEA in the liver induces oxidative stress due to formation of reactive oxygen species (ROS), which results in cellular damage and trigger hepatocyte proliferation, thus leading to the development of HCC (88). Prophylactic and therapeutic treatment with RCL5 to HCC-bearing rats exhibited a significant reduction in the activities of ALT, AST, ALP and GGT as compared to the disease control group. In several diseases raise in serum alpha fetoprotein (AFP) levels has been stated including hepatocellular

carcinoma (88). Like serum protein, AFP is similar in structure, size and amino acid composition to serum albumin; however it is measurable only in minute quantities in the serum of normal adults. It was observed that, exposure of hepatotoxic agents showed elevation in serum concentration of AFP protein in adults. The results showed that preventive and curative treatment with RCL5 significantly decrease ($P<0.001$) the AFP levels as compared to group II HCC bearing rats.

To improve the objectivity and reproducibility of the diagnostic pathology, Histopathological examinations of liver tissues offered another robust testimony for RCL beneficial effects in fighting NDEA-induced HCC. Commensurate with histological outcomes of previous research, administration of NDEA brought severe histopathological alterations in the liver tissue (90), possibly owing to the occurrence of multinucleate cells and tumor cells that shows genetic anomalies and abnormal divisions related with the malignant variations. Evidently, RSV and RCL5 therapies (prophylactic & therapeutic) give rise to marked attenuation in the NDEA-induced alterations in the liver histological architecture and with a relative superiority to RCL5 over free RSV.These results are well in agreement with those reported by Rajasekaran et al., that prophylactic and curative treatment of RSV showed substantial reduction in cell crowding, alteration in the cellular architecture, and decreased in the liver size compared with the NDEA exposed rats (91). In another study, RSV targeted multiple cellular targets like invasion, metastasis, angiogenesis, cellular proliferation and growth - apoptosis, which avoid or slow the advancement of various inflammation-related illnesses, including cancer (6). Based on all in-vitro and in-vivo studies, RCL5 demonstrated improved drug accumulation and has promising anticancer activity and adequate tolerability in NDEA induced HCC in rats.

6. SUMMARY

Resveratrol is a pleiotropic molecule with wide range pharmacological effects such as antiaging, antidiabetic, cardioprotective, antiobesity, antioxidant, and antitumor activities. Mounting evidence suggested that RSV has huge remedial potential in the prevention and treatment of various cancers including cervical cancer, skin cancer, glioblastoma, and prostate cancer. The high therapeutic potential and the multi-targeting ability of RSV makes it a perfect candidate for the treatment of HCC. However, the reduced aqueous solubility and susceptible to oxidative decomposition were the major hindrances for its formulation development. In the present research, resveratrol loaded cationic liposomes (RCL) was formulated and evaluated for their potential in the treatment of HCC. Summary of the present research is described as mentioned below.

1. The preliminary identification of the RSV was done by FTIR and DSC studies. A reversed phase-HPLC method validated in agreement with ICH guidelines was used for the quantification of RSV. Preliminary screening studies were performed to select the levels of formulation variables that can influence the characteristics of liposomes. The RCL was successfully formulated and optimized by using 3^2 factorial design (two-factor, three-level) (3^2) in Design-Expert® software. The two independent variables/factors (SL:Chol molar ratio and SA concentration) were assessed each at 3 altered levels (low, medium and high). The contour graphs and response surface plots were produced to understand the relationship between the dependent and independent variables. According to factorial design, nine formulations were prepared and the optimized batch was selected based on the optimum vesicle size, zeta potential and higher entrapment efficiency. Morphological examination of liposomes was evaluated

by TEM which clearly showed spherical morphology with uniform size distribution. Finally, 5%w/v mannitol (cryoprotectant) was mixed to optimized RCL5 dispersion and lyophilized (CHRIST Alpha 1-2 LD plus, Germany) for further studies. DSC thermograms and FTIR spectroscopic studies confirmed the loading of RSV in liposomes. In-vitro drug release of RSV from optimized RCL5 at pH 5.5 and 7.4 was performed by using ready-to-use dialysis tubes and the release data was subjected in different release kinetic models. The results showed sustained and complete drug release in 48h and Hixon-crowell model was indicated as the best fit model for RSV release from liposomes owing to its maximum R^2 value. Optimized RCL5 formulation was found to stable in both dispersion and lyophilized form after 3 months of storage at 4 ºC.

2. The in-vitro cytocompatibility against normal mouse fibroblast (L929) and cytotoxicity against HepG2 cell line of RSV, BL and optimized RCL5 was investigated by MTT assay. Absence of cytotoxicity against L929 cell lines confirms its cytocompatibility. In cytotoxicity assay RSV and RCL5 showed dose and time dependent changes in which RCL5 confirmed significantly higher cytotoxicity against HepG2 in comparison with free RSV. These findings are also supported by the cell uptake study which suggested improved uptake of RCL5 as compare to free drug.

3. In in-vivo toxicity studies, animals treated with RSV and RCL5 did not induce toxicity in the liver, spleen, and kidneys. The biochemical evaluation was further corroborated with histopathological examinations, suggesting a nontoxic behavior of free RSV and RCL5.

4. In-vivo pharmacokinetic evaluation of RCL5 demonstrated localization of encapsulated RSV in liver cancerous tissues by 3.2- and 2.2-fold increase in AUC and

Cmax, respectively, when compared to those of the free RSV. A pharmacodynamic investigation revealed a significant reduction in hepatocyte nodules and liver marker enzymes in RCL5 treated animals when compared to free RSV. Findings were supported by histopathological analysis, and demonstrate that NDEA induced detrimental effect on rat livers was successfully reversed with the treatment of RCL5 formulation.

7. CONCLUSION

In spite of its well-known application in cancer therapeutics, use of RSV is restricted due to its physiological properties such as poor bioavailability and low half-life. Liposomes are one of the potential formulation systems approved by FDA for application in cancer therapeutics. In the present investigation, we attempted to improve the bio-availability and the kinetic profile of RSV by using cationic liposomes as a carrier for HCC. RCL was successfully prepared and optimized using 3^2 factorial design. The optimized liposomal formulation (RCL5) showed spherical morphology with uniform size with appropriate vesicle size, zeta potential and greater entrapment efficiency. The DSC and FT-IR studies revealed the successful entrapment of RSV into the liposomal vesicular formulation. The in-vitro biocompatible nature of RCL was confirmed by the nonexistence of cytotoxicity against fibroblast (L929) cell lines. In-vitro cell culture assay showed an improved quantitative and qualitative internalization of cationic liposomes in HepG2 cells, resulting in better killing ability towards tumor cell when compared to the free drug. This may possibly due to high affinity of positive charged liposomes towards negative charge of phosphatidylserine exposed on cancer cells. In-vivo pharmacokinetic studies, RCL5 treated animal showed enhanced drug concentration in liver cancer tissue as compared to animals treated with free drug. In-vivo pharmacodynamic investigation demonstrated that RCL exerted both chemopreventive and therapeutic effect on NDEA initiated HCC. According to our result, it can be concluded that the RCL delivery system has a promising potential to treat HCC and will require preclinical efficacy study in large groups to prove the concept.

8. REFERENCES

1. Bray F, Ferlay J, Soerjomataram I, Siegel RL, Torre LA, Jemal A. Global cancer statistics 2018: GLOBOCAN estimates of incidence and mortality worldwide for 36 cancers in 185 countries. CA Cancer J Clin. 2018;68(6):394–424.
2. Daher S, Massarwa M, Benson AA, Khoury T. Current and future treatment of hepatocellular carcinoma: an updated comprehensive review. J Clin Transl Hepatol. 2018;6(1):69.
3. Bteich F, Di Bisceglie AM. Current and future systemic therapies for hepatocellular carcinoma. Gastroenterol Hepatol (N Y). 2019;15(5):266.
4. Llovet JM, Ricci S, Mazzaferro V, Hilgard P, Gane E, Blanc J-F, et al. Sorafenib in advanced hepatocellular carcinoma. N Engl J Med. 2008;359(4):378–90.
5. Bishayee A, Politis T, Darvesh AS. Resveratrol in the chemoprevention and treatment of hepatocellular carcinoma. Cancer Treatment Reviews. 2010;36(1):43-53.
6. Bishayee A, Dhir N. Resveratrol-mediated chemoprevention of diethylnitrosamine-initiated hepatocarcinogenesis: Inhibition of cell proliferation and induction of apoptosis. Chem Biol Interact. 2009;179!2-3):131-144.
7. Simonetti RG, Liberati A, Angiolini C, Pagliaro L. Treatment of hepatocellular carcinoma: a systematic review of randomized controlled trials. Ann Oncol. 1997;8(2):117–136.
8. Kensler TW, Qian G-S, Chen J-G, Groopman JD. Translational strategies for cancer prevention in liver. Nat Rev Cancer. 2003;3(5):321–329.

9. Okusaka T, Ikeda M. Immunotherapy for hepatocellular carcinoma: current status and future perspectives. ESMO open. 2018;3(Suppl 1):e000455.

10. Chikara S, Nagaprashantha LD, Singhal J, Horne D, Awasthi S, Singhal SS. Oxidative stress and dietary phytochemicals: Role in cancer chemoprevention and treatment. Cancer Lett. 2018;413:122–134.

11. Hu Y, Wang S, Wu X, Zhang J, Chen R, Chen M, et al. Chinese herbal medicine-derived compounds for cancer therapy : A focus on hepatocellular carcinoma. J. Ethnopharmacol. 2013;149:601–612.

12. Coimbra M, Isacchi B, van Bloois L, Torano JS, Ket A, Wu X, et al. Improving solubility and chemical stability of natural compounds for medicinal use by incorporation into liposomes. Int J Pharm. 2011;416(2):433–442.

13. Scheepens A, Tan K, Paxton JW. Improving the oral bioavailability of beneficial polyphenols through designed synergies. GENES NUTR. 2010;5(1):75–87.

14. Bishayee A. Cancer Prevention and Treatment with Resveratrol : From Rodent Studies to Clinical Trials. Cancer Prev. Res. 2009;2(5):409–419.

15. Yin S, Xia C, Wang Y, Wan D, Rao J, Tang X, et al. Dual receptor recognizing liposomes containing paclitaxel and hydroxychloroquine for primary and metastatic melanoma treatment via autophagy-dependent and independent pathways. J Control Release. 2018;288:148-160.

16. Öztürk E, Arslan AKK, Yerer MB, Bishayee A. Resveratrol and diabetes: A critical review of clinical studies. Biomedicine and Pharmacotherapy. 2017;95:230-234.

17. Lu Y, Lu X, Wang L, Yang W. Resveratrol attenuates high fat diet-induced mouse cardiomyopathy through upregulation of estrogen related receptor-α.

Eur J Pharmacol. 2019;843:88-95.

18. Jagwani S, Jalalpure S, Dhamecha D, Hua GS, Jadhav K. A Stability Indicating Reversed Phase HPLC Method for Estimation of trans -Resveratrol in Oral Capsules and Nanoliposomes. Anal Chem Lett. 2019;9(5):711-726.
19. Robinson K, Mock C, Liang D. Pre-formulation studies of resveratrol. Drug Dev Ind Pharm. 2015;41(9):1464–1469.
20. Amri A, Chaumeil JC, Sfar S, Charrueau C. Administration of resveratrol: What formulation solutions to bioavailability limitations?. J Control Release. 2012;158(2):182–193.
21. Sallem F, Haji R, Vervandier-Fasseur D, Nury T, Maurizi L, Boudon J, et al. Elaboration of Trans-Resveratrol Derivative-Loaded Superparamagnetic Iron Oxide Nanoparticles for Glioma Treatment. Nanomaterials. 2019;9(2):287.
22. Pangeni R, Sahni JK, Ali J, Sharma S, Baboota S. Resveratrol : review on therapeutic potential and recent advances in drug delivery. Expert Opin. Drug Deliv. 2014;11(8):1285–1298.
23. Smoliga JM, Blanchard O. Enhancing the Delivery of Resveratrol in Humans: If Low Bioavailability is the Problem, What is the Solution? Molecules. 2014;19(11):17154–17172.
24. Hossen S, Hossain MK, Basher MK, Mia MNH, Rahman MT, Uddin MJ. Smart nanocarrier-based drug delivery systems for cancer therapy and toxicity studies: A review. J Adv Res. 2019;15:1–18.
25. Alexis F, Pridgen EM, Langer R, Farokhzad OC. Nanoparticle technologies for cancer therapy. InDrug delivery. Springer; 2010:55–86.
26. Bozzuto G, Molinari A. Liposomes as nanomedical devices. Int J Nanomedicine. 2015;10:975.

27. Alexis F, Pridgen EM, Langer R, Farokhzad OC. Drug Delivery. Schäfer-Korting M, editor. Berlin, Heidelberg: Springer Berlin Heidelberg; 2010 [cited 2015 Apr 16]. (Handbook of Experimental Pharmacology; vol. 197). Available from: http://link.springer.com/10.1007/978-3-642-00477-3

28. Sercombe L, Veerati T, Moheimani F, Wu SY, Sood AK, Hua S. Advances and challenges of liposome assisted drug delivery. Front. Pharmacol. 2015;6:286.

29. Alavi M, Hamidi M. Passive and active targeting in cancer therapy by liposomes and lipid nanoparticles. Drug Metab Pers Ther. 2019;34(1).

30. Felgner PL, Gadek TR, Holm M, Roman R, Chan HW, Wenz M, et al. Lipofection: a highly efficient, lipid-mediated DNA-transfection procedure. Proc Natl Acad Sci. 1987;84(21):7413–7417.

31. De M, Ghosh S, Sen T, Shadab M, Banerjee I, Basu S, et al. A Novel Therapeutic Strategy for Cancer Using Phosphatidylserine Targeting Stearylamine-Bearing Cationic Liposomes. Mol Ther - Nucleic Acids [Internet]. 2018;10(March):9–27. Available from: https://doi.org/10.1016/j.omtn.2017.10.019

32. Soares MM, King SW, Thorpe PE. Targeting inside-out phosphatidylserine as a therapeutic strategy for viral diseases. Nat Med. 2008;14(12):1357-1362.

33. Deshpande PP, Biswas S, Torchilin VP. Current trends in the use of liposomes for tumor targeting. Nanomedicine. 2013;8(9):1509–1528.

34. Torchilin VP. Passive and active drug targeting: drug delivery to tumors as an example. In: Drug delivery. Springer; 2010; 3–53.

35. Llovet JM, Villanueva A, Lachenmayer A, Finn RS. Advances in targeted therapies for hepatocellular carcinoma in the genomic era. Nature Reviews Clinical Oncology. 2015;12(7):408.

36. Li Y, Martin RCG. Herbal medicine and hepatocellular carcinoma: applications and challenges. Evid Based Complement Alternat Med [Internet]. 2011 Jan [cited 2015 Apr 11];2011:541209. Available from: http://www.pubmedcentral.nih.gov/articlerender.fcgi?artid=3140057&tool=pmcentrez&rendertype=abstract

37. Athar M, Back JH, Kopelovich L, Bickers DR, Kim AL. Multiple molecular targets of resveratrol: Anti-carcinogenic mechanisms. Arch Biochem Biophys. 2009;486(2):95–102.

38. Bishayee A, Dhir N. Resveratrol-mediated chemoprevention of diethylnitrosamine-initiated hepatocarcinogenesis: inhibition of cell proliferation and induction of apoptosis. Chem Biol Interact. 2009;179(2–3):131–144.

39. Bu L, Gan L-C, Guo X-Q, Chen F-Z, Song Q, Gou X-J, et al. Trans-resveratrol loaded chitosan nanoparticles modified with biotin and avidin to target hepatic carcinoma. Int J Pharm. 2013;452(1–2):355–362.

40. Bilensoy E. Cationic nanoparticles for cancer therapy. Expert Opin Drug Deliv. 2010;7(7):795–809.

41. Wang M, Liu Y, Zhang X, Luo L, Li L, Xing S, et al. Gold nanoshell coated thermo-pH dual responsive liposomes for resveratrol delivery and chemo-photothermal synergistic cancer therapy. J Mater Chem B. 2017;5(11)2161-2171.

42. Cosco D, Paolino D, Maiuolo J, Marzio L Di, Carafa M, Ventura CA, et al. Ultradeformable liposomes as multidrug carrier of resveratrol and 5-fluorouracil for their topical delivery. Int J Pharm. 2015;489(1-2):1-0.

43. Caddeo C, Teskač K, Sinico C, Kristl J. Effect of resveratrol incorporated in

liposomes on proliferation and UV-B protection of cells. Int J Pharm. 2008;363(1–2):183–191.

44. Caddeo C, Nacher A, Vassallo A, Armentano MF, Pons R, Fernàndez-Busquets X, et al. Effect of quercetin and resveratrol co-incorporated in liposomes against inflammatory/oxidative response associated with skin cancer. Int J Pharm. 2016;513(1-2):153-163.

45. Jhaveri A, Deshpande P, Pattni B, Torchilin V. Transferrin-targeted, resveratrol-loaded liposomes for the treatment of glioblastoma. J Control Release. 2018;277:89-101.

46. Pozo-Guisado E, Merino JM, Mulero-Navarro S, Lorenzo-Benayas MJ, Centeno F, Alvarez-Barrientos A, et al. Resveratrol-induced apoptosis in MCF-7 human breast cancer cells involves a caspase-independent mechanism with downregulation of Bcl-2 and NF-κB. Int J Cancer. 2005;115(1):74-84.

47. Narayanan NK, Nargi D, Randolph C, Narayanan BA. Liposome encapsulation of curcumin and resveratrol in combination reduces prostate cancer incidence in PTEN knockout mice. Int J Cancer. 2009;125(1):1-8.

48. ICH I. ICH Harmonised Tripartite Guideline: Validation of Analytical Procedures. InMethodology, Q2 (R1), International Conference on Harmonisation of Technical Requirements fot Registrations of Pharmaceuticals for Human Use (ICH) 2005.

49. Bangham AD, Standish MM, Watkins JC. Diffusion of univalent ions across the lamellae of swollen phospholipids. Journal of molecular biology. 1965;13(1):238-IN27.

50. Jain S, Kumar D, Swarnakar NK, Thanki K. Polyelectrolyte stabilized multilayered liposomes for oral delivery of paclitaxel. Biomaterials.

2012;33(28):6758-68.

51. Yang T, Cui FD, Choi MK, Cho JW, Chung SJ, Shim CK, Kim DD. Enhanced solubility and stability of PEGylated liposomal paclitaxel: in vitro and in vivo evaluation. Int. J. Pharm. 2007;338(1-2):317-26.

52. Hioki A, Wakasugi A, Kawano K, Hattori Y, Maitani Y. Development of an in vitro drug release assay of PEGylated liposome using bovine serum albumin and high temperature. Biol. Pharm. Bull. 2010;33(9):1466-70.

53. Shah SM, Goel PN, Jain AS, Pathak PO, Padhye SG, Govindarajan S, Ghosh SS, Chaudhari PR, Gude RP, Gopal V, Nagarsenker MS. Liposomes for targeting hepatocellular carcinoma: use of conjugated arabinogalactan as targeting ligand. Int. J. Pharm. 2014;477(1-2):128-39.

54. Karn PR, Cho W, Park HJ, Park JS, Hwang SJ. Characterization and stability studies of a novel liposomal cyclosporin A prepared using the supercritical fluid method: comparison with the modified conventional Bangham method. Int J Nanomedicine. 2013;8:365.

55. Dhamecha D, Jalalpure S, Jadhav K, Jagwani S, Chavan R. Doxorubicin loaded gold nanoparticles: Implication of passive targeting on anticancer efficacy. Pharmacol Res. 2016;113:547-56.

56. Rajeshwari HR, Dhamecha D, Jagwani S, Patil D, Hegde S, Potdar R, Metgud R, Jalalpure S, Roy S, Jadhav K, Tiwari NK. Formulation of thermoreversible gel of cranberry juice concentrate: Evaluation, biocompatibility studies and its antimicrobial activity against periodontal pathogens. Mater Sci Eng C. 2017;75:1506-14.

57. Garg NK, Singh B, Kushwah V, Tyagi RK, Sharma R, Jain S, et al. The ligand (s) anchored lipobrid nanoconstruct mediated delivery of methotrexate: An

effective approach in breast cancer therapeutics. Nanomedicine Nanotechnology, Biol Med. 2016;12(7):2043-2060.

58. El Mesallamy HO, Metwally NS, Soliman MS, Ahmed KA, Abdel Moaty MM. The chemopreventive effect of Ginkgo biloba and Silybum marianum extracts on hepatocarcinogenesis in rats. Cancer Cell Int. 2011;11(1):38.

59. Abdel Messih HA, Ishak RAH, Geneidi AS, Mansour S. Nanoethosomes for transdermal delivery of tropisetron HCl: multi-factorial predictive modeling, characterization, and ex vivo skin permeation. Drug Dev Ind Pharm. 2017;43(6):958–71.

60. Shelke S, Shahi S, Jalalpure S, Dhamecha D. Poloxamer 407-based intranasal thermoreversible gel of zolmitriptan-loaded nanoethosomes: Formulation, optimization, evaluation and permeation studies. J Liposome Res. 2016;26(4):313–23.

61. Aggarwal N, Goindi S. Dermatopharmacokinetic and pharmacodynamic evaluation of ethosomes of griseofulvin designed for dermal delivery. J nanoparticle Res. 2013;15(10):1983.

62. Kotyńska J, Figaszewski ZA. Adsorption equilibria at interface separating electrolyte solution and phosphatidylcholine–stearylamine liposome membrane. Biophys Chem. 2007;127(1–2):84–90.

63. Akbarzadeh A, Rezaei-Sadabady R, Davaran S, Joo SW, Zarghami N, Hanifehpour Y, et al. Liposome: classification, preparation, and applications. Nanoscale Res Lett. 2013;8(1):102.

64. Mirahmadi N, Babaei MH, Valia M, Dadashzadeh S. Effect of liposome size on peritoneal retention and organ distribution after intraperitoneal injection in mice. Int J Pharm. 2010;383(1–2):7–13.

65. El Maghraby GMM, Campbell M, Finnin BC. Mechanisms of action of novel skin penetration enhancers: phospholipid versus skin lipid liposomes. Int J Pharm. 2005;305(1–2):90–104.

66. Dhamecha D, Jalalpure S, Jadhav K. Nepenthes khasiana mediated synthesis of stabilized gold nanoparticles: characterization and biocompatibility studies. J Photochem Photobiol B Biol. 2016;154:108–117.

67. Casals E, Soler M, Gallardo M, Estelrich J. Electrophoretic behavior of stearylamine-containing liposomes. Langmuir. 1998;14(26):7522-7526.

68. González-Rodríguez ML, Rabasco AM. Charged liposomes as carriers to enhance the permeation through the skin. Expert Opinion on Drug Delivery. 2011;8(7)857-871.

69. Mbah CC, Builders PF, Attama AA. Nanovesicular carriers as alternative drug delivery systems :ethosomes in focus. Expert Opin Drug Deliv. 2014;11(1):45–59.

70. Abdellatif MM, Khalil IA, Khalil MAF. Sertaconazole nitrate loaded nanovesicular systems for targeting skin fungal infection: In-vitro, ex-vivo and in-vivo evaluation. Int J Pharm. 2017;527(1-2):1.

71. Wan S, Zhang L, Quan Y, Wei K. Resveratrol-loaded PLGA nanoparticles: Enhanced stability, solubility and bioactivity of resveratrol for non-alcoholic fatty liver disease therapy. R Soc Open Sci. 2018;5(11):181457.

72. Hammoud Z, Gharib R, Fourmentin S, Elaissari A, Greige-Gerges H. Drug-in-hydroxypropyl-β-cyclodextrin-in-lipoid S100/cholesterol liposomes: Effect of the characteristics of essential oil components on their encapsulation and release. Int J Pharm. 2020;579:119151.

73. Karve S, Kempegowda GB, Sofou S. Heterogeneous domains and membrane

permeability in phosphatidylcholine - Phosphatidic acid rigid vesicles as a function of pH and lipid chain mismatch. Langmuir. 2008;24(11):5679-5688.

74. Shishir MRI, Karim N, Gowd V, Xie J, Zheng X, Chen W. Pectin-chitosan conjugated nanoliposome as a promising delivery system for neohesperidin: Characterization, release behavior, cellular uptake, and antioxidant property. Food Hydrocoll. 2019;95:432-444.

75. BrushiML. Mathematical models of drug release. In: Strategies to Modify the Drug Release from Pharmaceutical Systems. 2015.

76. Wójcik-Pastuszka D, Krzak J, Macikowski B, Berkowski R, Osiński B, Musiał W. Evaluation of the release kinetics of a pharmacologically active substance from model intra-articular implants replacing the cruciate ligaments of the knee. Materials (Basel). 2019;12(8):1202.

77. Mahmoudi M, Simchi A, Milani AS, Stroeve P. Cell toxicity of superparamagnetic iron oxide nanoparticles. J Colloid Interface Sci. 2009;336(2):510-518.

78. Wang H, Thorling CA, Liang X, Bridle KR, Grice JE, Zhu Y, et al. Diagnostic imaging and therapeutic application of nanoparticles targeting the liver. Journal of Materials Chemistry B. 2015;3(6):939-958.

79. Treuel L, Jiang X, Nienhaus GU. New views on cellular uptake and trafficking of manufactured nanoparticles. Journal of the Royal Society Interface. 2013;10(82):20120939.

80. Gubernator J. Active methods of drug loading into liposomes : recent strategies for stable drug entrapment and increased in vivo activity. 2011;8(5):565–580.

81. Saadat M, Zahednezhad F, Zakeri-Milani P, Heidari HR, Shahbazi-Mojarrad J, Valizadeh H. Drug targeting strategies based on charge dependent uptake of

nanoparticles into cancer cells. J Pharm Pharm Sci. 2019;22:191–220.

82. Behzadi S, Serpooshan V, Tao W, Hamaly MA, Alkawareek MY, Dreaden EC, et al. Cellular uptake of nanoparticles: Journey inside the cell. Chemical Society Reviews. 2017;46(14):4218-4244.

83. De Smet L, Ceelen W, Remon JP, Vervaet C. Optimization of Drug Delivery Systems for Intraperitoneal Therapy to Extend the Residence Time of the Chemotherapeutic Agent. Sci World J. 2013;2013.

84. Kenis H, Reutelingsperger C. Targeting Phosphatidylserine in Anti-Cancer Therapy. Curr Pharm Des. 2009;15(23):2719–2723.

85. Fidler IJ, Schroit AJ, Connor J, Bucana CD, Fidler IJ. Elevated Expression of Phosphatidylserine in the Outer Membrane Leaflet of Human Tumor Cells and Recognition by Activated Human Blood Monocytes. Cancer Res. 1991;51(11):3062-3066.

86. Riedl S, Rinner B, Asslaber M, Schaider H, Walzer S, Novak A, et al. In search of a novel target - Phosphatidylserine exposed by non-apoptotic tumor cells and metastases of malignancies with poor treatment efficacy. Biochim Biophys Acta - Biomembr. 2011;1808(11):2638-2645.

87. Ran S, Downes A, Thorpe PE. Increased exposure of anionic phospholipids on the surface of tumor blood vessels. Cancer Res. 2002;62(21):6132-6140.

88. Rajesh V, Kavitha KNVK, Vishali K, Raju C, Gayathri K, Sruthi A. Protective effect Courouptia guianensis flower extract against N-nitrosodiethylamine-induced hepatic damage in wistar albino rats. Orient Pharm Exp Med. 2015;15(1):83-93.

89. Farazuddin M, Dua B, Zia Q, Khan AA, Joshi B, Owais M. Chemotherapeutic potential of curcumin-bearing microcells against hepatocellular carcinoma in

model animals. Int J Nanomedicine. 2014;9:1139.

90. Zhu X, Tsend-Ayush A, Yuan Z, Wen J, Cai J, Luo S, et al. Glycyrrhetinic acid-modified TPGS polymeric micelles for hepatocellular carcinoma-targeted therapy. Int J Pharm. 2017;529(1-2):451-464.

91. Rajasekaran D, Elavarasan J, Sivalingam M, Ganapathy E, Kumar A, Kalpana K, et al. Resveratrol interferes with N-nitrosodiethylamine-induced hepatocellular carcinoma at early and advanced stages in male Wistar rats. Mol Med Rep. 2011;4(6):1211-1217.

9. ANNEXURES

Animal ethical committee approval letter

KLE University's
College of Pharmacy
(Recognized by PCI, AICTE & Accredited by NBA & 'A' grade By NAAC)
A constituent Unit of KLE Academy of Higher Education and Research
[Under section 3UGC Act, 1956 vide Govt. of India Notification No. F.9-19/2000-U.3 (A)]
Nehru Nagar, Belagavi – 590 010, Karnataka, India
Phone: 0831-2471399 **Fax:** 0831-2472387 **Web:** http://www.klepharm.edu **E-mail:** principal@klepharm.edu

Ref: No. KLEUCOP/_____ Date: 10/10/15

CERTIFICATE

This is to certify that the research project," **Evaluation of the chemotherapeutic potential of resveratol entrapped nanoliposomes for targeting hepatocellular carcinoma",** Submitted by **Mr.SatveerJagwani** has been approved in the Institutional Animal Ethics Committee meeting held on 10th October 2015, resolution No. KLECOP/IAEC/Res.22-10/10/2015 and was permitted to use ---------- 72- male Rats/ Mice/ Rabbits/Guinea pig.

You are hereby informed to strictly adhere to the protocol submitted for approval. Further you are required to keep the account of animals used for the project in specified Performa, **Form D.**

MEMBER SECRETARY
Institutional Animal Ethical Committee,
KLES's College of Pharmacy,
BELGAUM - 590010

10/10/2015
CPCSEA Nominee
Institutional Animal Ethics Committee
KLES's College of Pharmacy,
BELGAUM.

ACS Biomaterials SCIENCE & ENGINEERING

pubs.acs.org/journal/abseba Article

Pharmacokinetic and Pharmacodynamic Evaluation of Resveratrol Loaded Cationic Liposomes for Targeting Hepatocellular Carcinoma

Satveer Jagwani,*,⊥ Sunil Jalalpure,* Dinesh Dhamecha,⊥ Kiran Jadhav, and Raghvendra Bohara

Cite This: https://dx.doi.org/10.1021/acsbiomaterials.0c00429 Read Online

ACCESS | Metrics & More | Article Recommendations | Supporting Information

ABSTRACT: Hepatocellular carcinoma (HCC) is one of the leading causes of cancer-related death worldwide. The destructive nature of the disease makes it difficult for clinicians to manage the condition. Hence, there is an urgent need to find new alternatives for HCC, as the role of conventional cytotoxic drugs has reached a plateau to control HCC associated mortality. Antioxidant compounds of plant origin with potential anti-tumor effect have been recognized as alternate modes in cancer treatment and chemoprevention. Resveratrol (RS) is a model natural nonflavonoid drug known for its anti-cancer activity. However, its clinical application is limited due to its poor bioavailability. The current research work aims to formulate, optimize, and characterize RS loaded cationic liposomes (RLs) for specific delivery in HCC. The optimized liposomes formulation (RL5) was spherical with a vesicle size (VS) of 145.78 ± 9.9 nm, ζ potential (ZP) of 38.03 ± 9.12 mV, and encapsulation efficiency (EE) of 78.14 ± 8.04%. *In vitro* cytotoxicity studies in HepG2 cells demonstrated an improved anti-cancer activity of RL5 in comparison with free RS. These outcomes were supported by a cell uptake study in HepG2 cells, in which RL5 exhibited a higher uptake than free RS. Furthermore, confocal images of HepG2 cells after 3 and 5 h of incubation showed higher internalization of coumarin 6 (C6) loaded liposomes (CL) as compared to those of the free C6. Pharmacokinetic and pharmacodynamic (prophylactic and therapeutic treatment modalities) studies were performed in *N*-nitrosodiethylamine (NDEA-carcinogen) induced HCC in rats. Pharmacokinetic evaluation of RL5 demonstrated increased localization of RS in cancerous liver tissues by 3.2- and 2.2-fold increase in AUC and Cmax, respectively, when compared to those of the free RS group. A pharmacodynamic investigation revealed a significant reduction in hepatocyte nodules in RL5 treated animals when compared to those of free RS. Further, on treatment with RL5, HCC-bearing rats showed a significant decrease in the liver marker enzymes (alanine transaminase, alkaline phosphatase, aspartate transaminase, total bilirubin levels, γ-glutamyl transpeptidase, and α-fetoprotein), in comparison with that of the disease control group. Our findings were supported by histopathological analysis, and we were first to demonstrate that NDEA induced detrimental effect on rat livers was successfully reversed with the treatment of RL5 formulation. These results implied that delivery of RS loaded cationic liposomes substantially controlled the severity of HCC and that they can be considered as a promising nanocarrier in the management of HCC.

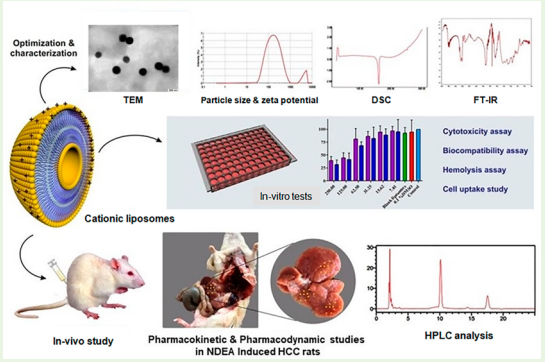

KEYWORDS: *Resveratrol, cationic liposomes, biocompatibility, hepatocellular carcinoma, pharmacokinetics, pharmacodynamics*

1. INTRODUCTION

Noncommunicable diseases (NCD) are one of the significant causes of mortality in the 21st century, in which cancer stands on top of the list, reducing the life expectancy to significant levels worldwide. As per the GLOBOCAN 2018 report, cancer accounts for 20.3, 14.4, 57.3, and 7.3% mortality rates in Europe, USA, Asia, and Africa, respectively.[1] Hepatocellular carcinoma (HCC) is the fourth-leading cause of cancer-related deaths, which has led to a total of 841 080 new cases and 781 631 deaths in the year 2018 worldwide. Hence, there is an alarming need to improve novel drug delivery strategies in HCC.[1]

Currently, HCC is treated with invasive surgical and chemotherapeutical approaches, which often lead to serious side effects such as hand−foot syndrome and gastrointestinal, skin, and endocrine disorders.[2] Furthermore, these conventional approaches have not been successful in reducing the overall mortality rate. Currently, sorafenib (Nexavar) is the only USFDA approved drug for systemic administration in the management of advanced HCC. Active efforts have been made in the past to develop similar therapies, with some of the ongoing phases III trials focused on shedding light on cancer therapy with better outcomes and minimal/no side effects.[3]

Received: March 26, 2020
Accepted: July 27, 2020
Published: July 27, 2020

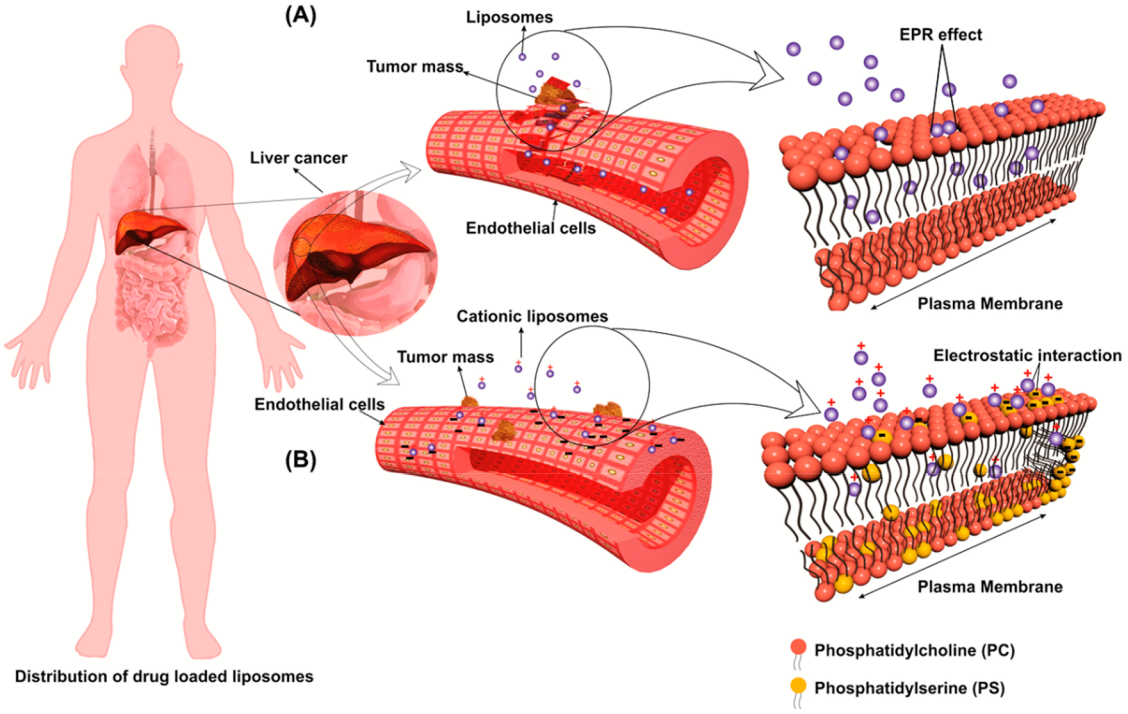

Figure 1. Depicting the mechanism of accumulation/targeting of cationic liposomes in the liver cancer. (A) Enhanced permeability and retention effect (EPR) in which the RLs with appropriate sizes (<200 nm) extravasate through large fenestrations between the tumor blood capillary endothelium (leaky endothelium) and enters the interstitial space. The gaps between the cancer endothelial cells are in the range 100−780 nm as opposed to those of a healthy endothelium, which are 5−10 nm. (B) Targeting of RLs based on the electrostatic interaction between anionic liver cells and cationic liposomes. In the plasma membrane of normal healthy cells, lipids are asymmetrically distributed across the inner and outer leaflets, with phosphatidylserine (PS) being the most abundant anionic phospholipid located predominantly on the inner leaflet. Due to the activation of the scramblase enzyme or oxidative stress in the tumor microenvironment, the symmetry of plasma membrane is lost, resulting in the exposure of PS on the surface, which is a unique feature of cancerous cells. RS loaded cationic liposomes are an easy way to target the anionic moiety of plasma membrane due to electrostatic interaction between them.

In the human body, the liver is the main detoxifying organ responsible for eliminating the metabolic byproducts/toxins to achieve homeostasis. However, the liver is susceptible to the accumulation of reactive oxidative species (ROS) due to imbalance between pro-oxidant and antioxidant compounds. Scientific literature suggests that there is a significant correlation between the increased levels of oxidative stress generated by these reactive oxygen species (ROS) and the severity of chronic liver diseases. It should be noted that HCC occurs in the background of chronic liver disease, making it often difficult to diagnosis at an initial stage.[4]

Antioxidant compounds of plant origin with potential anti-tumor effects have been recognized as alternate modes in cancer chemoprevention. Different phytochemicals, including nutrients and dietary agents, have been found to be effective against numerous types of cancers. Among the various available groups of natural products and plant metabolites, resveratrol (RS), a phytoalexin (plant antibiotic and anti-oxidant) found in peanuts, grapes, pines, berries, and various herbs such as *Polygonum cuspidatum* and *Vitis vinifera* L., plays an essential role as an antioxidant,[5] anti-tumor,[6] anti-aging,[7] anti-diabetic,[8] anti-inflammatory,[9] cardioprotective,[10] and anti-obesity.[11]

Looking toward the potential benefits of RS, its use in prophylaxis and therapeutics would be of great importance in the treatment of HCC. However, the use of free RS in the treatment of human cancer possesses certain limitations owing to the rapid metabolism and swift elimination from systemic circulation, resulting in low bioavailability (<1% oral viability) and low biological half-life (30−45 min).[12,13] Among several nanoparticles (poly-lactic-*co*-glycolic acid,[14,15] gold,[16,17] silver,[18] liposomes,[19] etc.) approaches, liposomes are the most successfully nanoscale formulations used to deliver therapeutic drugs and imaging agents. Encapsulating drugs in lipids offers structural properties similar to the natural cellular biomembrane, which provides several advantages including biocompatibility, higher stability, sustained release of the drug, biodegradability, safety, and industrial scalability.[20−22] Though there are reports for the use of RS loaded liposomes (RLs) in cancers such as cervical cancer,[23] skin cancer,[24−26] glioblastoma,[27] breast cancer,[28] and prostate cancer,[29] the efficacy of RL was never assessed for its use in the treatment of HCC. In HCC, the physiological changes in the surface properties of liver tissue generate large fenestration in the endothelium and anionic charge due to exposed phosphatidylserine (PS). These anionic moieties are exposed to the outer surface, which makes it an easy target to attract cationic liposomes for active targeting of liposomes. A schematic diagram depicting the probable targeting mechanism is shown in Figure 1.[30,31]

With this background, the present study aimed to encapsulate RS in a unique blend of a lipid and cationic charge generator for the formulation of cationic liposomes for selective delivery in HCC. The performance of optimized RL5 was evaluated with *in vitro* cytotoxicity assay, cellular uptake, *in vitro* cytocompatibility, *in vivo* pharmacokinetic profile, and pharmacodynamic study in NDEA induced HCC-bearing rats.

https://dx.doi.org/10.1021/acsbiomaterials.0c00429
ACS Biomater. Sci. Eng. XXXX, XXX, XXX−XXX

Table 1. Independent and Dependent Variables Used in the 3^2 Factorial Design Approach for Optimizing Liposomal Formulation[a]

Independent variables	levels			Dependent variables
	−1	0	+1	
molar ratio of SL/Chol	6:2	7:2	8:2	
concentration of SL and Chol (mg) based on molar ratio	343:57	350:50	357:43	vesicle size (VS), ζ potential (ZP), and encapsulation efficiency (EE)
concentration of SA (mg)	2.5	5.0	7.5	

[a]Concentrations of all the excipients are mentioned for the final batch of 20 mL with 20 mg of resveratrol (RS). SL, soya lecithin; Chol, cholesterol; SA, stearyl amine.

2. MATERIALS AND METHODS

2.1. Materials. RS (>98%) was supplied by M/s Sami Laboratories (Bangalore, India). Lipoid S100 soyalecithin (N94% phosphatidylcholine, SL) was provided by Lipoid GmbH, Ludwigshafen, Germany. Cholesterol (Chol) was purchased from Loba Chemie Pvt. Ltd., Mumbai, India. HPLC-grade acetonitrile was purchased from M/s Merck, Mumbai, India, and *N*-nitrosodiethylamine (NDEA-N0258), coumarin6 (442631), and stearylamine (SA-74750) were purchased from Sigma-Aldrich, Bangalore, India. Serum aspartate amino transferase (AST), serum alanine transaminase (ALT), alkaline phosphatase (ALP), total bilirubin (TB), total protein (TP), and γ-glutamyl transpeptidase (GGT) kits were purchased from ERBA Diagnostics Mannheim GmbH, Bangalore India. Rat α-fetoprotein (AFP) ELISA kit was purchased from Qayee-Biotechnology Co., Ltd., New Delhi, India. HepG2 cell lines and normal mouse fibroblasts were obtained from the National Centre of Cell Sciences, Pune, India. Fetal bovine serum (FBS), Pen-Strep (a mixture of streptomycin and penicillin), and Dulbecco's modified eagle medium (DMEM) were procured from HiMedia Laboratories Pvt. Ltd., Bangalore, India.

2.2. Preparation of Resveratrol Entrapped Cationic Liposomes. On the basis of preliminary studies, a 3^2 factorial approach (Design Expert Software (version 7, State-Ease Inc.) was used to optimize the RLs, in which the molar ratios of soya lecithin/cholesterol (SL/Chol) and SA were selected as independent variables. The mean vesicle size (VS), ζ potential (ZP), and encapsulation efficiency (EE) were selected as dependent variables (Table 1). The generated polynomial equation was used for the evaluation of the response,

$$Y = b_0 + b_1X_1 + b_2X_2 + b_{12}X_1X_2 + b_{11}X_1^2 + b_{22}X_2^2 \quad (1)$$

RLs were prepared by a thin film hydration method, as described by Bangham et al. in 1965.[32] Briefly, RS (20 mg), SA, SL, and Chol were solubilized in the mixture of organic solvent chloroform and methanol (2:1 v/v). The organic solvent was evaporated on rotavapor R-210 under reduced pressure (vacuum pump, V-700 Buchi) for 1 h at 40 °C to obtain a thin film. The film was then treated with a stream of nitrogen gas and kept in a vacuum overnight to remove any final traces of solvents. The lipid film was hydrated at 40 °C with 20 mL of phosphate buffer (pH 6.4) to aid in the formation of liposomes. Formulated RLs were sonicated for 2 min on an ice bath using a high intensity probe ultrasonic generator (Rivotek) with a probe diameter of 15 mm (15 s on/off pulse). Following sonication, the resulting liposome dispersion was centrifuged (Kubota 6500) at 2000 rpm at 4 °C for 10 min to separate the undissolved RS. RLs were then filtered five times using syringe filters (0.44 and 0.22 μm) successively to yield monodispersed RLs. Finally, cryoprotectant (mannitol 5% w/v) was added to RL dispersion and lyophilized (CHRIST Alpha 1−2 LD plus) for further studies. For lyophilization, the RL dispersion was frozen at −80 °C for 24 h, followed by freeze-drying for 48 h. The lyophilizer was set with −55 °C as the condenser temperature and 0.023 mbar as the vacuum pressure. The lyophilized formulation was evaluated for the appearance of the cake, reconstitution time, ZP, VS, and EE.[33]

2.3. Characterization of Liposomes. Dynamic light scattering (zetasizer Nano-ZS90, Malvern Instruments) was used to measure VS, PDI, and ZP of all RL formulations, and the surface morphology was analyzed by using a transmission electron microscope (TEM; Philips CM12 Electron Microscope). For TEM analysis, the aqueous dispersion of RL5 was stained with 1% phosphotungustic acid (sequential two-droplet method) and was visualized under TEM. For Fourier transform infrared spectroscopy (FT-IR, Shimadzu), each chemical components of the formulation and lyophilized RL were analyzed using a KBr pellet technique. For differential scanning colorimetry (DSC) studies, dried samples of raw material and optimized RLs were analyzed by using a DSC 823 instrument (Mettler Toledo,). Briefly, each sample (4−5 mg) was weighed, compressed into an aluminum pan, and scanned in the temperature range from 50 to 300 °C at a heating rate of 10 °C/min.

2.4. Estimation of Entrapment Efficiency (EE) and Drug Loading (DL). The EE of RLs was determined using an indirect method,[34] which involves measuring the amount of free drug available in nano dispersion. RL dispersion was centrifuged (Kubota 6500) at 2000 rpm (using rotor model AG-1212) at 4 °C for 10 min, and the supernatant was then separated. The pellet of the unentrapped drug (free drug) was determined by using a reverse-phase HPLC method.[13] The EE and DL[35] were calculated by the formulas shown below.

$$\text{percent EE} = \frac{(\text{WT} - \text{WF})}{\text{WT}} \times 100 \quad (2)$$

$$\text{percent DL} = \frac{\text{WR}}{\text{WL}} \times 100 \quad (3)$$

where WT is the weight of RS used for liposome formation, WFis the weight of unencapsulated RS, WR is the weight of RS in liposomes, and WL is the total weight of lipid and RS added in formulation.

2.5. *In Vitro* Drug Release and Release Kinetic Studies of RL. *In vitro* release of RS from liposomes was performed by ready-to-use dialysis tubes (Spectrum Laboratories, Rancho Dominguez, CA) having a MWCO of 12 400 Da, a pore size of <10 nm, and 10 cm length with a membrane diameter of 10 mm with a seal at one end and attached to a floatable cap. Release studies were performed in phosphate buffer saline (PBS) (pH 7.4- simulated blood pH) and PBS (pH 5.5- simulated tumor micro environment pH), both containing 0.1% v/v polyethylene glycol (PEG-400) to solubilize the released RS. Briefly, RL5 (5 mL equivalent to 4 mg RS) was transferred to dialysis bag, which was immersed into a 200 mL bottle containing 100 mL of PBS (pH 5.5 and 7.4). Bottles were placed on a magnetic stirrer pre-equilibrated at 37 ± 0.5 °C with a stirring speed of 100 rpm. At specific time intervals, the aliquots (0.5 mL) were withdrawn and replaced with an equal amount of fresh PBS. All aliquots were filtered by using a 0.45 μm syringe filter, and the amount of RS released was analyzed by HPLC.[36,37] In order to understand the drug release mechanism of optimized formulation (RL5), different kinetics models such as zero order, first order, Higuchi model, Korsmeyer -Peppas model, and Hixson Crowell model were evaluated. The best model was evaluated on the basis of the maximum value of the correlation coefficient (R^2).[36]

2.6. Stability Studies of RL. RL5 dispersion and lyophilized formulations were stored at 4 °C over a period of 3 months for stability studies. Both RL5 dispersion and lyophilized form were evaluated for VS, ZP, and EE for confirmation of stability.[33,38] After 3 months, the dispersion was centrifuged for 10 min at 2000 rpm and the supernatant liposomes were evaluated for the entrapped RS.

https://dx.doi.org/10.1021/acsbiomaterials.0c00429
ACS Biomater. Sci. Eng. XXXX, XXX, XXX−XXX

Table 2. Experimental Groups Used in the Study to Evaluate the Effect of Prophylactic and Therapeutic Treatment in HCC Induced Rats[a]

Group I (normal group)	rats fed with standard diet and were administered with vehicle (a mixture of 1% DMSO and 1% Tween 80 in PBS) twice a week.
Group II (disease control)	NDEA (carcinogen) intragastric administration until the 12th week
	prophylactic treatment
Group III received RS	NDEA administration until 12th week + simultaneous intraperitoneal dosing of RS (20 mg/kg body weight/twice a week)
Group IV received RL5	NDEA administration until 12th week + simultaneous intraperitoneal dosing of RL5 (equivalent to RS 20 mg/kg body weight/twice a week)
	therapeutic treatment
Group V received RS	NDEA administration until 12th week + intraperitoneal dosing of RS (20 mg/kg body weight/twice a week) starting from 9th week
Group VI received RL5	NDEA administration until 12th week + intraperitoneal dosing of RL5 (equivalent to RS 20 mg/kg body weight/twice a week) starting from 9th week

[a]Note: RS, resveratrol; RL5, optimized RS loaded liposomes; NDEA, *N*-nitrosodiethylamine.

Liposomes were dissolved in chloroform and methanol mixture to solubilize the lipids and RS. The solution was then diluted with acetonitrile (a component of HPLC solvent system), followed by centrifugation and filtration by using syringe filter (0.45 μm) for HPLC analysis.

2.7. *In Vitro* Biocompatibility Studies. *2.7.1. Blood Compatibility (Hemolysis Assay).* The blood biocompatibility of RL5 was confirmed by an erythrocyte lysis test.[39] Fresh blood was collected into the heparinized tubes from rats and centrifuged at 2500 rpm for 10 min at 4 °C for separation of red blood cells. The pellet was washed thrice with PBS and then finally resuspended in PBS and used for hemolysis assay. An equal volume (1 mL) of erythrocyte suspension and liposomal dispersion was mixed and incubated for 1 h at 37 °C under constant shaking. After 1 h, the mixture was subjected to centrifugation and the supernatant was analyzed at 540 nm for percent hemolysis using an UV−vis spectrophotometer (UV-1800 Shimadzu Corporation, Kyoto, Japan). The separated supernatant from the centrifuged blood sample was considered as blank and supernatant derived from the blood sample treated with 1% Triton w/v (hemolytic agent) was taken as the positive control. The experiments were performed in triplicates, and the percent hemolysis was calculated by using formula shown below:

$$\text{percent hemolysis} = \frac{\text{TA} - \text{BA}}{\text{PCA} - \text{BA}} \times 100 \quad (4)$$

where TA is test absorbance, BA is blank absorbance, and PCA is positive control absorbance.

2.7.2. Cytocompatibility Assay. The cytocompatible behavior of RS and RL5 was assessed using standard MTT (3-(4,5-dimethylthiazol-2-yl)-2,5-diphenyltetrazolium bromide) assay. Briefly, normal mouse fibroblasts (L929) cell lines were grown in a mixture of Dulbecco's modified eagle medium (DMEM), fetal bovine serum (FBS, 10%), and Pen-Step antibiotics (1%) in a CO_2 incubator (Eppendorf, New Brunswick, Galaxy 170R) at 37 °C with 95% humidity. Seeding of L929 cell lines at the densities of 1×10^4 cells/well in the 96 well plate was carried out, and the plates were incubated for 24 h in a CO_2 incubator to allow for cell adhesion. The media was discarded and swapped with fresh media with varying concentrations of RS and RL5 (250, 125, 62.5, 31.25, 15.63, and 7.81 μg/mL), and the control wells were treated with equivalent volumes of media without any test compound, followed by incubation for a period of 24 h. After the completion of the incubation period, the media in each well was discarded and wells were gently washed with PBS. Cells were then treated with 100 μL of MTT solution (0.5 mg/mL in phosphate buffer saline), and the plate was incubated at 37 °C for 4 h. After 4 h, the supernatant was discarded and DMSO (100 μL) was added to each well to dissolve formed formazan crystals and analyzed by plate reader (Lisa plus) to calculate the percent cell viability.[40,41]

2.8. *In Vitro* Cytotoxicity Assay. The cytotoxicity of RS and RL5 against HepG2 cell lines was performed as per the procedure mentioned in section 2.7.2. HepG2 cell lines were incubated with RS and RL5 of varying concentrations (250, 125, 62.5, 31.25, 15.63, and 7.81 μg/mL) equivalent to free RS for 24 and 48 h. After completion of the incubation period, percent cell viability was estimated by MTT assay method.

2.9. Quantitative and Qualitative Cell Uptake Assay. For qualitative cell uptake analysis, coumarin 6 (C6) was used as a model fluorescent dye to evaluate the extent of cellular uptake of liposomes. HepG2 cells were seeded in 6-well culture plates (50 000/well) and were incubated overnight for the attachment of the cells. The efficacy of cellular uptake as a function of RL5 was evaluated by *in vitro* incubation of HepG2 cells with free C6 and C6 loaded liposomes (CLs) (equivalent to 1 μg/mL C6) for 3 and 5 h.[42] The free C6 solution was prepared by solubilizing in 0.1% DMSO to yield a final concentration of 1 μg/mL.[43] CLs were prepared by following the method mentioned in section 2.2 and replacing RS with C6. After the given time of incubation of C6 and CL, the medium was aspirated and cells were washed with PBS five times, fixed with 4% paraformaldehyde (Merck), and were observed under a confocal laser scanning microscope (CLSM) (Olympus FV1000). For quantitative cell uptake analysis, HepG2 cells were treated with RS and RL5 (equivalent to 10 μg/mL RS) and further incubated for 3 and 5 h to determine cell uptake over time. Media was removed, and cells were washed thrice with PBS and then lysed with 0.1% Triton X-100. Lysed cells were then extracted with ACN for the complete dissolution of internalized RS. Finally, the cell lysate was centrifuged at 10 000 rpm for 10 min and supernatant was analyzed by HPLC.[42]

2.10. *In Vivo* Organ Toxicity Studies. Biochemical parameters of hepatic and renal functions such as alanine transaminase (ALT), aspartate transaminase (AST), blood urea nitrogen (BUN), and creatinine were assessed by commercially available diagnostic kits (Erba Diagnostics, Inc.). Organs such as liver, kidney, and spleen tissues of rats were stained with hematoxylin and eosin (H&E) for histopathological assessments.

2.11. Pharmacokinetic Study and Hepatic Accumulation of RS by HPLC. Animal studies were approved by the Institutional Animal Ethical Committee (KLECOP/IAEC/Res.22-10/10/2015), KLE College of Pharmacy, Belagavi, India. Studies involving animals were conducted in strict accordance with Animal Research: Reporting of *In Vivo* Experiments (ARRIVE) guidelines.[44] For *in vivo* pharmacokinetic study, male Wistar albino rats (200 ± 20 g) were obtained from our institution's animal housing facility and were housed in cages at room temperature 25 ± 2 °C and relative humidity of 50−60% under a 12 h light/dark cycle. Rats were fed with a pellet diet (VRK Nutritional Solutions, Pune, Maharashtra, India), with water, *ad libitum* for 1 week before experiments. NDEA was used to induce HCC in 6−7 week old healthy male rats. NDEA solution reconstituted in saline was administered intragastrically at a dose of 10 mg/kg body weight with the frequency of 5 times a week for 12 weeks.[45] HCC induced animals were randomly divided in two groups (n = 3 for each time point) and were administered with 20 mg/kg body weight of RS and equivalent RL5. Free RS was solubilized in a mixture of 1% DMSO and 1% Tween-80 solution in phosphate buffer saline (PBS).[46] On the basis of the permissible limit (less than 10 mL) for intraperitoneal injection,[47] the injection volume was kept around 1 mL considering the weight of the rats. Experimental rats were anaesthetized, and blood samples (1 mL) were collected in

https://dx.doi.org/10.1021/acsbiomaterials.0c00429
ACS Biomater. Sci. Eng. XXXX, XXX, XXX−XXX

Table 3. Observed Responses from 3^2 Factorial Design of Resveratrol Loaded Liposomes[a]

	independent variable		dependent variable			
formulation code	A	B	EE (%)	VS (nm)	ZP (mV)	DL (%)
RL1	−1	−1	49.26 ± 9.72	153.33 ± 7.50	07.57 ± 3.66	2.38 ± 0.45
RL2	−1	0	62.57 ± 7.45	140.30 ± 10.16	25.98 ± 5.82	2.99 ± 0.34
RL3	−1	1	58.91 ± 7.06	134.73 ± 5.09	29.26 ± 7.40	2.80 ± 0.32
RL4	0	−1	62.76 ± 6.17	176.43 ± 7.16	15.88 ± 4.27	3.02 ± 0.28
RL5	**0**	**0**	**78.14 ± 8.04**	**145.78 ± 9.9**	**38.03 ± 9.12**	**3.71 ± 0.36**
RL6	0	1	65.31 ± 5.59	138.18 ± 12.35	62.58 ± 4.13	3.10 ± 0.26
RL7	1	−1	63.65 ± 4.63	187.54 ± 7.29	11.73 ± 2.58	3.06 ± 0.21
RL8	1	0	70.74 ± 5.99	152.46 ± 7.52	35.00 ± 7.04	3.33 ± 0.25
RL9	1	1	65.85 ± 7.54	148.91 ± 7.27	56.43 ± 9.14	3.12 ± 0.34

[a]Note: (A) molar ratio of SL/Chol, (B) concentration of SA (mg). Each value represents the mean ± SD, $n = 3$. The composition of each batch is given in Table 1. The optimized values are represented in bold.

heparinized tubes *via* cardiac puncture at 15, 30, 60, and 120 min and sacrificed by cervical dislocation. Major organs such as heart, spleen, liver, lung, and kidney were excised, washed twice with ringer's solution, and immediately frozen until analysis. Isolated organs were weighed, minced thoroughly, and homogenized (RQT-127AD, Remi Elektrotechnik Ltd., Vasai, India) in 50% aqueous acetonitrile. Homogenized samples were centrifuged (12 000 rpm for 12 min), and the supernatant was preserved at −20 °C for further analysis. For estimation of RS in rat plasma, blood samples were centrifuged at 4000 rpm for 10 min at 4 °C for plasma separation and were preserved at −20 °C for further sample analysis. RS from frozen isolated organs and plasma were estimated by using a modified HPLC method.[48] Separated biological samples from both tissue homogenate and plasma (150 μL) were vortex-mixed with 150 μL of ACN for deproteinization, followed by centrifugation at 12 000 rpm for 12 min. Supernatants were separated, filtered through 0.22 μm membrane filter (Millipore), and finally analyzed by the HPLC system. The pharmacokinetic investigation was performed by one compartmental model using Kinetica software (Thermo-Scientific) to estimate the parameters such as area under curve (AUC), peak plasma concentration (Cmax), half-life ($t_{1/2}$), and mean residence time (MRT).[49]

2.12. Pharmacodynamics Activity: Prophylactic and Therapeutic Anti-Cancer Activity. The experimental animals were divided into six groups (Table 2) with six animals in each group. Group 2 (NDEA induced HCC rats: disease control) consisted of two more rats to ensure the successful generation of HCC at the end of the ninth week of the experiment. At the 13th week, rats in each group were sacrificed and liver specimens were removed and weighed. Plasma was collected from the blood by centrifugation at 4000 rpm for 10 min at 4 °C for biochemical estimation of alanine transaminase (ALT), alkaline phosphatase (ALP), aspartate transaminase (AST), total bilirubin levels, γ-glutamyl transpeptidase (GGT), and α-fetoprotein (AFP). After dissection, the liver was isolated and the tumor nodules were counted and stored in buffered formalin for histopathological examination.

3. RESULT AND DISCUSSION

3.1. Formulation and Optimization of RS Loaded Cationic Liposomes. Physicochemical properties and stability are the key factors to be considered while developing a new drug delivery system in all the formulation stage, especially those proposed for parenteral administration. In the present investigation, the RLs obtained from the 3^2 factorial design confirmed that the independent variables such as (A) the molar ratio of SL/Chol and (B) the concentration of SA had a significant effect on dependent variables such as EE, VS, and ZP (Table 3). The quadratic equation generated from Design-Expert Software (Stat-Ease Inc., Minneapolis, MN) for EE is

$$EE = 75.09 + 4.92A + 2.40B - 1.86AB - 6.91A^2 - 9.53B^2 \quad (5)$$

The positive sign indicates that EE is directly proportional to both the independent variables. The literature reveals that the increase in the concentration of SL subsequently increases EE, the reason for which could be attributed to the fact that lipophilic drugs like RS tend to easily dissolve in lipid resulting in a higher EE.[50] SA at the same time alters the membrane permeability or the electric charge density, resulting in enhanced EE of the liposomes.[51]

$$VS = 145.46 + 10.25A - 15.32B - 6.40AB - 0.38A^2 + 9.92B^2 \quad (6)$$

where the positive sign indicates that VS is directly proportional to A (molar ratio of SL/Chol) and the negative sign indicates inversely proportional to B (concentration of SA). The reduction in the VS could be due to the ability of SA to generate a net positive charge on the surface of RLs. An increase in the surface charge increases the intervesicular Brownian moment, keeping the particles stable. It also avoids the ripening of vesicles over time, which could be a key reason for a smaller VS.[52,53] The equation further advocates that VS was directly proportional to the concentration of SL, for which the reason could be attributed to the propensity of SL molecules to coalescence, leading to an increase in VS.[54] Hence, an optimum concentration of SL and SA is a prime requirement to obtain stable monodisperse nanoliposomes.

$$ZP = 38.53 + 5.36A + 20.41B + 3.40AB - 9.84A^2 + 1.05B^2 \quad (7)$$

All the formulations were analyzed for ZP as a part of the formulation development process. ZP is a useful tool to indicate the vesicle surface charge, which is used to predict the stability of colloidal dispersion. In general, ZP is the balance between the surface positive and negative charges and is directly proportional to the magnitude of the potential.[55] On the basis of the result, the positive sign indicates that the ZP is directly proportional to A and B. Our experiments were supported by the literature, which states that an increase in the concentration of SA consequently increases the ZP. In the present investigation, the ZP in all the formulations was maintained on the positive side, owing to the charge imparted by SA. Cationic lipid SA is an amphiphilic molecule, which has a lipophilic region (hydrocarbon chain) and a hydrophilic

https://dx.doi.org/10.1021/acsbiomaterials.0c00429
ACS Biomater. Sci. Eng. XXXX, XXX, XXX−XXX

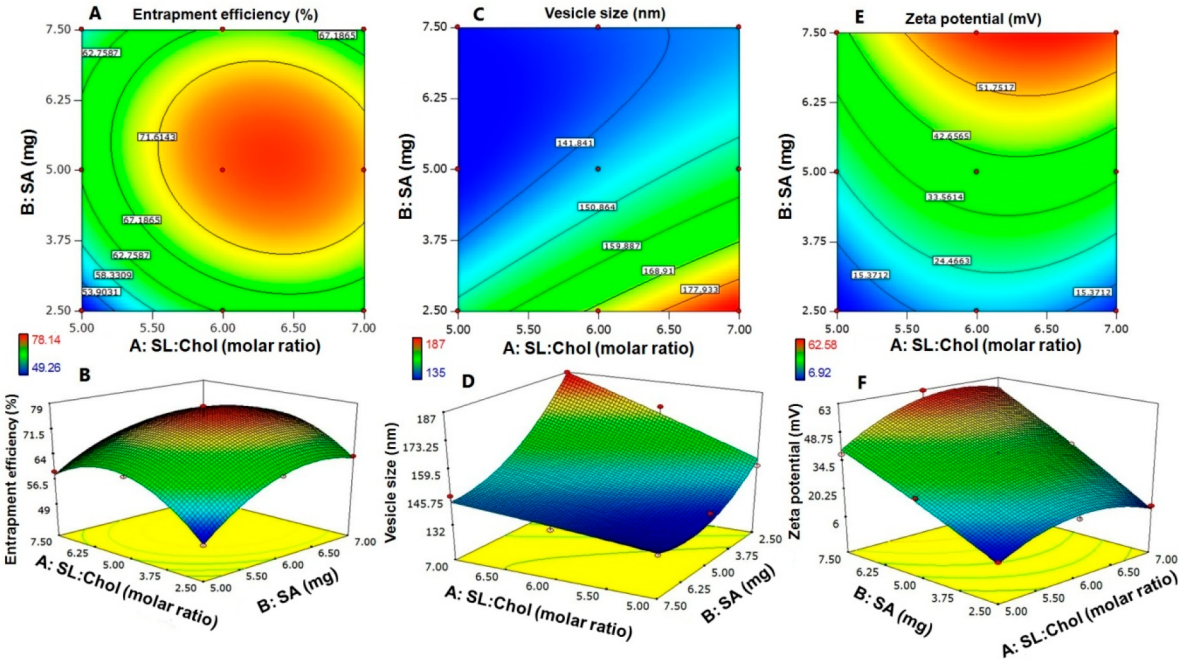

Figure 2. 2D contour and 3D response plots (design expert software) for (A and B) entrapment efficiency, (C and D) vesicle size, and (E and F) ζ potential, respectively. The 3^2 level factorial design demonstrated the significant influence of lipid and cholesterol molar ratio and stearyl amine concentration on ζ potential, vesicle size, and encapsulation efficiency. SL, soya lecithin; Chol, cholesterol; SA, stearyl amine.

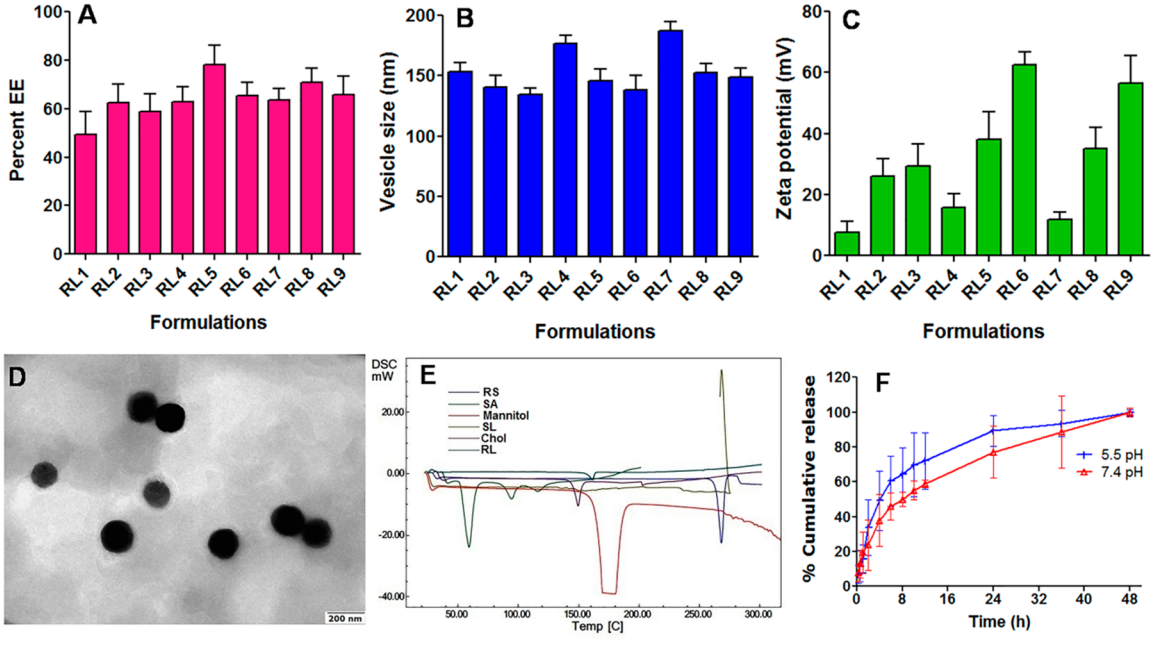

Figure 3. (A) Percent entrapment efficiency of RL1−RL9 by varying the ratio of SL/Chol. On the basis of the design of experiments, RL5 formulation was selected, owing to its highest EE for further *in vitro* cell uptake and animal study. (B) Graph showing the hydrodynamic diameters of RL1−RL9 in deionized water at pH 7.0. The figure shows that all formulations were in the range 134.73 ± 5.09−187.54 ± 7.29 nm, from which the optimized formulation RL5 was found to be 145.78 ± 9.9 nm in diameter. (C) Bar graph showing the ζ potential of RL1−RL9 in deionized water at pH 7.0. All formulations were in the range 7.57 ± 3.66−62.58 ± 4.13 mV, from which the optimized formulation RL5 was found to be 38.03 ± 9.12 mV, representing a stable RL dispersion. (D) Surface morphology of RL5 was confirmed and determined by TEM, which clearly showed spherical morphology with uniform size distribution. (E) DSC thermogram of RS, exhibiting a sharp endotherm at 256.45 °C, indicating its melting point, and conforming its crystalline nature, whereas SA, Chol, mannitol, and soya lecithin exhibited sharp endotherm peaks at 52, 149, 166.0, and 20.5 °C, respectively, corresponding to their melting points. The endotherm peak almost disappeared in the thermogram of RL5, suggesting that RS was entrapped in liposomes. RL5 shows clear peak of mannitol at 166.0 °C, which corresponds to crystallized mannitol. (F) *In vitro* drug release of RS from RL5 at pH 5.5 and 7.4 showed a faster release trend pH 5.5 when compared to pH 7.4. SL, soya lecithin; Chol, cholesterol; SA, stearyl amine, RL, resveratrol loaded cationic liposomes.

https://dx.doi.org/10.1021/acsbiomaterials.0c00429
ACS Biomater. Sci. Eng. XXXX, XXX, XXX−XXX

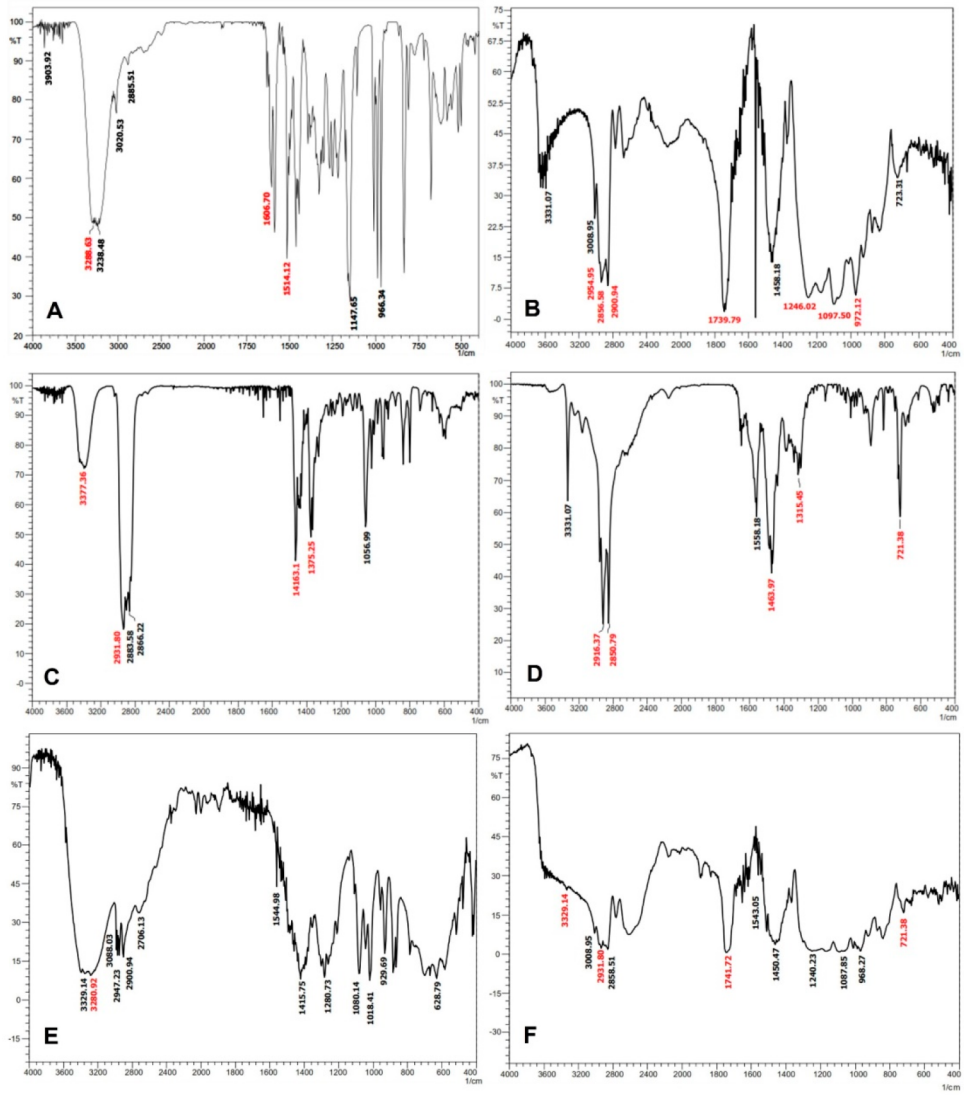

Figure 4. (A) FT-IR spectrum of RS, which revealed the intense absorption band of phenolic hydroxyl group at 3288 cm^{-1}, benzene ring absorption peaks of C═C at 1606 cm^{-1}, and medium absorption peak at 1514 cm^{-1}. (B) FT-IR spectrum of SL (LIPOID S100), in which characteristic peaks at 2954 cm^{-1} (hydroxyl stretching), 2900 and 2856 cm^{-1} (C—H stretching of long fatty acid chain), 1739 cm^{-1} (carbonyl stretching of the fatty acid ester), 1246 cm^{-1} (P═O stretching band), 1097 cm^{-1} (P—O—C stretching), and 972 cm^{-1} $(N^{+}(CH_3)_3$ stretching were observed. (C) FT-IR spectrum of Chol displayed a characteristic band between 2866−2931 cm^{-1} representing asymmetric and symmetric stretching vibrations of CH_2 and CH_3 groups and a broad and intense band nearly at 3377.36 cm^{-1} due to —OH stretching. The additional bands at 1463 and 1375 cm^{-1} is due to asymmetric stretching vibrations and bending vibration of $—CH_2$ and $—CH_3$ groups. (D) FT-IR spectrum of SA showed peaks at 2916 and 2850 cm^{-1}, owing to —C—H stretching, and 1463 cm^{-1}, owing to —N—H bending. Further, a sharp peak at 1315 cm^{-1} could be attributed to C—N stretching and a peak at 721 cm^{-1} represents —N—H wagging vibration. (E) FT-IR spectra of mannitol showed a broad characteristic peak at 3280 cm^{-1} assigned to the hydroxyl group. (F) FT-IR spectra of lyophilized RL5 showed characteristics peaks of mannitol, Chol, and SA but did not show any characteristics peaks of RS, which indicates the complete entrapment of RS inside the liposomes.

region comprising a positively charged polar amine group. The previous reported literature by Casals et al., clearly shows that SA is asymmetrically distributed in the lipid bilayer, which was predominantly on the outer surface as compared to the inner core. A high positive ζ potential value of the formulated liposomes confirms that a significant SA is available on the outer surface, imparting the cationic charge on the liposomes.[56,57] The application of ANOVA (Table S1) on the outcomes confirms the significance of the model from F and P values. The surface response curve and contour plots (Figure 2) reveal the effect of SL and SA on EE, VS, and ZP. The evaluation of liposomes suggested that RL5 demonstrated desirable properties, i.e., more than 78% EE, ZP of 38 mV, and the VS of less than 150 nm when compared with other formulations. Finally, the optimized liposomes RL5 were lyophilized by using cryoprotectant mannitol. The lyophilized RL5 cake was found to be intact and fluffy in nature with a reconstitution time less than 35 s.

3.1.1. Evaluation of Optimized Liposomes Formulation. VS, ZP, PDI, and EE of optimized liposomal formulation RL5 were found to be 145.78 ± 9.9 nm, 38.03 ± 9.12 mV, 0.359 ± 0.03, and 78.14 ± 8.04% (Figure 3A−C) respectively. Results revealed that VS, EE, and ZP values of liposomes were directly related to the concentration of SL and SA used in the formulation. The morphological examination of liposomes evaluated by TEM clearly showed a spherical morphology with

https://dx.doi.org/10.1021/acsbiomaterials.0c00429
ACS Biomater. Sci. Eng. XXXX, XXX, XXX−XXX

Table 4. Stability Studies of Optimized Liposomes RL5[a]

parameter →	vesicle size (nm)		ζ potential (mV)		EE (%)	
storage condition ↓	initial	after 3 months	initial	after 3 months	initial	after 3 months
RL5, liquid dispersion at 4 °C	142.17 ± 6.20	149.14 ± 12.62	37.3 ± 4.53	34.43 ± 4.80	76.57 ± 2.51	72.77 ± 3.05
RL5, lyophilized at 4 °C	143.76 ± 4.77	147.80 ± 10.30	36.66 ± 2.65	35.03 ± 3.27	76.44 ± 2.27	75.36 ± 0.929

[a]The data is expressed as mean ± SD (n = 3). The data were evaluated by Student's paired t-test, which showed no significant difference.

an uniform size distribution (Figure 3D) of vesicles. The reason for the formation of spherical morphology could be due to the hydrophobic nature of the lipids, which, when exposed to an aqueous environment, led to the spontaneous formation of closed bilayers, exposing the polar hydrophilic layer to the outer surface of liposomes. The shape and surface morphology of the liposomes was found to be smooth with no vesicular aggregation, which indicates the stability of the prepared liposomes.

DSC thermograms of RS, SL, SA, Chol, mannitol, and freeze-dried RL5 are shown in Figure 3E. The DSC thermogram of RS exhibited a sharp endotherm at 256.45 °C, which indicates the crystalline state of RS and confirms its melting point. The melting peak almost disappeared in the thermogram of RL5, suggesting that RS was entrapped in liposomes and the formulation changed from the crystalline state to the amorphous state. The DSC of pure SL exhibited endothermic peaks at 20.5 °C, indicating the transition temperature (Tm), which served as the basis for optimizing the temperature required for the film formulation of lipids. Further, SA and Chol thermograms showed strong endotherms at 52 and 149 °C, corresponding to their melting points, respectively, confirming their purity. These peaks were however not observed in the thermograms of RL5, which signifies the interaction between RS and other lipid components of the bilayer. RL5, however, shows a clear peak of mannitol at 166.0 °C, which was used as a cryoprotectant for lyophilization.

FT-IR spectroscopic studies were performed to analyze the drug and polymer/excipients interaction. The FT-IR spectra of lyophilized RL showed characteristics peak of mannitol but did not show any characteristics peaks of RS, which indicates the complete entrapment of RS inside the liposomes (Figure 4). The clear peak of amine groups at 1450 cm^{-1} in the FT-IR spectra of lyophilized RL5 could be attributed to the coating of SA onto the liposomes.

3.2. *In Vitro* Release Study of RL5. *In vitro* drug release profiles of RS from RL5 at pH 5.5 and 7.4 were obtained by plotting the graph of cumulative percentage of the drug released over time (Figure 3F). During the release study, 0.1% (v/v) of PEG was added in release medium PBS (pH 5.5 and 7.4) to solubilize the released RS. Initially, a burst release phase, releasing approximately 30% of resveratrol in both pH medium was observed in the first 2 h, followed by sustained and complete drug release in 48 h. No significant difference was found for the release of RS from RLs over the entire study period. A comparative faster release of RS at pH 5.5 (tumor microenvironment) could be due to use of heterogeneous lipids (SL and SA) used in the formulation of liposomes. SL (Lipoid S 100: lipid mixture)[58] and SA have an 18 carbon chain as their backbone. Liposomes prepared with heterogeneous lipids when exposed to a decreased pH lead to an increase in the membrane permeability and ultimately released the payloads. Our results are in corroboration with the studies performed by Karve et al., wherein they assessed the release behavior of vesicles formulated by different sets of lipids (DPPC (16 carbon containing lipid; 1,2-dipalmitoyl-*sn*-glycero-3-phosphocholine,) and DSPA (18 carbon containing; 1,2-distearoyl-*sn*-glycero-3-phosphate, sodium salt) lipids, DPPC and DPPA lipids, and DSPC and DSPA lipids) in different pH. Vesicles prepared with different chain lengths (DPPC and DSPA) showed an increased membrane permeability and higher release of encapsulated calcein at a lower pH when compared to the vesicles prepared by lipids with same chain length (DPPC−DPPA and DSPC−DSPA).[59] The drug release mechanism can be defined as the way of the release of payload from the nanocarrier. It is dependent of the nature of the polymer/lipid used in the formulation and the release conditions, which can follow several mechanisms such as dissolution, diffusion, swelling, erosion, and degradation.[36]

To examine the release mechanism of RS from the RL5, five kinetic models were applied to fit the release data. On the basis of the analysis (Figure S1A−E), the Hixson−Crowell model showed the highest R^2 value for RL5 at pH 5.5 (R^2 value: 0.937) and 7.4 (R^2 value: 0.971). Hence, the release of RS from RL5 follows the Hixson−Crowell model, which occurs through surface dissolution and is dependent on the surface area and the diameter of vesicle.[60,61]

3.3. Stability Studies. Physical stability of liposomes is indirectly proportional to the vesicle size and directly proportional to the ζ potential of the dispersion. Aggregation of vesicles, which represents poor stability, could be observed during formulation processing and/or upon storage. The increase in the diameter of liposomes results in a rapid uptake by the reticuloendothelial system with subsequent clearance, resulting in a short half-life. Therefore, preparing stable liposomes with small and uniform size distribution is the most significant aspect in drug product development. Table 4 represents the storage stability studies conducted for optimized RL5 after storage at 4 °C for 3 months in both dispersion and lyophilized forms (reconstituted with water). After 3 months of storage at 4 °C, there was no significant difference in the VS, ZP, and EE, which indicates a desirable stability of the formulation.

3.4. *In Vitro* Biocompatibility Studies. *3.4.1. Blood Compatibility (Hemolysis Assay) Studies.* Outlining the mechanism of liposomal interaction with red blood cells (RBCs) is an important step toward establishing the plausibility of using liposomes as delivery tools for biomedical applications. Formulations are expected to be inert and biocompatible with cells, blood, and blood components. In the present investigation, RL5 formulation (equivalent to 20 mg/mL RS) and free RS (20 mg/mL) were evaluated for hemolysis as compared to positive control (1% w/v Triton in PBS) and negative control (0.1% v/v DMSO in PBS), as depicted in Figure S2. Percent hemolysis values below 10% were considered to be nonhemolytic.[62] It was observed that formulated cationic RL5 caused 1.88% hemolysis, which is under the permissible limit (less than 10% lysis). Hemolysis assay suggests that the concentration of SA used in the

https://dx.doi.org/10.1021/acsbiomaterials.0c00429
ACS Biomater. Sci. Eng. XXXX, XXX, XXX−XXX

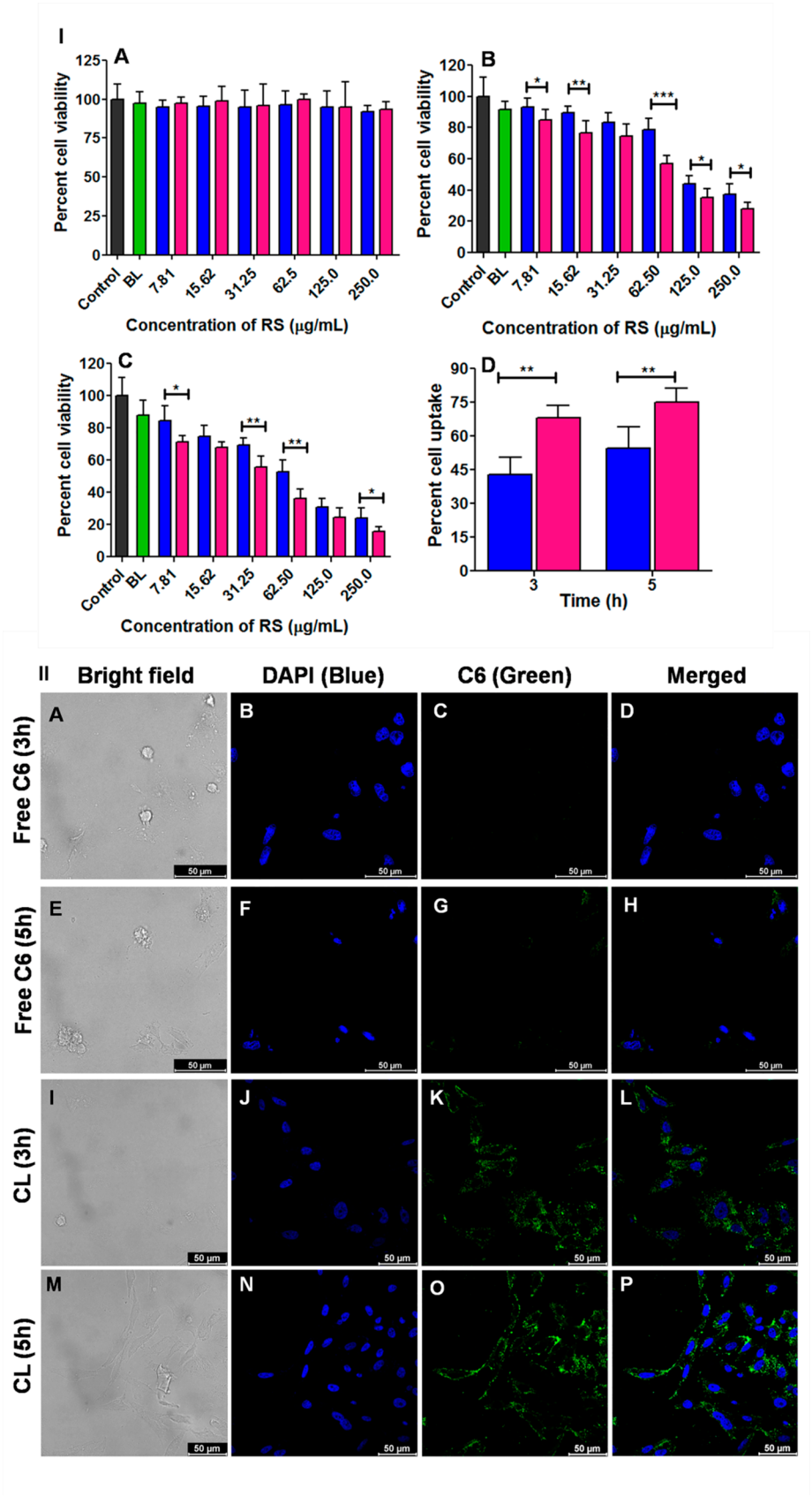

Figure 5. (I)(A) Cytocompatibility of RS and RL5 determined by evaluating the cytotoxicity against normal mouse fibroblast cell lines (L929) using colorimetric MTT assay. RS and RL5 were found to be biocompatible at the concentration range 7.812−250 μg/mL. (B and C) Graph showing cytotoxicity studies of BL, RS, and RL5 on HepG2 cell lines over a period of 24 and 48 h, and cell viability was estimated by MTT assay at different drug concentrations. BL were found to be biocompatible and showed no significant cytotoxicity against HepG2, whereas RS and RL5 showed dose- and time-dependent changes in which RL5 demonstrated a significantly higher cytotoxicity against HepG2 compared to that of RS.

https://dx.doi.org/10.1021/acsbiomaterials.0c00429
ACS Biomater. Sci. Eng. XXXX, XXX, XXX−XXX

Figure 5. continued

The half-maximal inhibitory concentration (IC50) values of RS after 24 and 48 h of incubation were 84.49 and 68.23 μg/mL and for RL5 were 63.65 and 42.26 μg/mL, respectively. (D) Bar graph showing quantitative cell internalization of RS and RL5 in HepG2 cancer cells, which were evaluated at 3 and 5 h time points by HPLC. The time-dependent cellular uptake showed augmented cellular internalization of RL5 as compared to RS throughout the incubation time ($p < 0.05$). Results demonstrated 54.16 ± 9.61 and 74.98 ± 6.33% cellular internalization after 5 h of incubation with RS and RL5, respectively. (II) Qualitative cell uptake study of C6 and CL showing time-dependent cellular uptake, wherein a higher uptake of CL by HepG2 was observed as compared to that free C6 at 3 (A−D and I−L) and 5 h (E−H and M−P). Scale bar is 50 μm.

formulation of RL5 is blood biocompatible and can be used for *in vivo* administration.

3.4.2. Cytocompatibility Assay. Cytocompatibility is the key parameter to be assessed for any bionanomaterial proposed for *in vivo* drug delivery system. In the present investigation, the cytocompatibility of RS and RL5 was evaluated against primary mouse fibroblast culture (L929) using colorimetric MTT assay. Cytotoxicity of samples was compared with control (untreated) cells that were considered as 100% viable (Figure 5IA). Fibroblast cells were treated with RS and RL5 at varying concentrations of 250, 125, 62.5, 31.25, 15.62, and 7.812 μg/mL and were evaluated for cell viability after 24 h. Both RS and RLs showed no significant difference in cell viability, which confirms its cytocompatibility.

3.5. Cytotoxicity Assay. Cytotoxicity studies of blank liposomes, free RS, and RL5 were tested on a HepG2 cell line over a period of 24 and 48 h using MTT viability assay at different drug concentrations (Figure 5IB,C). The half-maximal inhibitory concentration (IC50) was calculated by using Graph Pad Prism version 7.0, which signifies a quantitative measure of the concentration of a drug required to inhibit a given biological process by half. Blank liposomes were found to be biocompatible and showed no significant cytotoxicity against HepG2 when compared to control. RS and RL5 showed dose- and time-dependent changes in which RL5 demonstrated a significantly higher cytotoxicity against HepG2 when compared to RS. The IC50 of RS and RL after 24 h of exposure were found to be 84.49 and 63.65 μg/mL, respectively. After 48 h of incubation, the IC50 values of RS and RL were 68.23 and 42.26 μg/mL, respectively. Our results are in corroboration with the studies performed by Su et al., which showed that the IC50 values of free RS were around 68.4 and 34.2 μg/mL after 48 and 72 h, respectively.[63] The reason for improved activity and lower IC50 of RL5 in comparison to those of RS could be because of the enhanced uptake of liposomes and improved solubility of RS in nanoliposomes formulation.[64] Further, the negative charge on hepatocytes is more likely to attract positively charged liposomes, which increases the cell uptake of nanovesicles.[65,66] Similar outcomes were reported by De et al., wherein they developed SA based camptothecin loaded cationic liposomes. They reported that camptothecin loaded cationic liposomes demonstrated a manifold enhancement in the anti-cancer therapeutic efficacy both *in vivo* and *in vitro* in comparison with free camptothecin. This enhanced anti-cancer effect of liposomes was due to the attraction between the SA containing cationic liposomes toward the exposed PS group present on liver cancer cells.[67]

3.6. Qualitative and Quantitative Cell Uptake Assay. Cellular uptake efficiency was evaluated quantitatively by HPLC and qualitatively by CLSM. The cellular uptake showed an enhanced cellular internalization of RL5 as compared to that of RS throughout the incubation time ($P < 0.01$). HPLC analysis of cell extract after 5 h showed 54.16 ± 9.61 and 74.98 ± 6.33% cellular internalization of RS and RL5, respectively (Figure 5ID). By intending to evaluate the cellular internalization of developed liposomes, we developed CL and evaluated it using CSLM. C6 is a derivative of coumarin and is obtained from the plant origin. Owing to its fluorescent and lipophilic nature, it is used as a model fluorescent agent to qualitatively check the internalization of developed liposomes *via* fluorescence in both *in vitro* or *in vivo* experimental systems.[68] In our research investigation, CLSM results confirm that the HepG2 cells demonstrated a higher uptake of CL as compared to free C6, which was evident from confocal images of cells after 3 and 5 h of incubation (Figure 5IIL,P). An intense green fluorescence of CL was observed around the nucleus within the cytoplasm of HepG2 cells, whereas free C6 demonstrated a weak fluorescence signal (Figure 5IIC,G). Upon incubation of CL with HepG2 cells, the increased fluorescence intensity in the HepG2 cell membrane could be due to the accumulation of CL into the lysosomal compartment along with diffusion into the cytoplasm. Similar results were demonstrated by Parvathaneni et al., in which free C6 showed a reduced cell internalization than its corresponding CL.[69] This difference could be attributed to the relatively enhanced lipophilic nature of CL than C6. Out of the several reasons, lipophilic nature, solubility of test compound, and the time of incubation with cells are the key factors determining the uptake of the compound by cells. The literature suggests that C6, when suspended in aqueous media, is known to have a lesser uptake when compared with that of C6 solubilized in DMSO. This means that solubility of the compound is directly proportional to the cell uptake.[70,71]

Cationic nanoparticles with a net positive surface charge emerge as a promising option owing to their very strong cellular interaction and desirable cellular uptake.[30] As explained above, apart from PS on the surface of cancerous cells, it also contains strong negatively charged elements such as chorionic gonadotropin, sialic acid, and anionic residues of RNA as compared to normal cell surfaces.[72,73] On the basis of this fundamental electrostatic interaction, cationic liposomes have a high tendency to accumulate in cancer cells through endocytosis.[72]

3.7. *In Vivo* Toxicity Studies. The toxicity profiling of RS and RL5 were carried out using different toxicity markers. BUN, and plasma creatinine levels were determined for evaluating nephrotoxicity, while plasma ALT and AST levels were determined for evaluating the hepatotoxicity. Untreated animals served as the control for the comparison. As shown in Figure S3I, animals treated with RS and RL5 did not induce toxicity in the liver, spleen, and kidneys. The biochemical evaluation was further corroborated with histopathological examinations, suggesting a nontoxic behavior of free RS and RL5. Histological sections of liver, kidney, and spleen (Figure S3II) demonstrated normal parenchymal cell physiology, indicating no signs of inflammation and necrosis.

https://dx.doi.org/10.1021/acsbiomaterials.0c00429
ACS Biomater. Sci. Eng. XXXX, XXX, XXX−XXX

Table 5. Pharmacokinetic Parameters of RS and RL5 in Rat Plasma and Organs Following ip Administration

parameters		C_{max}	AUC_{total} (μg/mL·min)	$T_{1/2}$ (min)	MRT (min)
blood	RL5	2.15	225.98	56.24	95.70
	RS	1.74	125.06	48.86	83.58
liver	RL5	3.51	223.54	35.75	72.16
	RS	1.50	69.85	37.36	58.29
spleen	RL5	2.83	74.32	18.92	40.99
	RS	2.50	113.15	18.65	38.66
lung	RL5	0.49	10.56		
	RS	1.10	19.66		
heart	RL5	0.39	19.01	33.09	56.00
	RS	0.22	23.40	65.40	102.00
kidney	RL5	2.34	63.53	29.30	39.70
	RS	2.82	132.25	26.25	45.07

3.8. *In Vivo* Pharmacokinetic and Tissue Distribution. Liposome drug delivery systems (DDS) are excellent candidates to circumvent the limitations of free RS. An assessment of pharmacokinetic profile of RL5 in comparison with that of free RS was performed by using standard protocols. Results of the pharmacokinetic evaluation of RL5 after intraperitoneal injection in Wistar rats are shown in Table 5. The higher concentration of RS from RL5 in the plasma and liver was achieved when compared to the animal group, which received free RS. The increase in the plasma concentration of RS in animals treated with RL5 could be due to opsonization and macrophage uptake of liposomes.[30] Furthermore, the positive charge on liposome slows down the absorption rate due to the electrostatic interaction between the positively charged liposomes and the negatively charged peritoneal mesothelium surface. The slow absorption is further prolonged due to the low uptake of positive liposomes by peritoneal macrophages.[74] Vesicle size is known as one of the critical parameters that impact the absorption, retention, and lymphatic uptake of liposomes following intraperitoneal injection.[75] Hirano and Hunt et al. explained that the stability of liposomes is important for the delivery of intact liposomes after intraperitoneal injection. Poor stability of large liposomes leads to fusion of liposomes and subsequent undesirable leakage of payload in the peritoneal cavity.[76] Lee et al. and Dadashzadeh et al. also suggested that there is a possibility of aggregation of cationic liposomes after intraperitoneal injection due to an increase in vesicle size. Hence, size is considered as an important factor for the efficient delivery of liposomes through intraperitoneal injection.[75,77] In terms of distribution, cationic liposomes were concentrated maximum in the liver, followed by the spleen (C_{max} 2.83 μg/mL, half-life of 30 min) as compared to other organs. This difference in the distribution could be attributed to the EPR effect and/or electrostatic interaction, as explained in Figure 1.[65,67] Electrostatic interaction between the positively charged liposomes and negatively charged hepatocellular cancer cells makes the drug delivery system a potential way of targeting anti-cancer drugs to liver cancer. In a healthy condition, the liver comprises PS, which is positioned internally (unexposed) in healthy liver tissue and is mediated by a membrane protein or ATP-dependent transporter, amino phospholipid translocase.[78,79] This symmetry of PS phospholipid is lost in cancer tissues because of decreased functional activity of enzyme-translocase and/or oxidative stress in the tumor microenvironment or activation of the scramblase enzyme. The loss of symmetry thus exposes the PS on the surface of cancer tissue, which is a salient feature of cancerous cells specifically endothelial cells (ECs).[31,80] The exposure of PS on the surface of cells, known as the death knell, generates a negative charge on liver cancer tissue.[67,81] Pharmacokinetic evaluation, therefore, serves as clear indicative of this mechanism, explaining the use of cationic liposomes as a potential targeting approach to the hepatocellular carcinoma.[82−84]

3.9. Anti-Cancer Efficiency of RS and RL5 in the Experimentally Induced Animal Model. Prophylactic and therapeutic anti-cancer properties of RL5 were assessed in NDEA induced HCC rats. The morphologies of liver, histopathology, relative body/liver weight ratio, tumor nodules, and liver enzyme levels (alanine transaminase (ALT), alkaline phosphatase (ALP), aspartate transaminase (AST), total bilirubin levels, γ-glutamyl transpeptidase (GGT) and α-fetoprotein (AFP)) were assessed in all groups to compare the efficiency of RL5 with free RS. At the end of ninth week of the experiment, two rats from the disease control group were dissected and liver samples were examined through histopathology to confirm successful induction of cancer in the liver. The morphology of liver specimens was analyzed after 12 weeks of the experimental period for all the groups (Figure 6 IA−F). The administration of RS and RL5 to HCC-bearing rats (Groups III−VI) showed very few hepatic nodules (Figure 6IIIB), as compared to the disease control group. The preventive and therapeutic RL5 treated rats (Groups IV and VI) showed a marked suppression in tumor development with significant changes in liver morphology, as compared to the disease control group.

Histological examination revealed that administration of NDEA induced granular cytoplasm with a condensed nucleus with the presence of Councilman bodies, mononuclear inflammatory cells, Kupffer cell hyperplasia, and neoplastic lesion (Figure 6 IIB−E). In both prophylactic and therapeutic treatment groups, the administration of RS and RL5 showed that RL5 was better than free RS in the prevention of damage and reduced the number of neoplastic lesions (Figure 6IIF−I). RS is known to prevent the progression of cancer by targeting multiple cellular targets affecting the cellular proliferation and growth: apoptosis, inflammation, invasion, angiogenesis, and metastasis. Bishayee et al. demonstrated that RS inhibits hepatic carcinogen-activating enzymes such as cytochrome P450 1A1(CYP1A1) and CYP3A/2 *in vitro* and *in vivo*.[85] Similar observations were reported by Dhir et al. and Rajasekaran et al. which showed that RS significantly decrease the number of nodules and progression of cancer in NDEA induced HCC in rodents.[86,87] NDEA administration to rats

https://dx.doi.org/10.1021/acsbiomaterials.0c00429
ACS Biomater. Sci. Eng. XXXX, XXX, XXX−XXX

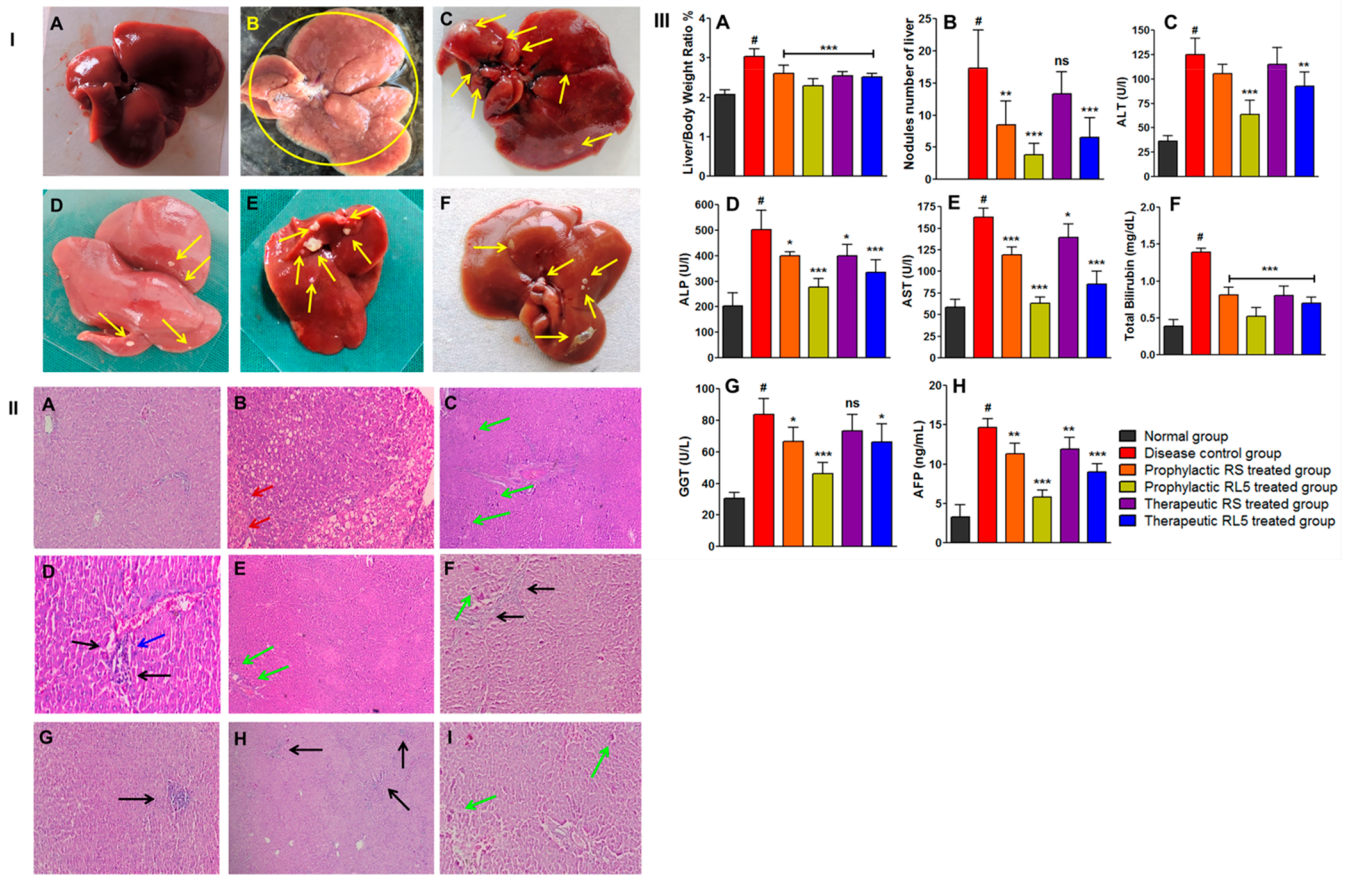

Figure 6. (I) Representative images of rat's livers: (A) normal group liver tissue appears normal with no macroscopically detectable pathological changes. (B) Disease control group liver tissues demonstrated significant changes in terms of color, consistency, and the surface texture. Tissue appeared pale pink in color with increased size and corrugated surface with multiple macroscopic nodules (yellow arrows). (C) Prophylactic RS treated group demonstrated very few nodules (yellow arrows) and lesions. (D) Prophylactic RL5 treated group in rats showed marked reduction in the number of nodules and damaged caused by NDEA. (E and F) Therapeutic RS and RL5 treated groups in rats showed reduction in the number of nodules. (II) Histopathological images of rat's livers: (A) Normal group showed normal hepatic lobule between the central vein and normal peripheral interlobular septum with the portal area comprising a portal vein, hepatic arteries bile ducts, and lymphatic vessels. (B–E) Disease control group showed injuries mainly as enlarged hepatocytes with granular cytoplasm with condensed nucleus (ballooning degeneration) with the presence of Councilman body (red arrows) and infiltration by mononuclear inflammatory cells (black arrows), kupffer cell hyperplasia (blue arrows), and neoplastic lesion, which is multicentric in origin (green arrows), was seen. (F) Prophylactic RS treated group showed neoplastic lesions with inflammatory cells, revealing the moderate improvement over the NDEA treated animals. (G) Prophylactic RL5 treated group showed hepatocyte maintaining normal architecture. (H) Therapeutic RS treated group showed neoplastic lesions. (I) Therapeutic RL5 treated group showed inflammatory cells in portal tract with moderate improvement over those of the disease control group. (III) (A) Liver/body weight ratio significant reduction in the liver/body weight ratio after administration of RS and RL5 as compared to disease control group. (B) Number of nodules on liver in each group; prophylactic and therapeutic RLs treated groups showed a significantly ($P < 0.001$) less number of nodules. (C–H) Enzyme estimations: the activities of serum alanine transaminase (ALT), alkaline phosphatase (ALP), aspartate transaminase (AST), total bilirubin levels, γ-glutamyl transpeptidase (GGT), and α-fetoprotein (AFP) were measured to assess the degree of hepatic cell damage. The data were shown as mean ± SD of six animals and statistically analyzed by one way ANOVA. Statistical significance was considered at $^{\#}P < 0.001$ when compared with the normal group; $^{***}P < 0.001$, $^{**}P < 0.01$, $^{*}P < 0.05$, and ns: no significance when compared with the disease control group.

lead to a marked elevation in levels of serum AST, ALT, ALP total bilirubin, and GGT levels, as shown in Figure 6IIIC–G, which is an indication of hepatocellular damage. Metabolism of NDEA in the liver causes damage to liver cells due to generation of reactive oxygen species (ROS). This process triggers uncontrolled proliferation of hepatocyte, ultimately leading to the generation of HCC.[88,89] RL5 treatment to HCC-bearing rats showed a significant decrease in the activities of AST, ALT, ALP, and GGT as compared to the disease control group.

Serum α fetoprotein (AFP) is considered as one of the key marker enzymes that is reported to increase in several diseases/disorders including hepatocellular carcinoma.[88] The effect of RS and RL5 on α-fetoprotein protein levels in NDEA induced liver damage is shown in Figure 6IIIH. Comparative AFP levels estimation of HCC induced rats treated with RS and RL5 clearly shows that RL5 treated rats had lower AFP levels than rats treated with free RS. Preventive and therapeutic treatment with RS and RL5 showed a significant decrease ($P < 0.001$) in AFP levels compared to those of disease control rats.

Overall, the cell uptake studies described above clearly support the idea that cationic liposomes have an inherent inclination toward PS groups present on the cancer cells, which was evident by higher internalization of RL5 than RS. These outcomes represent a novel strategy to target cancerous cells and can be used as an effective platform for the delivery of drugs and biological molecules for the treatment of HCC. The outcomes corroborate with the *in vivo* results discussed above,

https://dx.doi.org/10.1021/acsbiomaterials.0c00429
ACS Biomater. Sci. Eng. XXXX, XXX, XXX−XXX

which not only shows improvement in the therapeutic efficiency of the optimized RL5 compared to free RS but also confirms the biocompatible nature of the liposomes. Looking forward, it would be worth performing an experiment in combination with sorafenib (USFDA approved drug) to evaluate the effect of combination therapy.

4. CONCLUSION

In spite of its well-known application in cancer therapeutics, the use of RS is limited due to its physiological properties such as poor bioavailability and low half-life. Liposomes are one of the potential formulation systems approved by the FDA for application in cancer therapeutics. In the present investigation, we attempted to improve the bioavailability and the kinetic profile of RS by using cationic liposomes as a carrier for HCC. Optimized RL5 with a SL/Chol ratio of 7:2 and SA (5 mg) demonstrated desirable VS (145.78 ± 9.9 nm), ZP (38.03 ± 9.12 mV), and EE (78.14 ± 8.04%) values. The *in vitro* biocompatible nature of RLs was confirmed by the absence of cytotoxicity against fibroblast (L929) cell lines and blood erythrocytes. *In vitro* cell culture assay showed an enhanced uptake of RL5 in HepG2 cells, resulting in enhanced tumor cell killing ability when compared to free RS. This could be due to the high affinity of positively charged liposomes toward the negative charge of phosphatidylserine exposed on cancer cells. *In vivo* pharmacokinetic and pharmacodynamic studies revealed selective accumulation of RLs in liver cancer tissue, which demonstrated both chemopreventive and therapeutic effects on NDEA initiated HCC. Taken together, RS loaded cationic liposomes delivery system has a promising potential for the treatment of HCC and may provide a platform to enhance the delivery of small molecule anti-cancer drugs.

■ ASSOCIATED CONTENT

Supporting Information

The Supporting Information is available free of charge on the ACS Publications Web site. The Supporting Information is available free of charge at https://pubs.acs.org/doi/10.1021/acsbiomaterials.0c00429.

Table of results of analysis of variance test and figures of drug release kinetics models graphs, *in vitro* percentage hemolysis assay, and results of *in vivo* toxicity studies (PDF)

■ AUTHOR INFORMATION

Corresponding Authors

Satveer Jagwani − *KLE College of Pharmacy, Belagavi and Dr. Prabhakar Kore Basic Science Research Center, KLE Academy of Higher Education and Research, Belagavi 590010, Karnataka, India;* orcid.org/0000-0001-6754-174X; Phone: +91 8951002324; Email: satveerjagwani22@gmail.com

Sunil Jalalpure − *KLE College of Pharmacy, Belagavi and Dr. Prabhakar Kore Basic Science Research Center, KLE Academy of Higher Education and Research, Belagavi 590010, Karnataka, India;* orcid.org/0000-0001-7598-5973; Phone: +91 9448964057; Email: jalalpuresunil@rediffmail.com

Authors

Dinesh Dhamecha − *Dr. Prabhakar Kore Basic Science Research Center, KLE Academy of Higher Education and Research, Belagavi 590010, Karnataka, India*

Kiran Jadhav − *KLE College of Pharmacy, Belagavi, KLE Academy of Higher Education and Research, Belagavi 590010, Karnataka, India;* orcid.org/0000-0002-0502-1770

Raghvendra Bohara − *Centre for Interdisciplinary Research, D. Y. Patil Education Society (Institution Deemed to be University), Kolhapur 416006, Maharashtra, India; CÚRAM, SFI Research Centre for Medical Devices, National University of Ireland, Galway H91 W2TY, Ireland;* orcid.org/0000-0001-6654-9627

Complete contact information is available at: https://pubs.acs.org/10.1021/acsbiomaterials.0c00429

Author Contributions

⊥S.J. and D.D. contributed equally

Notes

The authors declare no competing financial interest.

■ ACKNOWLEDGMENTS

Authors would like to sincerely thank the KLE Academy of Higher Education and Research (formerly known as KLE University), Belagavi, Karnataka, India for providing financial support and the research facilities. The authors gratefully acknowledge Sami Labs, Bangalore, India for gifting pure trans-resveratrol and Lipoid GmbH, Ludwigshafen, Germany for providing (LIPOID S 100) phospholipid for the study. We would like to thank Dr. Ramesh Chavan, Department of Pathology, Jawaharlal Nehru Medical College, KAHER, Belagavi, for helping in the histopathology studies. The authors also would like to acknowledge SAIF, Indian Institute of Technology-Bombay, Mumbai, India for TEM analysis. Raghvendra Bohara would like to acknowledge the Irish Research Council, Ireland.

■ REFERENCES

(1) Bray, F.; Ferlay, J.; Soerjomataram, I.; Siegel, R. L.; Torre, L. A.; Jemal, A. Global Cancer Statistics 2018: GLOBOCAN Estimates of Incidence and Mortality Worldwide for 36 Cancers in 185 Countries. *Ca-Cancer J. Clin.* **2018**, *68* (6), 394−424.

(2) Llovet, J. M.; Villanueva, A.; Lachenmayer, A.; Finn, R. S. Advances in Targeted Therapies for Hepatocellular Carcinoma in the Genomic Era. *Nat. Rev. Clin. Oncol.* **2015**, *12*, 408−424.

(3) Okusaka, T.; Ikeda, M. Immunotherapy for Hepatocellular Carcinoma: Current Status and Future Perspectives. *ESMO open* **2018**, *3*, No. e000455.

(4) Chikara, S.; Nagaprashantha, L. D.; Singhal, J.; Horne, D.; Awasthi, S.; Singhal, S. S. Oxidative Stress and Dietary Phytochemicals: Role in Cancer Chemoprevention and Treatment. *Cancer Lett.* **2018**, *413*, 122−134.

(5) Bishayee, A. Cancer Prevention and Treatment with Resveratrol: From Rodent Studies to Clinical Trials. *Cancer Prev. Res.* **2009**, *2* (5), 409−418.

(6) Yin, S.; Xia, C.; Wang, Y.; Wan, D.; Rao, J.; Tang, X.; Wei, J.; Wang, X.; Li, M.; Zhang, Z.; Liu, J.; He, Q. Dual Receptor Recognizing Liposomes Containing Paclitaxel and Hydroxychloroquine for Primary and Metastatic Melanoma Treatment via Autophagy-Dependent and Independent Pathways. *J. Controlled Release* **2018**, *288*, 148−160.

(7) Teng, W.; Zhao, L.; Yang, S.; Zhang, C.; Liu, M.; Luo, J.; Jin, J.; Zhang, M.; Bao, C.; Li, D.; Xiong, W.; Li, Y.; Ren, F. The Hepatic-Targeted, Resveratrol Loaded Nanoparticles for Relief of High Fat

Diet-Induced Nonalcoholic Fatty Liver Disease. *J. Controlled Release* **2019**, *307*, 139−149.
(8) Öztürk, E.; Arslan, A. K. K.; Yerer, M. B.; Bishayee, A. Resveratrol and Diabetes: A Critical Review of Clinical Studies. *Biomed. Pharmacother.* **2017**, *95*, 230−234.
(9) Lu, Y.; Lu, X.; Wang, L.; Yang, W. Resveratrol Attenuates High Fat Diet-Induced Mouse Cardiomyopathy through Upregulation of Estrogen Related Receptor-α. *Eur. J. Pharmacol.* **2019**, *843*, 88−95.
(10) Cote, B.; Carlson, L. J.; Rao, D. A.; Alani, A. W. G. Combinatorial Resveratrol and Quercetin Polymeric Micelles Mitigate Doxorubicin Induced Cardiotoxicity in Vitro and in Vivo. *J. Controlled Release* **2015**, *213*, 128−133.
(11) Fernández-Quintela, A.; Milton-Laskibar, I.; González, M.; Portillo, M. P. Antiobesity Effects of Resveratrol: Which Tissues Are Involved? *Ann. N. Y. Acad. Sci.* **2017**, *1403* (1), 118−131.
(12) Sallem, F.; Haji, R.; Vervandier-Fasseur, D.; Nury, T.; Maurizi, L.; Boudon, J.; Lizard, G.; Millot, N. Elaboration of Trans-Resveratrol Derivative-Loaded Superparamagnetic Iron Oxide Nanoparticles for Glioma Treatment. *Nanomaterials* **2019**, *9* (2), 287.
(13) Jagwani, S.; Jalalpure, S.; Dhamecha, D.; Hua, G. S.; Jadhav, K. A Stability Indicating Reversed Phase HPLC Method for Estimation of Trans -Resveratrol in Oral Capsules and Nanoliposomes. *Anal. Chem. Lett.* **2019**, *9* (5), 711−726.
(14) Devulapally, R.; Foygel, K.; Sekar, T. V.; Willmann, J. K.; Paulmurugan, R. Gemcitabine and Antisense-MicroRNA Co-Encapsulated PLGA-PEG Polymer Nanoparticles for Hepatocellular Carcinoma Therapy. *ACS Appl. Mater. Interfaces* **2016**, *8* (49), 33412−33422.
(15) Chishti, N.; Jagwani, S.; Dhamecha, D.; Jalalpure, S.; Dehghan, M. H. Preparation, Optimization, and in Vivo Evaluation of Nanoparticle-Based Formulation for Pulmonary Delivery of Anticancer Drug. *Med.* **2019**, *55* (6), 294.
(16) Jadhav, K.; HR, R.; Deshpande, S.; Jagwani, S.; Dhamecha, D.; Jalalpure, S.; Subburayan, K.; Baheti, D. Phytosynthesis of Gold Nanoparticles: Characterization, Biocompatibility, and Evaluation of Its Osteoinductive Potential for Application in Implant Dentistry. *Mater. Sci. Eng., C* **2018**, *93*, 664−670.
(17) Dhamecha, D.; Jalalpure, S.; Jadhav, K. Doxorubicin Functionalized Gold Nanoparticles: Characterization and Activity against Human Cancer Cell Lines. *Process Biochem.* **2015**, *50* (12), 2298−2306.
(18) Jadhav, K.; Dhamecha, D.; Bhattacharya, D.; Patil, M. Green and Ecofriendly Synthesis of Silver Nanoparticles: Characterization, Biocompatibility Studies and Gel Formulation for Treatment of Infections in Burns. *J. Photochem. Photobiol., B* **2016**, *155*, 109−115.
(19) Tang, M.; Svirskis, D.; Leung, E.; Kanamala, M.; Wang, H.; Wu, Z. Can Intracellular Drug Delivery Using Hyaluronic Acid Functionalised PH-Sensitive Liposomes Overcome Gemcitabine Resistance in Pancreatic Cancer? *J. Controlled Release* **2019**, *305*, 89−100.
(20) H.R., R.; Dhamecha, D.; Jagwani, S.; Rao, M.; Jadhav, K.; Shaikh, S.; Puzhankara, L.; Jalalpure, S. Local Drug Delivery Systems in the Management of Periodontitis: A Scientific Review. *J. Controlled Release* **2019**, *307*, 393−409.
(21) Zhang, N.; Chen, H.; Liu, A. Y.; Shen, J. J.; Shah, V.; Zhang, C.; Hong, J.; Ding, Y. Gold Conjugate-Based Liposomes with Hybrid Cluster Bomb Structure for Liver Cancer Therapy. *Biomaterials* **2016**, *74*, 280−291.
(22) Kushwah, V.; Jain, D. K.; Agrawal, A. K.; Jain, S. Improved Antitumor Efficacy and Reduced Toxicity of Docetaxel Using Anacardic Acid Functionalized Stealth Liposomes. *Colloids Surf., B* **2018**, *172*, 213−223.
(23) Wang, M.; Liu, Y.; Zhang, X.; Luo, L.; Li, L.; Xing, S.; He, Y.; Cao, W.; Zhu, R.; Gao, D. Gold Nanoshell Coated Thermo-PH Dual Responsive Liposomes for Resveratrol Delivery and Chemo-Photothermal Synergistic Cancer Therapy. *J. Mater. Chem. B* **2017**, *5* (11), 2161−2171.
(24) Cosco, D.; Paolino, D.; Maiuolo, J.; Marzio, L. Di; Carafa, M.; Ventura, C. A.; Fresta, M. Ultradeformable Liposomes as Multidrug Carrier of Resveratrol and 5-Fluorouracil for Their Topical Delivery. *Int. J. Pharm.* **2015**, *489* (1−2), 1−10.
(25) Caddeo, C.; Teskač, K.; Sinico, C.; Kristl, J. Effect of Resveratrol Incorporated in Liposomes on Proliferation and UV-B Protection of Cells. *Int. J. Pharm.* **2008**, *363* (1−2), 183−191.
(26) Caddeo, C.; Nacher, A.; Vassallo, A.; Armentano, M. F.; Pons, R.; Fernàndez-Busquets, X.; Carbone, C.; Valenti, D.; Fadda, A. M.; Manconi, M. Effect of Quercetin and Resveratrol Co-Incorporated in Liposomes against Inflammatory/Oxidative Response Associated with Skin Cancer. *Int. J. Pharm.* **2016**, *513* (1−2), 153−163.
(27) Jhaveri, A.; Deshpande, P.; Pattni, B.; Torchilin, V. Transferrin-Targeted, Resveratrol-Loaded Liposomes for the Treatment of Glioblastoma. *J. Controlled Release* **2018**, *277*, 89−101.
(28) Pozo-Guisado, E.; Merino, J. M.; Mulero-Navarro, S.; Lorenzo-Benayas, M. J.; Centeno, F.; Alvarez-Barrientos, A.; Salguero, P. M. F. Resveratrol-Induced Apoptosis in MCF-7 Human Breast Cancer Cells Involves a Caspase-Independent Mechanism with Downregulation of Bcl-2 and NF-KB. *Int. J. Cancer* **2005**, *115* (1), 74−84.
(29) Narayanan, N. K.; Nargi, D.; Randolph, C.; Narayanan, B. A. Liposome Encapsulation of Curcumin and Resveratrol in Combination Reduces Prostate Cancer Incidence in PTEN Knockout Mice. *Int. J. Cancer* **2009**, *125* (1), 1−8.
(30) Bilensoy, E. Cationic Nanoparticles for Cancer Therapy. *Expert Opin. Drug Delivery* **2010**, *7* (7), 795−809.
(31) Fidler, I. J.; Schroit, A. J.; Connor, J.; Bucana, C. D.; Fidler, I. J. Elevated Expression of Phosphatidylserine in the Outer Membrane Leaflet of Human Tumor Cells and Recognition by Activated Human Blood Monocytes. *Cancer Res.* **1991**, *51* (11), 3062−3066.
(32) Bangham, A. D.; Standish, M. M.; Watkins, J. C. Diffusion of Univalent Ions across the Lamellae of Swollen Phospholipids. *J. Mol. Biol.* **1965**, *13* (1), 238−252.
(33) Jain, S.; Kumar, D.; Swarnakar, N. K.; Thanki, K. Biomaterials Polyelectrolyte Stabilized Multilayered Liposomes for Oral Delivery of Paclitaxel Q. *Biomaterials* **2012**, *33* (28), 6758−6768.
(34) Liu, J.; Wang, Z.; Li, F.; Gao, J.; Wang, L.; Huang, G. Liposomes for Systematic Delivery of Vancomycin Hydrochloride to Decrease Nephrotoxicity: Characterization and Evaluation. *Asian J. Pharm. Sci.* **2015**, *10* (3), 212−222.
(35) Nguyen, T. L.; Nguyen, T. H.; Nguyen, D. H. Development and in Vitro Evaluation of Liposomes Using Soy Lecithin to Encapsulate Paclitaxel. *Int. J. Biomater.* **2017**, *2017*, 1.
(36) Shishir, M. R. I.; Karim, N.; Gowd, V.; Xie, J.; Zheng, X.; Chen, W. Pectin-Chitosan Conjugated Nanoliposome as a Promising Delivery System for Neohesperidin: Characterization, Release Behavior, Cellular Uptake, and Antioxidant Property. *Food Hydrocolloids* **2019**, *95*, 432−444.
(37) Shah, S. M.; Goel, P. N.; Jain, A. S.; Pathak, P. O.; Padhye, S. G.; Govindarajan, S.; Ghosh, S. S.; Chaudhari, P. R.; Gude, R. P.; Gopal, V.; Nagarsenker, M. S. Liposomes for Targeting Hepatocellular Carcinoma: Use of Conjugated Arabinogalactan as Targeting Ligand. *Int. J. Pharm.* **2014**, *477* (1−2), 128−139.
(38) Karn, P. R.; Cho, W.; Park, H. J.; Park, J. S.; Hwang, S. J. Characterization and Stability Studies of a Novel Liposomal Cyclosporin a Prepared Using the Supercritical Fluid Method: Comparison with the Modified Conventional Bangham Method. *Int. J. Nanomed.* **2013**, *8*, 365−377.
(39) Jadhav, K.; Deore, S.; Dhamecha, D.; Hr, R.; Jagwani, S.; Jalalpure, S.; Bohara, R. Phytosynthesis of Silver Nanoparticles: Characterization, Biocompatibility Studies, and Anticancer Activity. *ACS Biomater. Sci. Eng.* **2018**, *4* (3), 892−899.
(40) Dhamecha, D.; Jalalpure, S.; Jadhav, K.; Jagwani, S.; Chavan, R. Doxorubicin Loaded Gold Nanoparticles: Implication of Passive Targeting on Anticancer Efficacy. *Pharmacol. Res.* **2016**, *113*, 547−556.
(41) Rajeshwari, H. R.; Dhamecha, D.; Jagwani, S.; Patil, D.; Hegde, S.; Potdar, R.; Metgud, R.; Jalalpure, S.; Roy, S.; Jadhav, K.; Tiwari, N. K.; Koduru, S.; Hugar, S.; Dodamani, S. Formulation of Thermoreversible Gel of Cranberry Juice Concentrate: Evaluation,

https://dx.doi.org/10.1021/acsbiomaterials.0c00429
ACS Biomater. Sci. Eng. XXXX, XXX, XXX−XXX

Biocompatibility Studies and Its Antimicrobial Activity against Periodontal Pathogens. *Mater. Sci. Eng., C* **2017**, *75*, 1506−1514.
(42) Garg, N. K.; Singh, B.; Kushwah, V.; Tyagi, R. K.; Sharma, R.; Jain, S.; Katare, O. P. The Ligand (s) Anchored Lipobrid Nanoconstruct Mediated Delivery of Methotrexate: An Effective Approach in Breast Cancer Therapeutics. *Nanomedicine* **2016**, *12* (7), 2043−2060.
(43) Pretor, S.; Bartels, J.; Lorenz, T.; Dahl, K.; Finke, J. H.; Peterat, G.; Krull, R.; Al-Halhouli, A. T.; Dietzel, A.; Büttgenbach, S.; Behrends, S.; Reichl, S.; Müller-Goymann, C. C. Cellular Uptake of Coumarin-6 under Microfluidic Conditions into HCE-T Cells from Nanoscale Formulations. *Mol. Pharmaceutics* **2015**, *12* (1), 34−45.
(44) Kilkenny, C.; Browne, W. J.; Cuthill, I. C.; Emerson, M.; Altman, D. G. The ARRIVE Guidelines Animal Research: Reporting in Vivo Experiments. *PLoS Biol.* **2010**, *8* (6), No. e1000412.
(45) El Mesallamy, H. O.; Metwally, N. S.; Soliman, M. S.; Ahmed, K. A.; Moaty, M. M. A. The Chemopreventive Effect of Ginkgo Biloba and Silybum Marianum Extracts on Hepatocarcinogenesis in Rats. *Cancer Cell Int.* **2011**, *11* (1), 38.
(46) Lee, E. O.; Lee, H. J.; Hwang, H. S.; Ahn, K. S.; Chae, C.; Kang, K. S.; Lu, J.; Kim, S. H. Potent Inhibition of Lewis Lung Cancer Growth by Heyneanol A from the Roots of Vitis Amurensis through Apoptotic and Anti-Angiogenic Activities. *Carcinogenesis* **2006**, *27* (10), 2059−2069.
(47) Diehl, K. H.; Hull, R.; Morton, D.; Pfister, R.; Rabemampianina, Y.; Smith, D.; Vidal, J. M.; Van De Vorstenbosch, C. A Good Practice Guide to the Administration of Substances and Removal of Blood, Including Routes and Volumes. *J. Appl. Toxicol.* **2001**, *21* (1), 15−23.
(48) Jagwani, S.; Jalalpure, S.; Dhamecha, D.; Hua, G. S.; Jadhav, K. Development and Validation of Reverse-Phase High-Performance Liquid Chromatographic Method for Determination of Resveratrol in Human and Rat Plasma for Preclinical and Clinical Studies. *Indian J. Pharm. Educ.* **2019**, *54* (1), 187−193.
(49) Tsai, Y. M.; Chien, C. F.; Lin, L. C.; Tsai, T. H. Curcumin and Its Nano-Formulation: The Kinetics of Tissue Distribution and Blood-Brain Barrier Penetration. *Int. J. Pharm.* **2011**, *416* (1), 331−338.
(50) Shelke, S.; Shahi, S.; Jalalpure, S.; Dhamecha, D. Poloxamer 407-Based Intranasal Thermoreversible Gel of Zolmitriptan-Loaded Nanoethosomes: Formulation, Optimization, Evaluation and Permeation Studies. *J. Liposome Res.* **2016**, *26* (4), 313−323.
(51) Kotyńska, J.; Figaszewski, Z. A. Adsorption Equilibria at Interface Separating Electrolyte Solution and Phosphatidylcholine−Stearylamine Liposome Membrane. *Biophys. Chem.* **2007**, *127* (1−2), 84−90.
(52) Villasmil-Sánchez, S.; Drhimeur, W.; Ospino, S. C. S.; Rabasco Alvarez, A. M.; González-Rodríguez, M. L. Positively and Negatively Charged Liposomes as Carriers for Transdermal Delivery of Sumatriptan: In Vitro Characterization. *Drug Dev. Ind. Pharm.* **2010**, *36* (6), 666−675.
(53) Ramana, L. N.; Sethuraman, S.; Ranga, U.; Krishnan, U. M. Development of a Liposomal Nanodelivery System for Nevirapine. *J. Biomed. Sci.* **2010**, *17* (1), 57.
(54) El Maghraby, G. M. M.; Campbell, M.; Finnin, B. C. Mechanisms of Action of Novel Skin Penetration Enhancers: Phospholipid versus Skin Lipid Liposomes. *Int. J. Pharm.* **2005**, *305* (1−2), 90−104.
(55) Dhamecha, D.; Jalalpure, S.; Jadhav, K. Nepenthes Khasiana Mediated Synthesis of Stabilized Gold Nanoparticles: Characterization and Biocompatibility Studies. *J. Photochem. Photobiol., B* **2016**, *154*, 108−117.
(56) Casals, E.; Soler, M.; Gallardo, M.; Estelrich, J. Electrophoretic Behavior of Stearylamine-Containing Liposomes. *Langmuir* **1998**, *14* (26), 7522−7526.
(57) González-Rodríguez, M. L.; Rabasco, A. M. Charged Liposomes as Carriers to Enhance the Permeation through the Skin. *Expert Opin. Drug Delivery* **2011**, *8* (7), 857−871.
(58) Hammoud, Z.; Gharib, R.; Fourmentin, S.; Elaissari, A.; Greige-Gerges, H. Drug-in-Hydroxypropyl-β-Cyclodextrin-in-Lipoid S100/Cholesterol Liposomes: Effect of the Characteristics of Essential Oil Components on Their Encapsulation and Release. *Int. J. Pharm.* **2020**, *579*, 119151.
(59) Karve, S.; Kempegowda, G. B.; Sofou, S. Heterogeneous Domains and Membrane Permeability in Phosphatidylcholine - Phosphatidic Acid Rigid Vesicles as a Function of PH and Lipid Chain Mismatch. *Langmuir* **2008**, *24* (11), 5679−5688.
(60) Bruschi, M. L. Mathematical Models of Drug Release. *Strategies to Modify the Drug Release from Pharmaceutical Systems*; Woodhead Publishing, 2015. .
(61) Wójcik-Pastuszka, D.; Krzak, J.; Macikowski, B.; Berkowski, R.; Osiński, B.; Musiał, W. Evaluation of the Release Kinetics of a Pharmacologically Active Substance from Model Intra-Articular Implants Replacing the Cruciate Ligaments of the Knee. *Materials* **2019**, *12* (8), 1202.
(62) Dhawan, V.; Magarkar, A.; Joshi, G.; Makhija, D.; Jain, A.; Shah, J.; Reddy, B. V. V.; Krishnapriya, M.; Róg, T.; Bunker, A.; Jagtap, A.; Nagarsenker, M. Stearylated Cycloarginine Nanosystems for Intracellular Delivery-Simulations, Formulation and Proof of Concept. *RSC Adv.* **2016**, *6* (114), 113538−113550.
(63) Su, D.; Cheng, Y.; Liu, M.; Liu, D.; Cui, H.; Zhang, B.; Zhou, S.; Yang, T.; Mei, Q. Comparision of Piceid and Resveratrol in Antioxidation and Antiproliferation Activities In Vitro. *PLoS One* **2013**, *8* (1), No. e54505.
(64) Lu, X.-Y.; Hu, S.; Jin, Y.; Qiu, L.-Y. Application of Liposome Encapsulation Technique to Improve Anti-Carcinoma Effect of Resveratrol. *Drug Dev. Ind. Pharm.* **2012**, *38* (3), 314−322.
(65) Wang, H.; Thorling, C. A.; Liang, X.; Bridle, K. R.; Grice, J. E.; Zhu, Y.; Crawford, D. H. G.; Xu, Z. P.; Liu, X.; Roberts, M. S. Diagnostic Imaging and Therapeutic Application of Nanoparticles Targeting the Liver. *J. Mater. Chem. B* **2015**, *3* (6), 939−958.
(66) Kristl, J.; Teskač, K.; Caddeo, C.; Abramović, Z.; Šentjurc, M. Improvements of Cellular Stress Response on Resveratrol in Liposomes. *Eur. J. Pharm. Biopharm.* **2009**, *73* (2), 253−259.
(67) De, M.; Ghosh, S.; Sen, T.; Shadab, M.; Banerjee, I.; Basu, S.; Ali, N. A Novel Therapeutic Strategy for Cancer Using Phosphatidylserine Targeting Stearylamine-Bearing Cationic Liposomes. *Mol. Ther.–Nucleic Acids* **2018**, *10*, 9−27.
(68) Miao, X.; Li, Y.; Wyman, I.; Lee, S. M. Y.; Macartney, D. H.; Zheng, Y.; Wang, R. Enhanced in Vitro and in Vivo Uptake of a Hydrophobic Model Drug Coumarin-6 in the Presence of Cucurbit [7] Uril. *MedChemComm* **2015**, *6* (7), 1370−1374.
(69) Parvathaneni, V.; Kulkarni, N. S.; Shukla, S. K.; Farrales, P. T.; Kunda, N. K.; Muth, A.; Gupta, V. Systematic Development and Optimization of Inhalable Pirfenidone Liposomes for Non-Small Cell Lung Cancer Treatment. *Pharmaceutics* **2020**, *12* (3), 206.
(70) Rivolta, I.; Panariti, A.; Lettiero, B.; Sesana, S.; Gasco, P.; Gasco, M. R.; Masserini, M.; Miserocchi, G. Cellular Uptake of Coumarin-6 as a Model Drug Loaded in Solid Lipid Nanoparticles. *J. Physiol. Pharmacol.* **2011**, *62* (1), 45−53.
(71) Zhao, S.; Dai, W.; He, B.; Wang, J.; He, Z.; Zhang, X.; Zhang, Q. Monitoring the Transport of Polymeric Micelles across MDCK Cell Monolayer and Exploring Related Mechanisms. *J. Controlled Release* **2012**, *158* (3), 413−423.
(72) Saadat, M.; Zahednezhad, F.; Zakeri-Milani, P.; Heidari, H. R.; Shahbazi-Mojarrad, J.; Valizadeh, H. Drug Targeting Strategies Based on Charge Dependent Uptake of Nanoparticles into Cancer Cells. *J. Pharm. Pharm. Sci.* **2019**, *22*, 191−220.
(73) Behzadi, S.; Serpooshan, V.; Tao, W.; Hamaly, M. A.; Alkawareek, M. Y.; Dreaden, E. C.; Brown, D.; Alkilany, A. M.; Farokhzad, O. C.; Mahmoudi, M. Cellular Uptake of Nanoparticles: Journey inside the Cell. *Chem. Soc. Rev.* **2017**, *46* (14), 4218−4244.
(74) De Smet, L.; Ceelen, W.; Remon, J. P.; Vervaet, C. Optimization of Drug Delivery Systems for Intraperitoneal Therapy to Extend the Residence Time of the Chemotherapeutic Agent. *Sci. World J.* **2013**, *2013*, 1.

https://dx.doi.org/10.1021/acsbiomaterials.0c00429
ACS Biomater. Sci. Eng. XXXX, XXX, XXX−XXX

(75) Lee, G.; Han, S.; Inocencio, I.; Cao, E.; Hong, J.; Phillips, A. R. J.; Windsor, J. A.; Porter, C. J. H.; Trevaskis, N. L. Lymphatic Uptake of Liposomes after Intraperitoneal Administration Primarily Occurs via the Diaphragmatic Lymphatics and Is Dependent on Liposome Surface Properties. *Mol. Pharmaceutics* **2019**, *16* (12), 4987−4999.
(76) Hirano, K.; Hunt, C. A. Lymphatic Transport of Liposome-encapsulated Agents: Effects of Liposome Size Following Intraperitoneal Administration. *J. Pharm. Sci.* **1985**, *74* (9), 915−921.
(77) Dadashzadeh, S.; Mirahmadi, N.; Babaei, M. H.; Vali, a M. Peritoneal Retention of Liposomes: Effects of Lipid Composition, PEG Coating and Liposome Charge. *J. Controlled Release* **2010**, *148* (2), 177−186.
(78) Kenis, H.; Reutelingsperger, C. Targeting Phosphatidylserine in Anti-Cancer Therapy. *Curr. Pharm. Des.* **2009**, *15* (23), 2719−2723.
(79) Soares, M. M.; King, S. W.; Thorpe, P. E. Targeting Inside-out Phosphatidylserine as a Therapeutic Strategy for Viral Diseases. *Nat. Med.* **2008**, *14* (12), 1357−1362.
(80) Riedl, S.; Rinner, B.; Asslaber, M.; Schaider, H.; Walzer, S.; Novak, A.; Lohner, K.; Zweytick, D. In Search of a Novel Target - Phosphatidylserine Exposed by Non-Apoptotic Tumor Cells and Metastases of Malignancies with Poor Treatment Efficacy. *Biochim. Biophys. Acta, Biomembr.* **2011**, *1808* (11), 2638−2645.
(81) Ran, S.; Downes, A.; Thorpe, P. E. Increased Exposure of Anionic Phospholipids on the Surface of Tumor Blood Vessels. *Cancer Res.* **2002**, *62* (21), 6132−6140.
(82) Bozzuto, G.; Molinari, A. Liposomes as Nanomedical Devices. *Int. J. Nanomed.* **2015**, *10*, 975−999.
(83) Reddy, L. H.; Couvreur, P. Nanotechnology for Therapy and Imaging of Liver Diseases. *J. Hepatol.* **2011**, *55* (6), 1461−1466.
(84) Zhu, X.; Tsend-Ayush, A.; Yuan, Z.; Wen, J.; Cai, J.; Luo, S.; Yao, J.; Bian, J.; Yin, L.; Zhou, J.; Yao, J. Glycyrrhetinic Acid-Modified TPGS Polymeric Micelles for Hepatocellular Carcinoma-Targeted Therapy. *Int. J. Pharm.* **2017**, *529* (1−2), 451−464.
(85) Bishayee, A.; Politis, T.; Darvesh, A. S. Resveratrol in the Chemoprevention and Treatment of Hepatocellular Carcinoma. *Cancer Treat. Rev.* **2010**, *36* (1), 43−53.
(86) Bishayee, A.; Dhir, N. Resveratrol-Mediated Chemoprevention of Diethylnitrosamine-Initiated Hepatocarcinogenesis: Inhibition of Cell Proliferation and Induction of Apoptosis. *Chem.-Biol. Interact.* **2009**, *179* (2−3), 131−144.
(87) Rajasekaran, D.; Elavarasan, J.; Sivalingam, M.; Ganapathy, E.; Kumar, A.; Kalpana, K.; Sakthisekaran, D. Resveratrol Interferes with N-Nitrosodiethylamine-Induced Hepatocellular Carcinoma at Early and Advanced Stages in Male Wistar Rats. *Mol. Med. Rep.* **2011**, *4* (6), 1211−1217.
(88) Rajesh, V.; Kavitha, K. N. V. K.; Vishali, K.; Raju, C.; Gayathri, K.; Sruthi, A. Protective Effect Courouptia Guianensis Flower Extract against N-Nitrosodiethylamine-Induced Hepatic Damage in Wistar Albino Rats. *Orient. Pharm. Exp. Med.* **2015**, *15* (1), 83−93.
(89) Farazuddin, M.; Bhavyata, D.; Zia, Q.; Khan, A. A.; Joshi, B.; Owais, M. Chemotherapeutic Potential of Curcumin-Bearing Microcells against Hepatocellular Carcinoma in Model Animals. *Int. J. Nanomed.* **2014**, *9*, 1139.

https://dx.doi.org/10.1021/acsbiomaterials.0c00429
ACS Biomater. Sci. Eng. XXXX, XXX, XXX−XXX

Original Article

Development and Validation of Reverse-Phase High-Performance Liquid Chromatographic Method for Determination of Resveratrol in Human and Rat Plasma for Preclinical and Clinical Studies

Satveer Jagwani[1,2], Sunil Jalalpure[1,2]*, Dinesh Dhamecha[2], Gan Siew Hua[3], Kiran Jadhav[1]

[1]KLE College of Pharmacy, KLE Academy of Higher Education and Research, Nehru Nagar, Belagavi, Karnataka, INDIA.
[2]Dr. Prabhakar Kore Basic Science Research Center, KLE Academy of Higher Education and Research, Nehru Nagar, Belagavi, Karnataka, INDIA.
[3]School of Pharmacy, Monash University Malaysia, Jalan Lagoon Selatan, Bandar Sunway, Selangor, MALAYSIA.

ABSTRACT

Aim: The aim of the study was to develop and validate a simple and precise reverse-phase High Performance Liquid Chromatography (RP-HPLC) method for quantitative analysis of trans-resveratrol in human and rat plasma. **Methods:** HPLC method was developed by using Phenomenex Luna C18 column (150 x 4.6 mm, 5 μm) and the optimized mobile phase comprised of acetonitrile/water in isocratic mode (30:70, v/v) with the flow rate of 1.0 mL/min. Trans-resveratrol was detected at a UV wavelength of 306 nm. Developed method was validated as per International Conference on Harmonization (ICH) M10 guidelines. **Results:** The proposed method was found simple, precise and linear with regression coefficient of 0.999 which could analyse the samples in nanograms levels with mean percent recovery in the acceptable range of 94.44 – 97.44%. The method was precise at the intra-day and inter-day levels as reflected by the relative standard deviation values (less than 3.36%). Trans resveratrol was found to be stable in plasma under different storage conditions. **Conclusion:** The present investigation demonstrated that the developed method was succesfully applied to accurately determine trans-resveratrol in human and rat plasma and therefore can be applicable for pre-clinical and clinical studies.

Key words: RP-HPLC, Trans resveratrol, Human plasma, Rat plasma, Storage stability studies.

INTRODUCTION

Recently, various food constituents, mainly polyphenols have gained wide attention either as a potential therapeutic or as prophylactic agent in the management of several diseases.[1] Resveratrol (3,5,4'- trihydroxystilbene), a well-known naturally occurring lipophilic polyphenol is first isolated from white hellebore and also present in wide range of other plant products including cranberry, grapevine, blueberry, bilberry and peanut.[2,3] Resveratrol has two isomers cis and trans from which, the trans-resveratrol is the therapeutically active form (Figure 1) responsible for health-promoting pharmacological effects like antioxidant, anti-aging, cardioprotective, neuroprotective, anti-inflammatory and anticancer properties.[4] Although trans-resveratrol has shown promising results in several diseases but its unfavorable pharmacokinetic properties such as low bioavailability, extensive metabolism and short half-life limits its use in clinical applications.[5] Currently, trans-resveratrol has been widely incorporated as a nutritional supplement in the day-today life and to consume it as a drug, it is important

Submission Date: 16-05-2019;
Revision Date: 22-08-2019;
Accepted Date: 03-12-2019

DOI: 10.5530/ijper.54.1.22

Correspondence:
Dr. Sunil Jalalpure,
Professor, KLE College of Pharmacy, KLE Academy of Higher Education and Research, Nehru Nagar, Belagavi, Karnataka, INDIA.
2Dr. Prabhakar Kore Basic Science Research Center, KLE Academy of Higher Education and Research, Nehru Nagar, Belagavi-590010 Karnataka, INDIA.
Phone: +91 9448964057
E-mail: jalalpuresunil@rediffmail.com

www.ijper.org

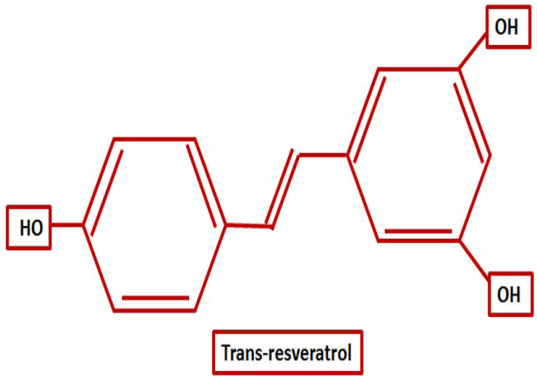

Figure 1: Structure of trans-resveratrol.

to develop an appropriate drug delivery systems which can overcome the problems related to its pharmacokinetic. Several HPLC methods are reported in the literature to quantify trans resveratrol in human and rat plasma.[2,5-9] However, the reported RP-HPLC methods present several limitations such as long run times, high flow rates, complicated gradient elutions and buffer solutions in mobile phase. The necessity for development of a reliable analytical method for drug assay in biological fluids is a prerequisite for pharmacokinetic studies in animal models and human subjects.

With this background, the aim of the study was to develop a simple, rapid and selective RP-HPLC method in accordance with U.S. Food and Drug Administration and ICH guideline[10,11] to quantify trans-resveratrol in human and rat plasma.

MATERIALS AND METHODS

Materials

Trans-resveratrol (99% pure) and carbamazepine were obtained as free samples from Ms. Sami Labs Ltd., Bangalore, India and Alkem Laboratories Ltd., Mumbai, India, respectively. HPLC-grade acetonitrile (ACN) and methanol were procured from Merck, Mumbai, India. Whole human blood was obtained from K.L.E.S. Dr. Prabhakar Kore Hospital and Medical Research Centre blood bank, (Nehru Nagar, Belagavi-590010, Karnataka, India) and was processed to obtained blank plasma. Deionized water used in the tests was prepared by filtering water through Millipore Direct-Q®-3 purification system (18.2 MΩ/cm) Millipore (Molsheim, France).

Instrument

The HPLC system (LC-20AD prominence system, Shimadzu, Kyoto, Japan) consisted of an LC-20AD pump, SIL-20 AC HT autosampler, SPD-M20A diode array detector and CBM-20A communication bus module, which was functioned by using computer based Shimadzu LC solution (version 1.25) software program to analyse the chromatograms. A reverse phase Luna C_{18} column (150 x 4.6 mm i.d., 5 µm particle size, Phenomenex, USA) equipped with a guard column (ODS; 4 x 3.0 mm ID, Phenomenex, CA, USA) with a similar particle size was used for separation.

Chromatographic conditions

System was operated with isocratic elution of ACN: Deionized water (30:70 v/v) as mobile phase at a flow rate of 1.0 mL/min under a controlled temperature (30°C) condition. Solvents were prepared by degassing in bath sonicator for 10 min followed by filteration through 0.45 µm membrane Millex HV polyvinylidene fluoride membrane filters (Millipore, Bedford, USA) by using vaccum pump. Drug samples (20 µl) was injected in HPLC system and detected at 306 nm.

Method validation

Developed method was validated for its selectivity, linearity, system suitability, Limit of Detection (LOD), Limit of Quantitation (LOQ), precision, accuracy and stability.

Human and rat plasma samples preparations

Animal experiments was approved by the Institutional Animal Ethical Committee, KLE College of Pharmacy, Belagavi, India. Human and rat blood samples were centrifuged at 3000 rpm for 10 min at 4°C for plasma separation.[12] The stock solution of the drug was spiked in rat and human plasma to get final concentrations of 2, 4, 6, 8, 10, 12 µg mL^{-1} (trans-resveratrol). Protein precipitation was performed by treating the spiked plasma samples (150 µL) with acetonitrile (100 µL) followed by centrifugation at 10000 rpm for 10 min at 4°C. Finally, the supernatant was carefully seperated and loaded into the HPLC autosampler for analysis.[13]

Stability experiments

Trans-resveratrol stability was determined in the human and rat plasma at different storage conditions as follows: stability for up to 6 h at 25°C, freezer stability up to 7 days (at -20°C) and freeze-thaw stability (at -20°C). In freeze-thaw stability, cycles were conducted for thrice and the samples were restored to the same condition after withdrawal of aliquots for analysis. The peak areas of the trans-resveratrol obtained at 0 h were used as the reference to determine the relative stability at various storage conditions. All the experiment were performed in triplicates and the samples were considered as stable if the assay values were within the acceptable limit of accuracy (i.e. ± 15% standard deviation).[14]

RESULTS AND DISCUSSION

Method development

Preceding to the validation step, the proposed method was developed in order to provide a simple and optimized procedure, with reduced time and cost of analysis. Therefore, different chromatographic parameters were considered, namely peak number of theoretical plates (N), symmetry (as described by the tailing factor, T), resolution, HETP and retention factor (k'). Initially, the developed RP-HPLC method was optimized by altering the mobile phase composition to obtain symmetrical peak. Varying ratios of solvents mainly consisting of ACN and deionized water with or without methanol was used to optimise the resolution of the peak. Solvent composition consisting of methanol and water in the ratio of 50:50 v/v might yield clear trans-resveratrol peak but had a undesirable impact on the theoretical plate number whereas, solvent composition consisting of ACN and deionized water 50:50 v/v yielded well resolved peak with minor tailing. For the separation of trans-resveratrol, several proportions of ACN and water were tested ranging from 90:10 to 40:60 and analysed to get sharp peak with negligible tailing and shorter retention time. Apart from the mobile phase selection, column temperature is one of the key parameter that demonstrate the significant effect on retention time and peak shape of trans-resveratrol. Experiments with colum temperature in the ranging from 25°C to 45°C revealed that 30°C demonstrated clear peak shape and shorter retention time when compared to others.

The developed HPLC system with Luna C_{18} column (150 x 4.6 mm i.d., 5µm) was validated by using a solvent mixture of ACN and deionized water (30:70) with isocratic elution at 1.0 mL/min. The injection volume was set up at 20 µL with column temperature of 30°C. Under these chromatographic conditions, trans-resveratrol was detected at wavelength of 306 nm with retention time of 6.1 min (Figure 2).

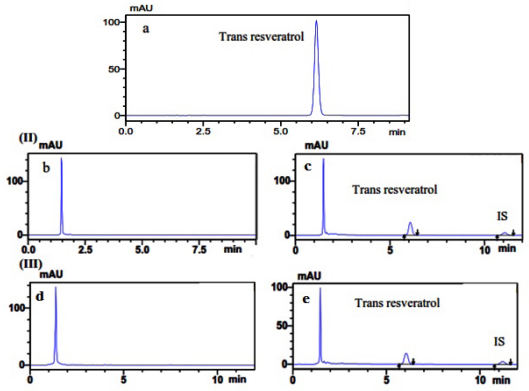

Figure 2: Representative chromatogram obtained from a) pure trans resveratrol (6µg mL^{-1}) b) blank human plasma c) human plasma spiked with pure trans resveratrol at 6µg mL^{-1} and internal standard (IS) carbamezapine at 20µg mL^{-1} d) blank rat plasma e) rat plasma spiked with pure trans resveratrol at 6µg mL^{-1} and internal standard (IS) carbamezapine at 20µg mL^{-1}. Retention time of pure resveratrol and IS are 6.1 and 11.2 min, respectively.

Table 1: System suitability parameters.

Parameter	Human plasma	Rat plasma	Acceptance criteria
Retention time (R_t, min)	6.055 ± 0.004	6.051 ± 0.003	-
Peak area	171352.3 ± 1173.212	172503.7 ± 1329.123	-
Tailing factor (T)	1.11	1.09	≤ 2.0
Theoretical plates (N)	8504.00	4454.00	> 2000
Resolution	26.21	10.92	>2
HETP	0.01	0.03	Smaller the value the higher column efficiency
retention factor (k')	3.16	3.10	> 2

Values are express as mean ± standard deviation (SD); (*n*=6)

Method validation

System suitability and selectivity tests

System suitability test is an vital part of the HPLC method development which defines the feasibility and acceptability of the proposed method for the estimation of trans-resveratrol in the plasma. The results of the tested parameters along with their acceptance criteria are summarized in Table 1. All the parameters such as retention factor (>2), tailing factor (< 2), resolution (>2) and theoretical plate number (>2000) were found to be within the acceptable limits demonstrating desirable resolution, peak symmetry, column efficiency and excellent chromatographic conditions which was used for further validation and sample analysis. Selectivity is described as the ability of a method to separate the analyte from all possibly interfering substance. The selectivity of the method was examined by analyzing blank human and rat plasma detection and spiking with pure compound. Figure 2 shows that there were no interference of plasma in resveratrol elution.

Linearity and range

The linearity of a method is defined as the relationship between the peak area and its corresponding concentrations in the sample solutions. The developed method was found to be linear (Figure 3) over the range of 2 –

12 µg mL^{-1} with correlation coefficient; r^2= 0.999 (Table 2) indicating acceptable linearity over the proposed concentration range.

LOD and LOQ

The LOD and LOQ were determined by diluting the known concentration of the drug until a signal to noise ratio of nearly 3:1 and 10:1 were obtained (Table 2). The lowest concentration of trans-resveratrol detected in human and rat plasma was 0.030 and 0.032 µg mL^{-1} respectively. Whereas, the limit of quantitation in the human plasma and rat plasma was found to be 0.090 and 0.099 µg mL^{-1} respectively.

Precision

The precision of an analytical method indicates the closeness of agreement between the series of measurements obtained from multiple samplings of the identical sample under the similar analytical conditions. Both inter-day (at three consecutive days) and intra-day (repeatability) assays were performed at three different concentrations (in triplicates) and results are shown in Table 3. The percent relative standard deviation (%RSD) of the total peak areas were <3.36% which indicates that the developed method is precise.

Accuracy

The accuracy of the bioanalytical method is defined as the percent difference between the mean experimental value and true value. Accuracy was evaluated by conducting a recovery experiment in pre-analysed biological fluid (human and rat plasma). The assay was performed by following standard addition method at three different concentrations (50%, 100% and 150%) of preanalysed trans-resveratrol samples in triplicates. The mean percent recovery of trans resveratrol from biological fluid were in the range of 94.44 to 97.44 % with < 1 % RSD. The results summarized in the Table 4. clearly indicate that the developed method displayed low variability and a strong agreement between experimental and true values.

Trans-resveratrol stability

Trans-resveratrol was stable for 6h at 23°C - 25°C and 7 days at freezing condition (-20°C). Trans resveratrol was also stable for 3 freeze-thaw (F/T) cycles (Table 5).

Comparison with previous published methods

Comparative analysis of methods described in the existing literature and the current study reveals the advantage of the developed method (Table 6). The developed method uses conventional solvents like water and ACN and has the flowrate of 1mL min^{-1} with retention time of 6 min which suggests that it is economic, cheap and

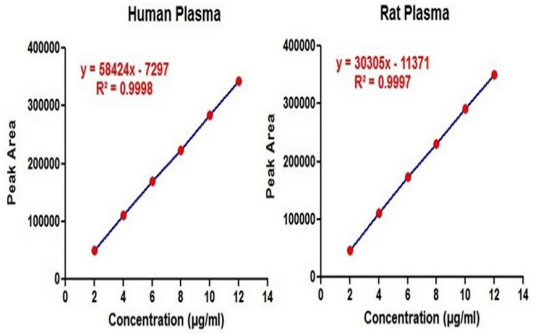

Figure 3: Linearity curve of trans resveratrol in human and rat plasma found to be linear over the range of 2 – 12 µg mL^{-1} with correlation coefficient; r^2= 0.999.

Table 2: Statistical evaluation of the calibration data.

Parameters	Human plasma	Rat plasma
Linearity range (µg mL $^{-1}$)	2 - 12	2 - 12
Slope	58424	30305
Intercept	-7297	-11371
Correlation coefficient	0.999	0.999
Limit of detection (µg mL $^{-1}$)	0.0301	0.0327
Limit of quantification (µg mL $^{-1}$)	0.0909	0.0992

Table 3: Intraday and interday precision of resveratrol.

Samples	Resveratrol concentration (µg mL^{-1})	Intraday (*n*=6) Percent RSD	Interday (*n*=3) Percent RSD		
			Day 1	Day 2	Day 3
Human plasma	2	1.042	1.208	1.690	1.684
	6	1.430	1.368	1.315	1.02
	10	1.652	1.120	1.515	1.304
Rat plasma	2	3.20	1.48	3.36	1.68
	6	1.37	1.42	1.99	2.37
	10	2.06	2.12	1.19	1.26

RSD (Relative standard deviation); *n* = number of replicate.

Table 4: Determination of accuracy based on percentage recovery (*n*=3).

Level of addition (%)	Human plasma	Rat plasma
50	94.44	94.68
Percent RSD	0.49	0.65
100	95.09	95.25
Percent RSD	0.27	0.36
150	97.44	96.29
Percent RSD	0.55	0.64

RSD (Relative standard deviation); *n* = number of replicate.

Table 5: Stability data of trans-resveratrol in human and rat plasma.

Spiked concentration (µg/mL^{-1})	Stability	Human plasma		Rat plasma	
		Mean ± SD[a] (µg/mL^{-1}), *n*= 3	Accuracy (%) [b]	Mean ± SD[a] (µg/mL^{-1}), *n* = 3	Accuracy (%) [b]
2	0 h	1.934 ± 0.022	-	1.958 ± 0.015	-
	3 F/T cycles	1.891 ± 0.027	95.33	1.771 ± 0.0132	92.37
	6 h	1.920 ± 0.012	98.45	1.919 ± 0.009	95.87
	7 days at -20°C	1.900 ± 0.016	92.39	1.941 ± 0.028	94.02
6	0 h	5.973 ± 0.006	-	5.978 ± 0.022	-
	3 F/T cycles	5.679 ± 0.023	95.07	5.837 ± 0.027	97.63
	6 h	5.753 ± 0.056	98.74	5.878 ± 0.019	98.74
	7 days at -20°C	5.190 ± 0.132	93.05	5.812 ± 0.028	97.21
10	0 h	9.876 ± 0.039	-	9.225 ± 0.099	-
	3 F/T cycles	9.325 ± 0.166	94.42	8.927 ± 0.202	96.76
	6 h	9.753 ± 0.056	98.74	8.966 ± 0.239	97.19
	7 days at -20°C	9.190 ± 0.132	93.05	8.872 ± 0.109	96.16

[a]Back calculated concentration, [b] (Mean assayed concentration/mean assayed concentration at o h) x 100.

Table 6: Comparison between HPLC methods reported in the literature.

No.	Column	Mobile phase	Separation time (min)	Limitations	Applicability	References
1	C_{18}	Gradient elution $NH_4CH_3CO_2$ -5mM CH_3OH, Propan-2-ol- 2%	18.6	Gradient elution; Longer run time; Expensive equipment	Human plasma and urine	9
2	C_{18}	3% CH_3COOH: CH_3CN (20:80, v/v)	11.7	Gradient elution; High flow rate; Expensive equipment and hence uneconomical	Rat plasma and tissue	7
3	C_{18}	H_3PO_4 0.5% v/v (pH 6.8): CH_3OH: (37:63 v/v)	3.94	Complete validation was not done; system suitability parameters were not mentioned	Spiked human plasma	15
9	C_{18}	CH_3OH: CH_3CN: 0.1% H_3PO_4 (60:10:30 v/v)	4.34	Method validation in plasma clearly not given; stability studies not given	PLGA nanoparticle and human plasma	16
10	ODS Hypersil	CH_3CN: 30µM PBS (pH 7.0) (30:70)	5.5	No system suitability data given	Rat plasma	5
14	C_{18}	CH_3CN: H_2O (30:70)	6.10	Economical, fast analysis, complete validation and stability studies of resveratrol in plasma	human and rat	Present method

fast when compared to other methods. Use of simple mobile phase without strong buffers/expensive HPLC grade solvents and a conventional C_{18} column makes the method versatile for the analysis of trans-resveratrol.

Comparison with previous published methods

Comparative analysis of methods described in the existing literature and the current study reveals the advantage of the developed method (Table 6). The developed method uses conventional solvents like water and ACN and has the flowrate of 1mL min^{-1} with retention time of 6 min which suggests that it is economic, cheap and fast when compared to other methods. Use of simple mobile phase without strong buffers/expensive HPLC grade solvents and a conventional C18 column makes the method versatile for the analysis of trans-resveratrol.

CONCLUSION

A simple, sensitive and rapid RP-HPLC method was successfully developed according to the ICH guideline for the estimation of trans-resveratrol in human and rat plasma. The simple chromatographic conditions and pre-treatment procedure is easy and fast to perform. The acceptable limit of selectivity, precision, accuracy and appropriate retention time only 6 min make it suitable for preclinical and clinical studies.

ACKNOWLEDGEMENT

The authors gratefully acknowledge Sami Labs, Bangalore, India for gifting sample of pure trans-resveratrol. The authors are thankful to KLE Academy of Higher Education and Research, Belagavi for providing facility to carry out the study.

CONFLICT OF INTEREST

The authors declares no conflict of interest.

ABBREVIATIONS

ACN: Acetonitrile; **ICH:** International Council for Harmonisation; **LC:** Liquid chromatography; **LOD:** Limit of detection; LOQ**:** Limit of Quantitation; **RP-HPLC:** Reverse Phase high performance liquid chromatography; **RSD:** Relative standard deviation; **UV:** Ultraviolet.

REFERENCES

1. Rajeshwari HR, Dhamecha D, Jagwani S. Formulation of thermoreversible gel of cranberry juice concentrate: Evaluation, biocompatibility studies and its antimicrobial activity against periodontal pathogens. Mater Sci Eng C. 2017;75:1506-14.
2. Lin HS, Ho PC. A rapid HPLC method for the quantification of 3, 5, 4′-trimethoxy-trans-stilbene (TMS) in rat plasma and its application in pharmacokinetic study. J Pharm Biomed Anal. 2009;49(2):387-92.
3. Kurangi B, Jalalpure S, Jagwani S. A validated stability-indicating HPLC method for simultaneous estimation of resveratrol and piperine in cubosome and human plasma. J Chromatogr B. 2019;1122-1123:39-48.
4. Zupančič Š, Lavrič Z, Kristl J. Stability and solubility of trans-resveratrol are strongly influenced by pH and temperature. Eur J Pharm Biopharm. 2015;93:196-204.
5. Das S, Ng KY. Quantification of trans-resveratrol in rat plasma by a simple and sensitive high performance liquid chromatography method and its application in pre-clinical study. J Liq Chromatogr Relat Technol. 2011;34(14):1399-414.
6. Katsagonis A, Atta PJ, Koupparis MA. HPLC Method with UV Detection for the Determination of trans-Resveratrol in Plasma. J Liq Chromatogr Relat Technol. 2015;28(9):1393-405.
7. Juan ME, Maijó M, Planas JM. Quantification of trans-resveratrol and its metabolites in rat plasma and tissues by HPLC. J Pharm Biomed Anal. 2010;51(2):391-8.
8. Frozza RL, Bernardi A, Paese K. Characterization of trans-resveratrol-loaded lipid-core nanocapsules and tissue distribution studies in rats. J Biomed Nanotechnol. 2010;6(6):694-703.
9. Boocock DJ, Patel KR, Faust GE. Quantitation of trans-resveratrol and detection of its metabolites in human plasma and urine by high performance liquid chromatography. J Chromatogr B. 2007;848(2):182-7.
10. U.S. Food and Drug Administration, Guidance for Industry: Bioanalytical Method Validation. Updated in 2013 and 2018. 2001. https://www.fda.gov/downloads/Drugs/ GuidanceComplianceRegulatoryInformation/Guidances/UCM070107.pdf
11. ICH guideline. M10: Validation of Analytical Procedure: Text and Methodology, International Conference on Harmonization. Available from: https://www.ich.org/fileadmin/Public_Web_Site/ICH_Products/Guidelines/Multidisciplinary/M10/M10EWG_Step2_DraftGuideline_2019_0226.pdf
12. Mohamed FA, Khashaba PY, Shahin RY, El-Wekil MM. Determination of donepezil in spiked rabbit plasma by high-performance liquid chromatography with fluorescence detection. Royal Soc Open Sci. 2019;6(1):181476.
13. Garg NK, Singh B, Kushwah V. The ligand (s) anchored lipobridnanoconstruct mediated delivery of methotrexate: An effective approach in breast cancer therapeutics. Nanomedicine. 2016;12:2043-60.
14. Chen X, He H, Wang G. Stereospecific determination of cis-and trans-resveratrol in rat plasma by HPLC: Application to pharmacokinetic studies. Biomed Chrom. 2007;21(3): 257-65.
15. Singh G, Pai RS, Pandit V. Development and validation of a HPLC method for the determination of trans-resveratrol in spiked human plasma. J Adv Pharm Technol Res. 2012;3(2):130.
16. Kumar S, Lather V, Pandita D. Stability indicating simplified HPLC method for simultaneous analysis of resveratrol and quercetin in nanoparticles and human plasma. Food Chem. 2016;197(PtA):959-64.

PICTORIAL ABSTRACT

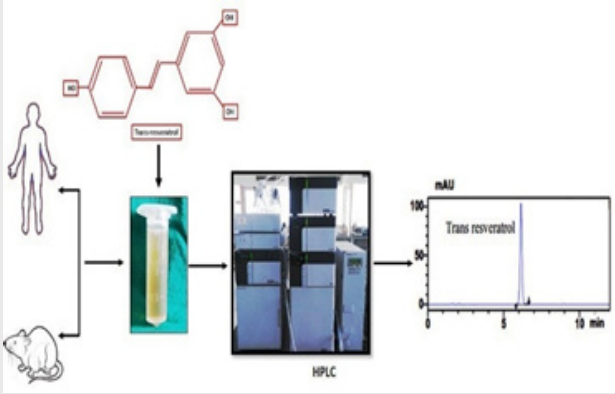

SUMMARY

Developed RP-HPLC method was validated as per ICH (M10) guidelines for quantitative analysis of trans-resveratrol in human and rat plasma. Separation of trans-resveratrol was carried out by using Phenomenex Luna C18 column (150 x 4.6 mm, 5 µm) with optimized mobile phase comprised of acetonitrile/water in isocratic mode (30:70, v/v) at the flow-rate of 1.0 mL/min. Trans-resveratroldetected at UV wavelength of 306 nm with retention time of 6.1 min. The developed bioanalytical method was rapid, simple and precise for the determination of trans resveratrol in plasma.

About Authors

Mr. Satveer Jagwani, is a PhD scholar at KLE College of Pharmacy, KLE Academy of Higher Education and Research, Belagavi. His current research interest are development of nanoparticles (lipid and metallic) and its biomedical application in the treatment of cancers, pharmacodynamic studies in animal models, cell culture based experiments.

Dr. Sunil Jalalpure is presently working as a Professor, Department of Pharmacognosy, KLE College of Pharmacy, K.L.E Academy of Higher Education and Research, Belagavi. His areas of research interests include isolation/ characterization of active principles from medicinal plants and their pharmacological screening for various biological activities and training the research students in Pharmacognosy, Phytochemistry and Biotechnological aspects with modern tools and techniques. He is recently involved in nanoparticle drug delivery system of herbal actives and green nanotechnology.

Dr. Dinesh Dhamecha has completed his PhD at KLE Academy of higher education and research. His PhD work involves design and characterization of metallic nanoparticles for anticancer activity. He is also involved in the area of drug delivery and nanomedicine.

Dr. Gan Siew Hua has a BSc from Manchester University, a Masters in Clinical Pharmacy and a PhD in pharmacology from Universiti Sains Malaysia (USM). Her research area is in the field of pharmacogenetics and toxicology.

Dr. Kiran Jadhav has completed her PhD at KLE Academy of higher education and research. and M. Pharmacy in Quality Assurance from C. U. Shah college of Pharmacy, SNDT University in the year 2010. Her PhD work involves design and characterization of metallic nanoparticles for antimicrobial activity. She has two years of industrial experience in solid oral and tropical dosage forms.

Cite this article: Satveer Jagwani S, Jalalpure S, Dhamecha D, Hua GS, Jadhav K. Development and Validation of Reverse-Phase High-Performance Liquid Chromatographic Method for Determination of Resveratrol in Human and Rat Plasma for Preclinical and Clinical Studies. Indian J of Pharmaceutical Education and Research. 2020;54(1):187-93.

Analytical Chemistry Letters

ISSN: 2229-7928 (Print) 2230-7532 (Online) Journal homepage: https://www.tandfonline.com/loi/tacl20

A Stability Indicating Reversed Phase HPLC Method for Estimation of *trans*-Resveratrol in Oral Capsules and Nanoliposomes

Satveer Jagwani, Sunil Jalalpure, Dinesh Dhamecha, Gan Siew Hua & Kiran Jadhav

To cite this article: Satveer Jagwani, Sunil Jalalpure, Dinesh Dhamecha, Gan Siew Hua & Kiran Jadhav (2019) A Stability Indicating Reversed Phase HPLC Method for Estimation of *trans*-Resveratrol in Oral Capsules and Nanoliposomes, Analytical Chemistry Letters, 9:5, 711-726, DOI: 10.1080/22297928.2019.1696227

To link to this article: https://doi.org/10.1080/22297928.2019.1696227

Taylor & Francis
Taylor & Francis Group

ISSN Print: 2229-7928
ISSN Online: 2230-7532

A Stability Indicating Reversed Phase HPLC Method for Estimation of *trans*-Resveratrol in Oral Capsules and Nanoliposomes

Satveer Jagwani [1, 2], Sunil Jalalpure [1, 2]*, Dinesh Dhamecha [1], Gan Siew Hua [3], Kiran Jadhav [2]

[1] Dr. Prabhakar Kore Basic Science Research Center, KLE Academy of Higher Education and Research, Nehru Nagar, Belagavi-590010, Karnataka, India
[2] KLE College of Pharmacy, KLE Academy of Higher Education and Research, Nehru Nagar, Belagavi-590010, Karnataka, India
[3] School of Pharmacy, Monash University Malaysia, Jalan Lagoon Selatan, 47500 Bandar Sunway, Selangor, Malaysia

Received 10 May 2019; accepted in revised form 20 November 2019

Abstract: *Trans*-resveratrol, a naturally occurring lipophilic polyphenol present in various foods, is well known for its therapeutic use. Owing to their exciting therapeutic potential, we developed a simple and precise stability indicating reverse-phase high performance liquid chromatography (RP-HPLC) method as per International Conference on Harmonization guidelines for quantitative analysis of trans-resveratrol in a commercial nutraceutical product and in-house nanoliposomes formulation. The chromatographic separation was attained on Phenomenex Luna C18 column (150 x 4.6 mm, 5 µm) at 30°C using UV detection at 306 nm. The optimized mobile phase consisted of acetonitrile/water (30:70, v/v) at the flowrate of 1.0 mL/min under isocratic mode of elution. The proposed method was found to be accurate, precise and linear with regression coefficient of 0.999 which could analyse the samples with as low as in nanograms with percent recovery in the acceptable range of 97.97 - 102.80 %. In addition, stress degradation study was also carried out wherein analyte peak was found to be well resolved. Hence, the present investigation confirmed that the developed method can be employed for the analysis of *trans*-resveratrol in different formulations, and also of huge benefit in careful selection of experimental conditions and its implication for storage and formulation development.

Key words: *Trans*-resveratrol; RP-HPLC; forced degradation studies; nanoliposomes.

Introduction

Recently, multifarious food constituents particularly polyphenols have gained extensive attention as either potential therapeutic or as preventive agents in the management of various diseases [1]. Resveratrol (3,5,4'- trihydroxystilbene), a well known naturally occurring low molecular weight lipophilic polyphenol, is produced as the secondary metabolite by various plants in response to environmental and pathogenic induced stress [2]. Resveratrol predominantly exists in a sensitive *trans*-resveratrol form, which gets isomerized to *cis* form on exposure to UV light [3-4] (Fig. 1). *Trans*-resveratrol is the active form responsible for cardioprotective, neuroprotective, anti-inflammatory, antioxidant, anti-aging and anticancer properties [5].

Numerous chromatographic techniques such as high performance liquid chromatography (HPLC), liquid chromatography mass spectro-

*Corresponding author (Sunil Jalalpure)
E-mail: < jalalpuresunil@rediffmail.com >

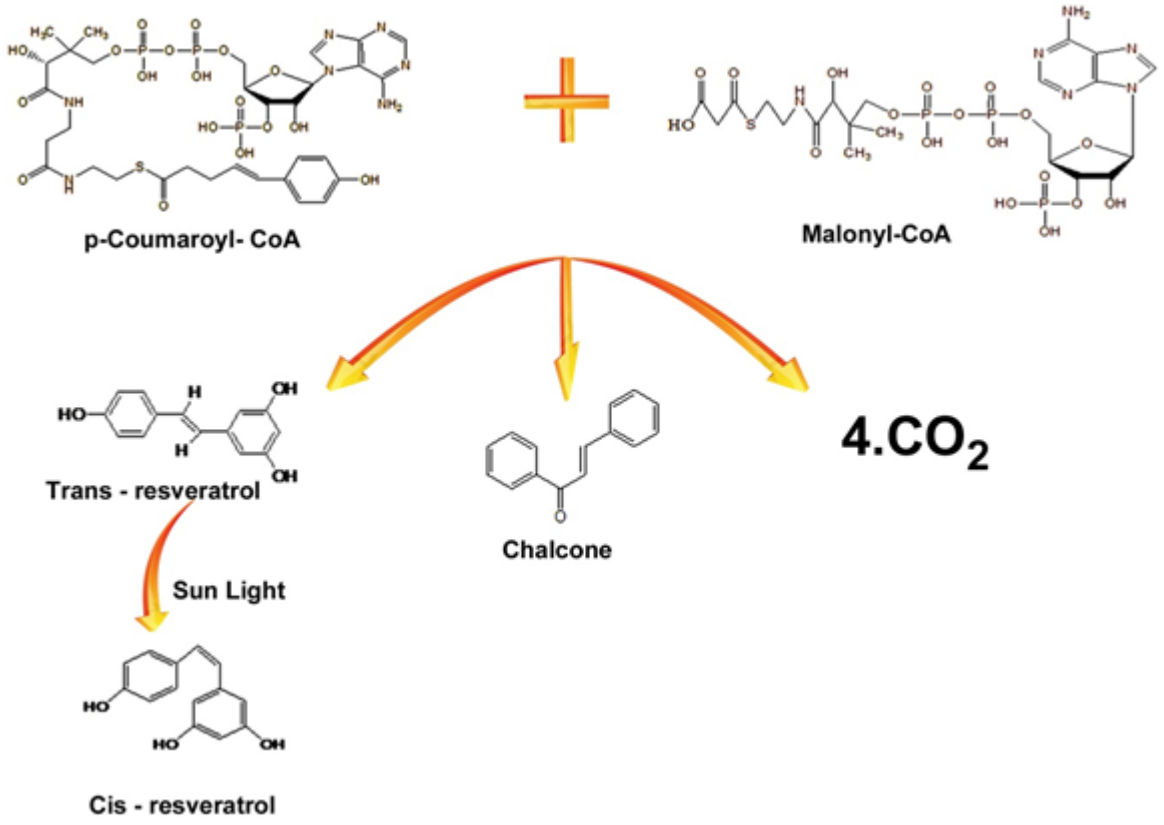

Figure 1. Synthesis of trans-resveratrol, Carbon dioxide (CO_2)

metry (LC/MS), fluorometric and electrochemical detection methods have been reported for the quantification of resveratrol in wine, grapes and nanoformulations [6-13]. However, the reported RP-HPLC methods have several limitations including long run times [14], high flow rates [15-16], complicated gradient elutions [17] and buffer solutions in mobile phase [7].

A wide range of resveratrol dosage forms (powders, tablets and capsules) are now commercially available as nutritional health supplements. However, these dosage forms fail to provide therapeutic benefits because of poor bioavailability, low water solubility, rapid degradation at alkaline pH and fast systemic clearance [18]. In addition, the sensitive nature of *trans*-resveratrol poses a concern towards its stability during formulation and analysis that may affect its therapeutic properties [19]. To overcome these limitations, nanocarrier systems like liposomes [20], solid lipid nanoparticles [21], nanoemulsions [22], micelles [23], and nanoparticles [24] have been investigated. Amongst these nanocarriers, liposomes are considered as the most useful vesicular system. However, the success of nanoformulation-based drug delivery systems depends upon the particle size [25], zeta potential [26], and encapsulation efficiency (EE) [27]. Estimation of drug entrapment is one of the key attributes in determining successful formation of nanoliposomes. In this regard, the present study focuses on formulating in-house *trans*-resveratrol loaded nanoliposomes followed by the evaluation of the application of the developed method for estimation of entrapment efficiency.

With this background, the present study (schematically represented in figure 2) was stemmed, to develop a simple, rapid and selective RP-HPLC method in accordance with International Council for Harmonization guideline (ICH, Q2(R1) [28] to quantify *trans*-resveratrol in commercial nutraceutical capsules and in-house resveratrol loaded nanoliposomes. To our knowledge, there is no single method that has been reported which can analyse *trans*-resveratrol concentration in various systems like commercial formulations and in-house complex lipid formulation. Subsequently,

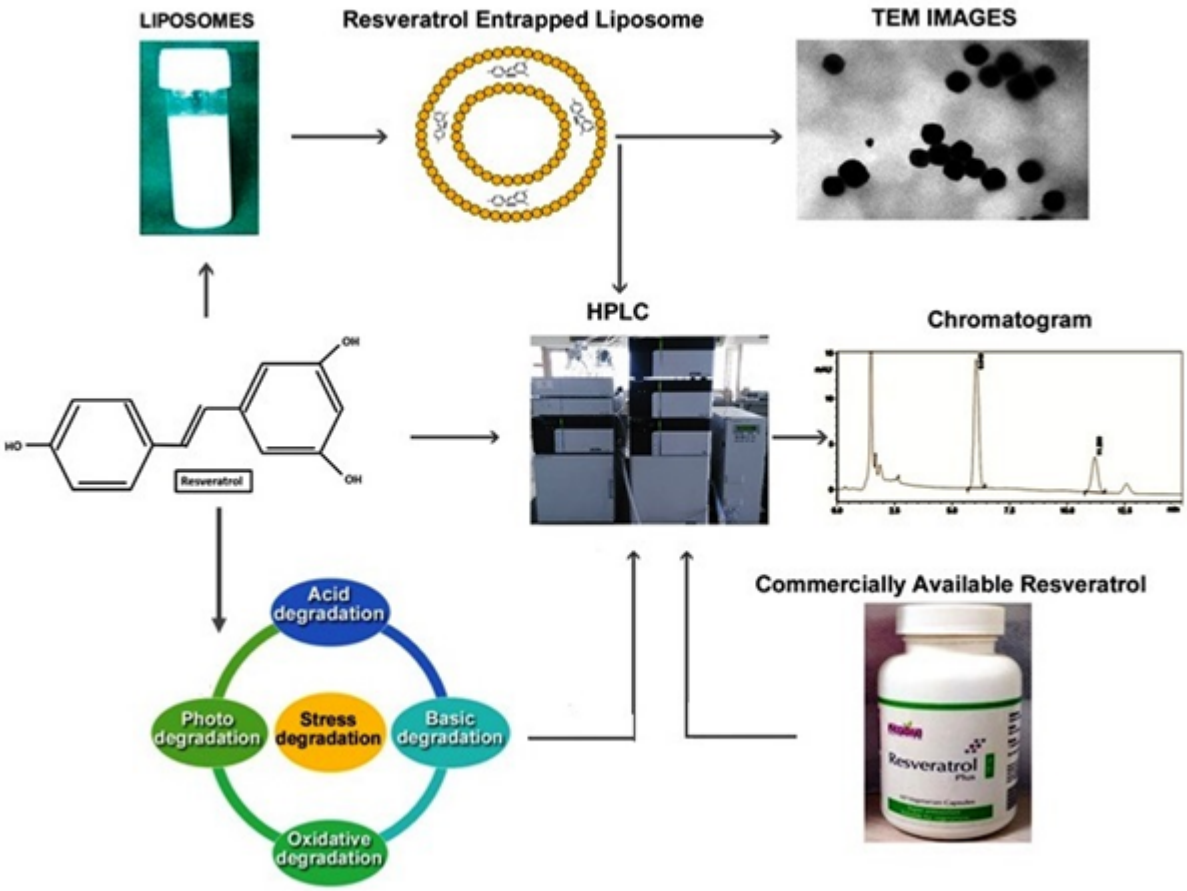

Figure 2. Schematic representation of stability indicating RP-HPLC method development validation and estimation of trans-resveratrol in oral capsules and nanoliposomes

the developed method was used to investigate the degradation behavior of *trans*-resveratrol under different conditions (acidic, basic, neutral, oxidation, UV-light and thermal degradation) which can aid in the careful selection of experimental conditions and its implication for storage, formulation development and analysis.

Materials and methods

Materials

Trans-resveratrol (99 % pure), Lipoid S 100 (94 % phosphatidylcholine) and carbamazepine donated by Ms. Sami Labs Ltd., Bangalore, India; Lipoid GmbH, Ludwigshafen, Germany and Alkem Laboratories Ltd., Mumbai, India, respectively. HPLC-grade acetonitrile (ACN) was procured from Merck, Mumbai, India. Deionized water used in the test was prepared via Millipore Direct-Q®-3 purification system (18.2 MÙ/cm) Millipore (Molsheim, France).

Experimental

Equipment setup and HPLC conditions

The Shimadzu HPLC system (LC-20AD prominence system, Kyoto, Japan) consisting of an LC-20AD pump, SIL-20 AC HT autosampler, SPD-M20A diode array detector and CBM-20A communication bus module, which was operated by using a computer based Shimadzu LC solution (version 1.25) software program. A reverse phase Luna C18 column (150 x 4.6 mm i.d., 5 µm particle size, Phenomenex, USA) equipped with a security guard column having (ODS; 4 x 3.0 mm ID, Phenomenex, USA) was used for separation. The system was operated under an isocratic elution of ACN:water (30:70 v/v) at 1.0 mL/min under a controlled temperature (30°C) condition. The solvents were prepared by degassing in an ultrasonic bath for 15 min followed by a vacuum pump which allows filteration through a Millex HV polyvinylidene fluoride membrane filter (0.45

µm) (Millipore, Bedford, USA). Drug samples 10 µl was injected into the HPLC system and was detected at 306 nm.

Preparation of calibration standards

Stock methonolic solution (1 mg mL^{-1}) of resveratrol and carbamazepine as the internal standard (IS) were prepared. Six working solutions of *trans*-resveratrol (2, 4, 6, 8, 10 and 12 µg mL^{-1}) and working solution of IS (20 µg mL^{-1}) were prepared by diluting *trans*-resveratrol and IS stock solution in the mobile phase respectively. The sample solutions were stored at 5ºC ± 3ºC until further use. The experiments were performed in dim light to prevent the possibility of photochemical isomerization.

Method validation

The developed method was validated for its selectivity, linearity, system suitability, limit of detection (LOD), limit of quantification (LOQ), precision, accuracy, stability, robustness and ruggedness as per ICH guideline (Q2R1).

Analysis of commercial dosage form

Commercially available resveratrol capsules (Resveratrol Plus capsules; marketed by Zenith Nutrition and manufactured by Medizen Labs Pvt. Ltd., Bangalore, India) were used for evaluating the assay of resveratrol in capsules. Resveratrol powder equivalent to 10 mg was accurately weighed and dissolved in 10 mL of methanol in amber volumetric flasks. The resulting mixture was sonicated for 15 min followed by filtration using a 0.45 µm syringe filter (Millipore, Bedford, USA). The solution was finally diluted to yield a solution of 10 µg mL^{-1}. Recovery studies were carried out by spiking the preanalyzed commercial resveratrol samples with 50, 100 and 150 % of resveratrol.

Preparation of an in-house nanoliposomes formulation

Resveratrol loaded nanoliposomes were prepared by a lipid film hydration method as previously described [29]. Briefly, 20 mg of *trans*-resveratrol and a previously optimized (not published yet) phosphatidylcholine and cholesterol mixture in the ratio of (7:2) was dissolved in methanol and chloroform (1:2 v/v). The solution was transferred to amber coloured round bottom flask (RBF). Subsequently, the organic solvent was evaporated under a reduced pressure for 1h at 40ºC using a Rotavapour R-210 (V-700 Buchi, Switzerland) to yield a thin lipid film. The lipid film was then flushed with a stream of nitrogen to remove any residual solvents.

The formation of nanoliposomes was achieved by hydrating the thin lipid film with phosphate buffer saline (PBS, pH 6.8) at 40ºC. Nanoliposomes were then subjected to a size reduction for 2 min (15s On/off pulse interval) on an ice bath using a probe sonicator (High Intensity Ultrasonic Generator, Rivotek, India) equipped with an S.S probe of 15 mm diameter. The final nanoliposomes dispersion was centrifuged (Kubota 6500, Japan) at 3000 rpm, 4ºC for 20 min to separate any undissolved drug. The develped HPLC method was used to analyze the encapsulation efficiency (EE) of the inhouse liposomal formulation. The formulated nanoliposomes were characterized for its particle size, polydispersity index (PI) and zeta potential (ZP) by using a Zetasizer Nano-ZS90 (Malvern Instruments, United Kingdom). The morphological characterization of the formulated nanoliposomes was done by using transmission electron microscopy (TEM; Philips CM12 Electron Microscope, Netherlands).

Stability experiments

Stability of *trans*-resveratrol in the mobile phase was determined at various storage conditions as follows: stability for up to 6 h at 25 ± 2°C, freezer stability up to 7 days at -20°C and freeze-thaw stability at -20°C. In the freeze-thaw stability test, the cycles were conducted thrice and were restored in similar condition following withdrawal of aliquots for analysis. The peak areas of *trans*-resveratrol obtained at baseline were used as a reference when determininig the relative stability at various storage conditions [30]. All experiments were performed in triplicates and the samples were considered as stable if the assay values were within the acceptable limit of accuracy (i.e. ± 15 % standard deviation).

Forced degradation studies

Accelerated stress degradation studies were performed for 5 h under the optimized HPLC method in various stress conditions as recommended in the ICH stability guideline (Q1A (R2)). In order to exclude the possible degradation effects of light on resveratrol, all degradation experiments were carried out in dim light except for the photo degradation test. For each degradation study, four samples were prepared 1) blank solution stored under ambient condition 2) blank solution subjected to degradation in a similar way as that of drug solution 3) zero time (baseline) sample with drug stored under ambient condition and 4) drug solution subjected to degradation. For acidic degradation study, 1 mL of drug solution was treated with 1 mL of 1 molar (M) hydrochloric acid (HCl). Prior to analysis, the mixture was refluxed at 80ºC for 5 h followed by neutralization using 1 mL of 1 M sodium hydroxide (NaOH). For alkaline degradation study, 1 mL of drug solution was treated with 1 mL of 1 M NaOH. Prior to analysis, the mixture was refluxed at 80ºC for 5 h followed by neutralization using 1 mL of 1 M HCl. Oxidative degradation was performed by treating the drug sample with 1 mL of 30 % hydrogen peroxide (H_2O_2) solution. On the other hand, dry heat degradation was performed by placing an approximate quantity of drug (100 mg) in a sealed ampoule and incubating the ampoule in a digital thermostatic hot air oven maintained at 100ºC for 5 h. Finally, photochemical stability of the drug was investigated at different time intervals (1, 3, 5 and 7 h) by exposing the drug solution directly to sunlight. In accelerated studies, all samples were diluted appropriately in mobile phase and followed by filteration prior to the HPLC analysis [31].

Results and discussion

Method development and optimization

In this study, a single stability indicating RP-HPLC method was developed for an accurate estimation of *trans*-resveratrol in marketed capsules, in-house nanoliposomes formulation and to investigate the degradation behavior of *trans*-resveratrol under different harassic conditions. The developed RP-HPLC method was optimized by altering the flow rate, mobile phase composition and column oven temperature to obtain desirable sharp and symmetrical peaks. Varying ratios of solvents such as ACN, methanol and water was used to optimise the peak resolution. Solvent composition consisting of methanol and water (50:50 v/v) yielded a tall *trans*-resveratrol peak but had a negative impact on the theoretical plate number. On the other hand solvent composition consisting of ACN and water (50:50 v/v) yielded a well resolved peak with a minor tailing. For the separation of *trans*-resveratrol, various proportions of ACN and water were tested and analysed to get a sharp peak with negligible tailing and shorter retention time. Apart from mobile phase selection, column temperature is another key parameter that impacts separation. Experiments with column temperatures range between 25°C and 45°C revealed that 30°C demonstrated clear peak shape and shorter retention time when compared to others and was therefore deemed to be ideal for the analysis The developed HPLC system attached to a Luna C18 column (150 x 4.6 mm i.d., 5 µm) was validated by using a mixture of ACN and water (30:70) with an isocratic elution at 1.0 mL/min. The injection volume was set up at 10 µL using the optimized column temperature 30ºC. Carbamazepine was used as the internal standard (IS) owing to its close structural resemblance to *trans*-resveratrol. Under these chromatographic conditions, *trans*-resveratrol and IS was detected at 306 nm with retention times of 6.1 and 11.2 min (Fig. 3).

Method validation

System suitability tests

System suitability test is an integral part of the HPLC method development which determines the feasibility of the proposed method for estimating *trans*-resveratrol concentration in routine pharmaceutical application (Table 1). All parameters such as retention factor (1 and 10), tailing factor (< 2), theoretical plate number (>2000) and percent relative standard deviation (RSD) (< 2 % of six consecutive injections) were within the acceptable limits demonstrating desirable resolution, peak symmetry, column efficiency and excellent chromatographic conditions which were used for further validation and sample analysis.

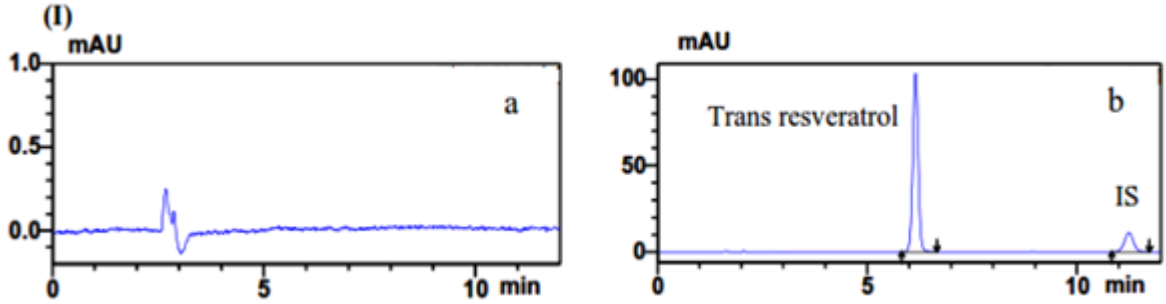

Figure 3. Representative chromatograms obtained from I(a) blank mobile phase and I(b) spiked with 6µg mL^{-1} trans resveratrol (t_R 6.1 min) and 20 µg mL^{-1} IS (t_R 11.2 min)

Table 1. System suitability parameters

Parameter		Acceptance criteria
Retention time (t_R, min)	6.073 ± 0.006	-
Percent RSD of retention time	0.10	< 1 for n ≥ 5
Peak area	480623.3 ± 411.1519	-
Percent RSD of peak area	0.08	< 1 for n ≥ 5
Tailing factor (T)	1.08	≤ 2.0
Theoretical plates (N)	9497.90	> 2000
retention factor (k')	2.63	> 2

Mean values ± standard deviation (SD); (n=6)

Linearity and range

The linearity of a method is defined as the relationship between the peak area and its corresponding concentrations in the sample solutions. The developed method was linear over the range of 2 - 12 µg mL^{-1}with correlation coefficient; r^2 = 0.999 (Table 2) indicating acceptable linearity over the investigated concentration range.

LOD and LOQ

The LOD and LOQ were determined by diluting the known concentration of the drug until a signal to noise ratio of approximately 3:1 and 10:1 were obtained (Table 2). The lowest concentration of *trans*-resveratrol was 0.008 µg mL^{-1} whereas, the lowest quantified concentration was 0.024 µg mL^{-1}.

Precision

The precision of an analytical method indicates the closeness of the agreement between a series of measurements obtained from multiple samplings of identical sample under similar analytical conditions. Both inter- (at three consecutive days) and intra-day (repeatability) assays were performed at three different concentrations (in triplicates) and the results (Table 3) suggest that the percent (RSD) of the total peak areas were < 2 % indicating that the developed method is precise.

Accuracy

The accuracy of an analytical method is defined as the percentage difference of mean experimental value from the true value. Accuracy was evaluated by conducting a recovery experiment in preanalysed commercial resveratrol capsules and nanoliposomes. The assay was performed by following standard addition method at three different concentrations (50 %, 100 % and 150 %) of preanalysed *trans*-resveratrol samples in triplicates. The mean percentage recovery of *trans*-resveratrol, including the commercial dosage form and in-house nanoliposomes formulation were between 97.97 and 102.8 % with < 1 % RSD (Table 4) which clearly indicates that there is low

Table 2. Statistical evaluation of the calibration data

Parameters	
Linearity range (µg mL $^{-1}$)	2 - 12
Slope	80745
Intercept	-35857
Correlation coefficient	0.999
SE of slope	2147.27
SE of intercept	5375.57
Limit of detection (µg mL $^{-1}$)	0.0082
Limit of quantification (µg mL $^{-1}$)	0.0246

SE: Standard error

Table 3. Intraday and interday precision of resveratrol

Resveratrol concentration (µg mL^{-1})	Intraday (n=6) Percent RSD	Interday (n=3) Percent RSD		
		Day 1	Day 2	Day 3
2	1.676	0.994	1.416	1.473
6	1.028	0.960	1.158	1.120
10	1.345	0.781	0.670	1.103

RSD (Relative standard deviation)
n = number of replicate

Table 4 Determination of accuracy based on percentage recovery

Level of addition (%)	Percent recovery		
	Mobile phase	Commercial dosage form	Nanoliposomes
50	97.97	100.39	101.65
Percent RSD	0.436	0.88	0.19
100	101.31	102.80	99.03
Percent RSD	0.176	0.19	0.50
150	99.88	98.22	100.83
Percent RSD	0.39	0.26	0.43

RSD (Relative standard deviation)

variability between the experimental and true values.

Robustness

Robustness is the ability of the developed method to remain unaltered by minor deliberate variations in the chromatographic parameters. In the present study, robustness of the developed RP-HPLC method was examined based on the percent RSD values and system suitability parameters after introducing small variations in the mobile phase ratio (± 2 %), flow rate (±0.2mL/min) and column temperature (±5ºC) while maintaining a constant concentration of *trans*-resveratrol. The results indicated that slight variations in the chromatographic conditions did not

affect the percentage RSD values and system suitability parameters (Table 5) thus confirming that the developed method is robust.

Characterization of nanoliposomes formulation

In the present study, we have successfully developed *trans*-resveratrol loaded nanoliposomes formulation by a thin film hydration method. Particle diameter, polydispersity index (PDI) and zeta potential (ZP) of the optimized *trans*-resveratrol were 149.7 nm, 0.39 and 29.1 mV respectively. The low PDI values confirmed the homogenous nature of the optimized formulation and correspond to the monodispersed particles [32]. ZP is a key indicator for predicting vesicle stability. Higher ZP values, either positive (+) or negative (-) indicates a better stability of the nanovesicular systems [33]. The morphological appearance of the developed nanoliposomes formulation was visualized with TEM which confirmed spherical morphology of the formulated vesicles (Fig. 4).

Analysis of commercial dosage form and nanoliposomes

The developed RP-HPLC method was used to determine *trans*-resveratrol concentration in commercial available capsules and to determine (% EE) of the newly optimized nanoliposomes formulation. The concentration of *trans*-resveratrol in commercial dosage form (capsules) matched (98.8 %) with the labeled claim whereas, the EE of the nanoliposomes was 75 %. The absence of interfering peaks in the chromatogram of the marketed capsule and in-house nanoliposomal formulation indicates that the excipients used in the capsules and in nanoliposomes formulation did not interfere with the peak of interest indicating that the proposed method is applicable for routine analysis of *trans*-resveratrol in quality control laboratories. The percentage recovery of the drug in the capsule and nanoliposomes were shown in 98 - 102 % range (Table 4).

***Trans*-resveratrol stability**

Trans-resveratrol was stable at 6h (if maintained at 23ºC - 25ºC), freezer condition at (-20°C) for seven days and three freeze-thaw (F/T) cycles (Table 6).

Forced degradation studies

The specificity and the stability indicating capability of the established method was judged by the good separation of the drug peak from the other degradation peaks. The study verified the applicability of the method since the analyte peaks were well separated from their degraded chemical entitites (Fig. 5). Treatment of *trans*-

Table 5. Robustness studies

Concentration (6 μg mL^{-1}) Conditions	Changes	Peak area	Mobile phase Tailing factor	Theoretical plate
Mobile phase (ACN: water)	(28:72)	471030.80 ± 432.84	1.0608 ± 0.001	10263.90 ± 9.73
	% RSD	0.0919	0.1388	0.0948
	(32:68)	479158.70 ± 160.07	1.1050 ± 0.002	8704.50 ± 25.50
	% RSD	0.03341	0.1954	0.2930
Flow rate(ml/min)	0.8	586780.70 ± 390.68	1.0758 ± 0.0008	10653.22 ± 27.40
	% RSD	0.0660	0.0690	0.2570
	1.2	399770.00 ± 148.36	1.0911 ± 0.0013	8311.18 ± 12.68
	% RSD	0.0370	0.1210	0.1520
Temperature (°C)	25	474765.80 ± 866.27	1.0696 ± 0.0022	9581.10 ± 49.26
	% RSD	0.1825	0.20195	0.5141
	35	475285.80 ± 191.13	1.0923 ± 0.0015	9383.48 ± 24.79
	% RSD	0.0402	0.1378	0.2642

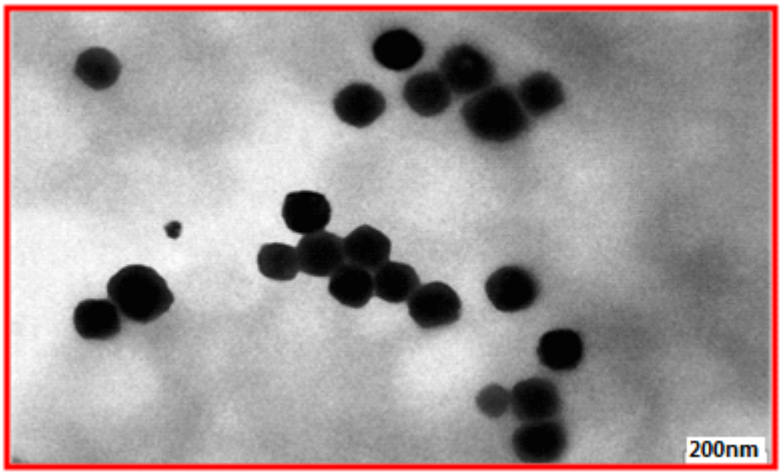

Figure 4. TEM image demonstrates the structure of trans-resveratrol loaded nanoliposomes (magnification 25000 X, scale bar 200 nm)

Table 6. Stability data of trans-resveratrol

Spiked concentration (μg/mL^{-1})	Stability	Mean ± SD[a] (μg/mL^{-1}), n = 3	Accuracy (%) [b]
2	0 h	2.088 ± 0.035	-
	3 F/T cycles	2.038 ± 0.002	97.60
	6 h	2.108 ± 0.008	100.96
	7 days at-20°C	2.065 ± 0.012	98.89
6	0 h	6.407 ± 0.044	-
	3 F/T cycles	6.310 ± 0.128	98.48
	6 h	6.485 ± 0.027	101.21
	7 days at-20°C	6.154 ± 0.157	96.05
10	0 h	10.258 ± 0.068	-
	3 F/T cycles	10.970 ± 0.080	97.19
	6 h	10.300 ± 0.124	100.41
	7 days at-20°C	9.912 ± 0.025	96.63

[a]Back calculated concentration,

[b] (Mean assayed concentration/mean assayed concentration

resveratrol with HCl (1M) leads to a 68 % degradation which was reflected by a degradation product, whereas alkaline hydrolysis led to an exponential increase in degradation resulting in 94 % degradation with the formation of a single degradation product (Table 7). The effect may be attributed to low *trans*-resveratrol stability in an alkaline pH, in which dissolution and degradation occurred at the same time, resulting in the increased concentration of degraded products as well as a decreased solubility [4]. The comparatively stable behavior of *trans*-resveratrol in an acidic medium when compared to an alkaline medium may be attributed to the fact that the hydroxyl groups present in *trans*-resveratrol were protected from radical oxidation generated by positively charged hydronium cation (H_3O^+) group that is released in an acidic condition. These results corroborate with some previous findings [19] wherein the pH dependence on degradation of *trans*-resveratrol was stable for at least 42 h in neutral aqueous buffers, 28 days in acidic media with an initial half-life of 1.6 h at pH 10.0 if the solution is kept protected from light. Our experiments re-

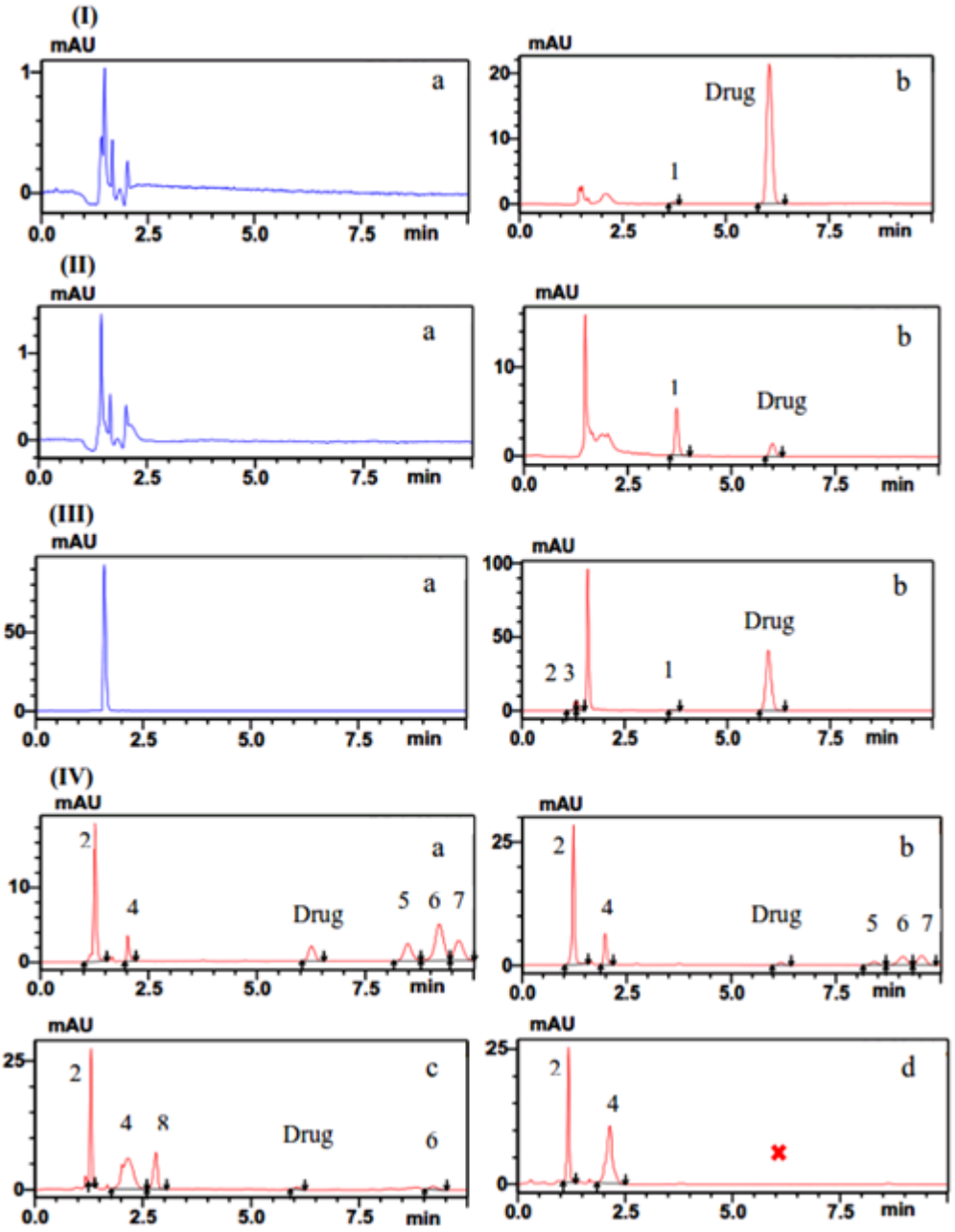

Figure 5. HPLC chromatogram of trans-resveratrol injected at 10 µg mL-1(Ia) blank sample following acid degradation; (Ib) drug after acid degradation; (IIa) blank after basic degradation; (IIb) drug after basic degradation; (IIIa) blank after oxidative degradation; (IIIb) drug after oxidative degradation; (IVa) photo degradation after 1 h; (IVb) photo degradation after 3h; (IVc) photo degradation after 5 h and (IVd) photo degradation after 7 h.

vealed that degradation of *trans*-resveratrol was also dependent on both pH and temperature. For example, in an acidic media, the drug was stable with temperature having minimal impact on degradation. In contrast, in an alkaline pH and in high temperatures, a high degradation rate occurs [19, 34].

In fact exposure of *trans*-resveratrol to oxidative stress (i.e. in the presence of 30 % H_2O_2) caused a 55.8 % degradation in the presence of three degradation peaks which may be attributed to the presence of oxygen in the medium and the subsequent promotion of free radical formation [4].

Table 7. Forced degradation studies

Stress conditions	Degradation time (h)	t_R of the yielded degradation product (min)	Percent degradation
HCl (1 M) at 80°C	5	3.68	68.00
NaOH (1 M) at 80°C	5	3.68	94.00
H_2O_2 (30%) at 80°C	5	1.28, 1.36 and 3.68	55.83
Dry heat at 80°C	5	No degradation	0.00
	1	1.28, 2.20, 8.47, 9.20 and 9.64	89.67
	3	1.28, 2.20, 8.47, 9.20 and 9.64	93.55
Photo degradation	5	1.28, 2.20, 2.75 and 9.20	93.79
	7	1.28 and 2.20	Complete degradation

On the other hand, there was no evidence of degradation in a dry heat condition suggesting higher stability of *trans*-resveratrol in powder form. Our findings corroborate with literature suggesting that *trans*-resveratrol is not stable in solution at either low or high temperatures, whereas the powder form is stable under "accelerated stability" conditions [19].

Exposure of *trans*-resveratrol solution to a direct sunlight demonstrated a time dependent degradation with a 100 % degradation at the 7th hour followed by the formation of two degradation products. These findings confirm the photosensitive nature of *trans*-resveratrol leading to isomerisation of *trans*-resveratrol to the *cis* form. In fact, the basic chemical structure of *trans*-resveratrol consists of two phenolic rings bonded together by a double styrene bond, forming the 3,5,4-trihydroxystilbene. The double bond is responsible for the isomeric c*is*-and *trans*-forms of resveratrol [35]. In addition, *trans*-resveratrol *cis*/*trans* isomerization is influenced by the wavelength and the time of irradiation. The conversion of *trans*-resveratrol is proportional to the light intensity, indicating that the number of photon absorbed by the system is proportional to the number of *trans*-resveratrol molecules being *trans*-formed [36]. To summarise the influence of individual factors in degradation profile, *trans*-resveratrol is not stable under the influence of pH, light and oxidation which may lead to isomerization of *trans*-resveratrol (therapeutic form) to the *cis* form or the formation of other degradation products which may subsequently have a strong biological impact. Therefore, based on the above forced degradation experiment, careful consideration is required when selecting the experimental and storage conditions of *trans*-resveratrol.

Comparison with previous published methods

Comparative analysis of methods described in the existing literature and the current study was conducted based on type of mobile phase, flow rate, analytical time, detection limits, accuracy, precision, peak shapes and applicability of the method (Table 8). To the best of our knowledge, there is no method developed till date which can used for multiple purposes like analysis of actives in different formulations and to study the degradation behavior using the same mobile phase and column conditions. The developed method which uses conventional solvents like ACN:water combination and has the flowrate of 1 mL min^{-1} with retention time of 6 min suggests that it is economic, cheap and fast when compared to other methods.

Conclusion

The present method was successfully developed and validated where the same mobile phase was used to estimate *trans*-resveratrol in nutraceuticals supplements, resveratrol-loaded nanoliposomes and to determine the degradation behaviour. The established RP-HPLC method was robust, accurate, simple and fulfill the FDA validation requirement for the quantitative determination of *trans*-

Table 8. Comparison between HPLC methods reported in the literature

No.	Column	Mobile phase	Separation time (min)	LOD & Flow rate	Limitations	Applicability	Ref.
1.	C18	KH_2PO_4(10 mM) (pH 6.8): CH_3OH: CH_3CN(30:63:7v/v/v)	3.26	20 ng mL^{-1}, 1 mL min^{-1}	Three solvents in the mobile phase; robustness of data not provided; low theoretical plates which reflects low column efficiency.	Poly(lactic-co-glycolic acid) (PLGA) Nanoparticles	9
2.	C18	CH_3COOH 0.25% v/v: CH_3OH (50:50, v/v)	6.20	25 ng mL^{-1} 1 mL min^{-1}	Robustness of data not provided	Different pH solutions	4
3.	C18	CH_3OH (35-95%): H_2O (65-5%)	15.44	-,-	Gradient elution; high separation time; flow rate and validation data like system suitability, LOD, accuracy & precision not given	Grape extract	37
4.	C18	Solvent A - CH_3OH: H_2O:CH_3COOH (10:90:10 v/v):Solvent B-CH_3OH:H_2O: CH_3COOH(10:90:10 v/v) Gradient program: 0.0 -18.0 min from 0 % to 4 0 % B; 18.0-25 min from 40 % to100 % B & 25-27 min 100 % B	21.85	0.9 pmol, 1.5 cm^3 min^{-1}	Complicated gradient elution; long separation time; high flow rate and hence expensive; Expensive equipment; Not available in all laboratories; no robustness and system suitability test conducted	Hungarian Wines	38
5.	SPE ODS C_{18}	CH_3CN: H_2O(40:60)	16.00	0.04 µg/g 0.3 mL min^{-1}	Long retention time; validation parameters such as system suitability, precision and robustness was not performed	Peanut & Peanut butter	39

table 8. (continued).

No.	Column	Mobile phase	Separation time (min)	LOD & Flow rate	Limitations	Applicability	Ref
7.	C18	H_2O:CH_3CN:CH_3COOH (70:29.9:0.1)	4.70	0.02 mg L^{-1}, 1.0 mL min^{-1}	System suitability, robustness was not performed,	Red grapes skin	40
8.	C18	CH_3OH: H_2O (51:49, v/v)	6.4	68.0 ng mL^{-1}, 0.9 mL min^{-1}	System suitability parameter not given; high LOD	Polymeric nanoparticles	41
9.	C18	Solvent A - H_2O: CH_3COOH (99:1 v/v): Solvent B - H_2O:CH_3CN: CH_3COOH (67:32:01 v/v) Solvent C – CH_3CN Gradientprogram: 0.0 min 20 % B; 18 min,100 % B; 28 min,100 % C; 33 min, 100 % B; 37 min, 20 % B	16.20	0.017 µg mL^{-1}, 0.8 mL min^{-1}	Complicated gradient elution; long separation time and hence expensive; expensive equipment; No system suitability and validation data given	dietary supplements	42
10.	C18	CH_3CN: H_2O (30:70)	6.10	0.008, µg mL^{-1}, 1.0 mL min^{-1}	Economical, fast analysis, fully validated analytical method with degradation study along with stability studies.	Commercial nutraceutical supplement, and Nanoliposomes	Present method

LOD- Limit of detection
CH_3OH – Methanol
CH_3COOH - Acetic acid
CH_3CN- Acetonitrile
$NH_4CH_3CO_2$ – Ammonium acetate
KH_2PO_4 – Potassium di hydrogen phosphate

resveratrol. Forced degradation studies revealed that the resveratrol is able to tolerate in oxidative, acidic as well as high temperature conditions, but more susceptible to degrade in photolytic and alkaline conditions. The outcomes of the degradation studies is effectively applied for determining the suitable conditions for formulation, development and storage. The absence of excipients peaks during *trans*-resveratrol analysis in nutraceutical supplements and nanoliposomes further demonstrated that the developed method can be used for the routine analysis of *trans*-resveratrol in different dosage forms.

Acknowledgements

The authors are grateful to Sami Labs, Bangalore, India for gifting pure *trans*-resveratrol sample and Lipoid GmbH, Ludwigshafen, Germany for providing (LIPOID S 100) phospholipid for the study. This work was financially supported by the KLE Academy of Higher Education and Research (formerly known as KLE University), Belagavi, Karnataka, India.

Competing interests

The authors declare that they have no competing interest.

References

1. **Rajeshwari, H.R., Dhamecha, D., Jagwani, S., Patil, D., Hegde, S., Potdar, R., Metgud, R., Jalalpure, S., Roy, S., Jadhav, K., Tiwari, N.K. (2017).** Formulation of thermoreversible gel of cranberry juice concentrate: Evaluation, biocompatibility studies and its antimicrobial activity against periodontal pathogens. Mater. Sci. Eng. C. 75: 1506-1514.
2. **Soo, E., Thakur, S., Qu, Z., Jambhrunkar, S., Parekhm H.S., Popat, A. (2016).** Enhancing delivery and cytotoxicity of resveratrol through a dual nanoencapsulation approach. J. Colloid Interface Sci. 462: 368-374.
3. **Hasan, M.M., Cha, M., Bajpai, V.K., Baek, K.H. (2013).** Production of a major stilbenephytoalexin, resveratrol in peanut (Arachishypogaea) and peanut products: a mini review. Reviews in Environmental Science and Bio/Technology. 12: 209-221.
4. **Zupanèiè,Š.,Lavriè, Z. (2015).** Kristl, J. Stability and solubility of trans-resveratrol are strongly influenced by pH and temperature. Eur. J. Pharm. Biopharm. 93: 196-204.
5. **Shah, P. and Patel, J. (2010).** Resveratrol and its biological actions. Int. J. Green Pharm. B4: 15-21.
6. **Katsagonis, A., Atta, P.J., Koupparis, M.A. (2015).** HPLC Method with UV Detection for the Determination of trans-Resveratrol in Plasma. J. LiqChromatogrRelat Technol. 28: 1393-1405.
7. **Das, S., Ng, K.Y. (2011).** Quantification of trans-resveratrol in rat plasma by a simple and sensitive high performance liquid chromatography method and its application in pre-clinical study. J. LiqChromatogrRelat Technol. 34: 1399-1414.
8. **Porgalý, E., Büyüktuncel, E. (2012).** Determination of phenolic composition and antioxidant capacity of native red wines by high performance liquid chromatography and spectrophotometric methods. Food Res. Int. 45: 145-154.
9. **Singh, G., Pai, R.S. (2014).** A Rapid Reversed-Phase HPLC Method for Analysis of Trans-Resveratrol in PLGA Nanoparticulate Formulation. ISRN Chromatography. 2014: 1-6.
10. **Domýnguez, C., Guillén, D.A., Barroso, C.G.(2001).** Automated solid-phase extraction for sample preparation followed by high-performance liquid chromatography with diode array and mass spectrometric detection for the analysis of resveratrol derivatives in wine. J. Chromatogr. A. 918: 303-310.
11. **Pezet, R., Pont, V., Cuenat, P. (1994).** Method to determine resveratrol and pterostilbene in grape berries and wines using high-performance liquid chromatography and highly sensitive fluorimetric detection. J. Chromatogr. A. 663: 191-197.
12. **Jeandet, P., Breuil, A.C., Adrian, M., Weston, L.A., Debord, S., Meunier, P., Maume, G., Bessis, R. (1997).** HPLC analysis of grapevine phytoalexins coupling photodiode array detection

and fluorometry. Anal. Chem. 69: 5172-5177.
13. **Kolouchová-Hanzlýìková, I., Melzoch, K., Filip, V., Šmidrkal J. (2004).** Rapid method for resveratrol determination by HPLC with electrochemical and UV detections in wines. Food Chem. 87: 151-158.
14. **Dourtoglou, V.G., Makris, D.P., Bois-Dounas, F., Zonas, C. (1999).** *Trans*-resveratrol concentration in wines produced in Greece. J. Food Compost. Anal. 12: 227-233.
15. **Juan, M.E., Maijó, M., Planas, J.M. (2010).** Quantification of trans-resveratrol and its metabolites in rat plasma and tissues by HPLC. J. Pharm. Biomed. Anal. 51: 391-398.
16. **Frozza, R.L., Bernardi, A., Paese, K., Hoppe, J.B., Silva, T.D., Battastini, A.M., Pohlmann, A.R., Guterres, S.S., Salbego, C. (2010).** Characterization of trans-resveratrol-loaded lipid-core nanocapsules and tissue distribution studies in rats. J. Biomed. Nanotechnol. 6: 694-703.
17. **Boocock, D.J., Patel, K.R., Faust, G.E., Normolle, D.P., Marczylo, T.H., Crowell, J.A., Brenner, D.E., Booth, T.D., Gescher, A., Steward, W.P. (2007).** Quantitation of *trans*-resveratrol and detection of its metabolites in human plasma and urine by high performance liquid chromatography. J. Chromatogr. B. 848: 182-187.
18. **Summerlin, N., Soo, E., Thakur, S., Qu,Zhi.,Jambhrunkar, S., Popat, A. (2015).** Resveratrol nanoformulations: challenges and opportunities. Int. J. Pharm. 479: 282-290.
19. **Francioso, A., Mastromarino, P., Masci, A., d'Erme, M., Mosca, L. (2014).** Chemistry, stability and bioavailability of resveratrol. Med. Chem. 10: 237-245.
20. **Caddeo, C., Teskaè, K., Sinico, C., Kristl, J. (2008).** Effect of resveratrol incorporated in liposomes on proliferation and UV-B protection of cells. Int. J. Pharm. 363: 183-191.
21. **Jose, S., Anju, S.S., Cinu, T.A., Aleykutty, N.A., Thomas, S., Souto, E.B. (2014).** *In vivo* pharmacokinetics and biodistribution of resveratrol-loaded solid lipid nanoparticles for brain delivery. Int. J. Pharm. 474: 6-13.
22. **Sessa, M., Balestrieri, M.L., Ferrari, G., Servillo, L., Castaldo, D.D., Onofrio, N., Donsì, F., Tsao, R. (2014).** Bioavailability of encapsulated resveratrol into nanoemulsion-based delivery systems. Food Chem. 147: 42-50.
23. **Lu, X., Ji, C., Xu, H., Li, X., Ding, H., Ye, M., Zhu, Z., Ding, D., Jiang. X,, Ding, X., Guo, X. (2009).** Resveratrol-loaded polymeric micelles protect cells from A β-induced oxidative stress. Int. J. Pharm. 375: 89-96.
24. **Singh, G., Pai, R.S. (2014).** Optimized PLGA nanoparticle platform for orally dosed trans-resveratrol with enhanced bioavailability potential. Expert Opin. Drug Deliv. 11: 647-59.
25. **Dhamecha, D., Jalalpure, S., Jadhav, K., Jagwani, S., Chavan, R. (2016).** Doxorubicin loaded gold nanoparticles: Implication of passive targeting on anticancer efficacy. Pharmacol. Res. 113: 547-56.
26. **Dhamecha, D., Jalalpure, S., Jadhav, K. (2016).** Nepenthes khasiana mediated synthesis of stabilized gold nanoparticles: characterization and biocompatibility studies. J. Photochem. Photobiol. 154: 108-17.
27. **Shelke, S., Shahi, S., Jadhav, K., Dhamecha, D., Tiwari, R., Patil, H. (2016).** Thermoreversible nanoethosomal gel for the intranasal delivery of Eletriptan hydrobromide. J. Mater. Sci. Mater. Med. 27(6):103.
28. **Validation of analytical procedure: (2005).** Methodology International Conference on Harmonisation. Q2 (R1).
29. **Bangham, A.D., Standish, M.M., Watkins, J.C. (1965).** Diffusion of univalent ions across the lamellae of swollen phospholipids. J. Mol. Biol. 13: 238-252.
30. **Chen, X., He, H., Wang, G., Yang, B., Ren, W., Ma, L., Yu, Q. (2007).** Stereospecific determination of *cis* and *trans* resveratrol in rat plasma by HPLC: application to pharmacokinetic studies. Biomed. Chrom. 21: 257-265.

31. **Abdelwahab, N.S., Abdelrahman, M.M. (2015).** Stability indicating RP-HPLC method for the determination of flubendazole in pharmaceutical dosage forms. RSC Adv. 5: 10927-109235.
32. **Jadhav, K., Rajeshwari, H.R., Deshpande, S., Jagwani, S., Dhamecha, D., Jalalpure, S., Subburayan, K., Baheti, D. (2018).** Phytosynthesis of gold nanoparticles: Characterization, biocompatibility, and evaluation of its osteoinductive potential for application in implant dentistry. Mater. Sci. Eng. C. 93:664-670.
33. **Jadhav, K., Deore, S., Dhamecha, D., Jagwani, S., Jalalpure, S., Bohara, R. (2018).** Phytosynthesis of Silver Nanoparticles: Characterization, Biocompatibility Studies, and Anticancer Activity. ACS BiomaterSci Eng. 4(3):892-9.
34. **Trela, B.C., Waterhouse, A.L. (1996).** Resveratrol: isomeric molar absorptivities and stability. J. Agric. Food Chem. 44(5): 1253-1257.
35. **Gambini, J., Inglés, M., Olaso, G., Lopez-Grueso, R., Bonet-Costa, V., Gimeno-Mallench, L., Mas-Bargues, C., Abdelaziz, K.M., Gomez-Cabrera, M.C., Vina, J., Borras, C. (2015).** Properties of resveratrol: *in vitro* and *in vivo* studies about metabolism, bioavailability, and biological effects in animal models and humans. Oxid. Med. Cell Longev. 2015.
36. **Silva, C.G., Monteiro, J., Marques, R.R., Silva, A.M., Martínez, C., Canle, M., Faria, J.L. (2013).** Photochemical and photocatalytic degradation of trans-resveratrol. Photochem. Photobiol. Sci. 12(4):638-644.
37. **Prokop, J., Abrman, P., Seligson, A.L., Sovak, M. (2006).** Resveratrol and its glyconpiceid are stable polyphenols. J. Med. Food. 9(1):11-4.
38. **Mark, L., Nikfardjam, M.S., Avar, P., Ohmacht, R.A.(2005).** validated HPLC method for the quantitative analysis of trans-resveratrol and trans-piceid in Hungarian wines. J. Chromatogr. Sci. 43(9): 445-449.
39. **Lee, S.S., Lee, S.M., Kim, M., Chun, J., Cheong, Y.K., Lee, J. (2004).** Analysis of trans-resveratrol in peanuts and peanut butters consumed in Korea. Food Res. Int. 37(3):247-251.
40. **Tzanova, M., Peeva, P. (2018).** Rapid HPLC Method for Simultaneous Quantification of trans-Resveratrol and Quercetin in the Skin of Red Grapes. Food Anal. Methods. 11(2): 514-521.
41. **Da Rocha Lindner, G., Khalil, N.M., Mainardes, R.M. (2013).** Resveratrol-loaded polymeric nanoparticles: validation of an HPLC-PDA method to determine the drug entrapment and evaluation of its antioxidant activity. Sci. World J. 2013. Article ID 506083, 9 pages.
42. **Moretón-Lamas, E., Lago-Crespo, M., Lage-Yusty, M.A., López-Hernández, J. (2017).** Comparison of methods for analysis of resveratrol in dietary vegetable supplements. Food Chem. 224: 219-223.